# EVALUATING INHIBITORY POTENTIAL TARGETING CHOLESTERYL ESTER TRANSFER PROTEIN (CETP) BY HYDROXYCITRIC ACID (HCA) FOUND IN *GARCINIA* SPECIES THROUGH KINETIC AND IN-SILICO TECHNIQUE.


**SURAYA BINTI ABDUL SANI**

**SCHOOL OF PHARMACY**
**FACULTY OF SCIENCE**
**Thesis submitted to the University of Nottingham for the degree of Doctor of Philosophy**
**MAY 2016**

*To my beloved husband, Mohammad Norfaizan Waie Sekol, My adorable daughter Uzma Amani, my beloved parent, Mr Abdul Sani Bujang & Mdm Senawati Sahani and my entire family. Thank you for being there for me through the thick and the thin of my PhD period.*

## DECLARATION

I, Suraya Abdul Sani, declare that this thesis is my own work. It is being submitted for the Degree of Doctor of Philosophy, at the School of Pharmacy, Faculty of Sciences, University of Nottingham, Malaysia. It has not been submitted before for any degree or examination at this or any other University.

……

(Suraya Abdul Sani)

……

(Date: )

# ACKNOWLEDGEMENT

I offer my greatest thanks to my dear husband, Mohammad Norfaizan Waie and my dear daughter, Uzma Amani for being there during my PhD period. Endless love for the entire family for their ongoing support and motivation.

I am grateful to my supervisor, Associate Professor Dr Khoo Teng Jin for his constant support and commitment throughout this research. Special thanks as well to my Co-supervisor, Professor Jonas Emsley for his endless enthusiasm and attention for my 1 year attachment in UK campus. I would also like to thank Dr Charles Laughton for his valuable expertise in Bioinformatics.

I would like to thank my bestfriend, Sree Vaneesa and Chiang Michelle for their help and guidance throughout my 3 years PhD work. It would be tough without them!

*"Doing a PhD is like a 7 dwarves,*
*At the start you are dopey and bashful,*
*In the middle you are usually sick (sneezy), sleepy and gumpy,*
*At the end they call you Doc and you're happy."*

Ronald Azuma

**ABSTRACT**

Cardiovascular disease has emerged in developing countries and becoming the leading cause of death recorded. Many scientific studies have been conducted in order to understand the specific mechanism on how atherosclerosis develop, searching for the real culprit that responsible in the progression of the disease and suggesting the possible prevention to overcome this problem. This piece of work examined and revealed the mechanism of action on how secondary metabolites that has been isolated from Malaysian local plants which have the properties to impede the action of cholesteryl ester transfer protein (CETP) in order to prevent the atherosclerosis. Preliminary results of the crude plant extracts from the initial screening showed positive results. A similar trend of inhibition can be obtained for twigs and leaves extracts of *Garcinia atroviridis* and *Garcinia parvifolia.* Ethanol extracts of fruit parts of *Garcinia atroviridis* give $IC_{50}$ of 19.28 ± 0.021 mg/ml which shows the highest inhibitory compared to the other extracts of other plant parts. The remarkable results that are obtain from fruit rinds of *Garcinia atroviridis* do give some hints that the secondary metabolites that are present might have the ability to inhibit CETP. Based on literature review, it is postulated hydroxycitric acid (HCA) might be responsible for inhibiting CETP activity and HCA has been selected for further studies. Kinetic studies have been employed in this piece of work in order to see the types of inhibition that HCA possess against CETP. The kinetic study has revealed that HCA is a noncompetitive inhibitor because of the Km (-0.12) that is unchanged for every substrate and the Vmax is increased when the concentration of the inhibitor increase. Further in-silico works such as molecular docking and molecular dynamic has been implemented as well in order to see the interaction and mechanism of action between HCA and CETP. The molecular docking work has revealed that HCA binds to the same side as torcetrapib does and the RMSD obtained was 2.703Å. Molecular dynamics has been

employed as well in order to see the extensive structural and functional analysis and also to evaluate the strengthness of the complex between HCA and CETP. The complex were found to be stable due to the existence of the hydrogen bonding to SER230 and the overall RMSD reading are between the range of 0.8Å, 2.4Å and 3.2Å. Overall, this work are pioneering and pave the way for further studies in establishing a new chemical template form of natural products for CETP research with an objective to extend the scope of work into in-vivo studies and x-ray crystallography in order to enable us to understand the mechanism of action in protein level. The in-silico studies in this work provides a preliminary understanding on the structural basis of CETP structure and its active sites which could accommodate the exact template of chemical molecule. With this new understanding, an inhibitor drug which are effective with lesser side effect, targeting atherosclerosis could be developed.

**LIST OF TABLES**

## List of figures

## List of abbreviations

| | |
|---|---|
| **CVD** | Cardiovascular disease |
| **WHO** | World Health Organization |
| **LDL-C** | Low density lipoprotein cholesterol |
| **LDL** | Low density lipoprotein |
| **HDL** | High density lipoprotein |
| **HDL-C** | High density lipoprotein cholesterol |
| **CETP** | Cholesteryl ester transfer protein |
| **CE** | Cholesterol ester |
| **TG** | Triglycerides |
| **SAR** | Structure Activity Relationship |
| **mmol/L** | Millimole per litre |
| **HMG-CoA** | 3-hydroxy-3-methylglutaryl Coenzyme A |
| **CoA** | Coenzyme A |
| **HMGCR** | 3-hydroxy-3-methylglutaryl Coenzyme A reductase |
| **IDL** | Intermediate density lipoprotein |
| **VLDL** | Very low density lipoprotein |
| **apoA-I** | Apolipoprotein A -I |
| **apoA-II** | Apolipoprotein A-II |
| **INTERHEART** | A global case-control study of risk factors for acute myocardial infarction |
| **Ox-LDL** | Oxidized low density lipoprotein |
| **SMC** | Smooth muscle cell |
| **MAP** | Mitogen activated protein |
| **VCAM-1** | Vascular cell adhesion molecule |
| **MCP-1** | Monocyte chemoattractant protein |
| **MMP** | Matrix metalloproteinase |
| **MCSF** | Macrophage colony stimulating factor |
| **TLR** | Toll like receptor |
| **µM** | micro molar |
| **ICAM** | Intercellular adhesion molecule |
| **$PGI_2$** | Prostacylin |

| | |
|---|---|
| **PAF** | Platelet activating factor |
| **SREBP** | Sterol regulatory element binding protein |
| **SREBP1a** | Sterol regulatory element binding protein 1a |
| **SREBP2** | Sterol regulatory element binding protein 2 |
| **LXRS** | Liver X receptors |
| **DR4** | Direct repeat separated by 4 elements |
| **CRE** | Cholesterol response element |
| **Å** | Amstrong |
| **KDA** | Kilo dalton |
| **PDB ID** | Protein Data Bank Identification |
| **2OBD** | Crystal structure of native CETP |
| **4EWS** | Crystal structure of CETP with torcetrapib |
| **GLY** | Glycine |
| **ALA** | Alanine |
| **VAL** | Valine |
| **LEU** | Leucine |
| **ILE** | Isoleucine |
| **PRO** | Proline |
| **PHE** | Phenylalanine |
| **TYR** | Tyrosine |
| **TRP** | Tryptophan |
| **SER** | Serine |
| **THR** | Threonine |
| **CYS** | Cysteine |
| **MET** | Methionine |
| **ASN** | Asparagine |
| **GLN** | Glutamine |
| **LYS** | Lysine |
| **ARG** | Arginine |
| **HIS** | Histidine |
| **ASP** | Aspartate |
| **GLU** | Glutamate |
| **ILLUMINATE** | A study examining torcetrapib/atorvastatin and atorvastatin effects on clinical CV events in patients with heart disease |

**REVEAL** Randomized Evaluation of the effects of anacetrapib through lipid-modification

**ACCELERATE** A study of evacetrapib in high risk vascular disease

**UNMC** University of Nottingham Malaysia Campus

**SD** Standard deviation

**ANOVA** One-way analysis of variance

**FTIR** Fourier Transform Infrared Spectroscopy

**ATR** Attenuated total reflectance

**HPLC** High performance Liquid Chromatography

**orgTh** Organizing thrombus

**NC** Necrotic core

**Th** Acute thrombus

**FC** Thin fibrous cap

**ACS** Acute coronary syndrome

**apoE** Apolipoprotein E

**WTD** Western type diet

**LDLR** Low density lipoprotein receptor

**CM** Chylomicrons

**RCT** Reverse cholesterol transport

**ACAT** CoA:cholesterol acyltransferase

**CD36** Cluster of differentiation 36

**SR-A** Macrophage scavenger type A

**LCAT** Lecithin: cholesterol acyltransferase

**ATP** Adenosine triphosphate

**ABCA** ATP binding cassette transporter

**ABCG-1** ATP binding cassette sub-family G member 1

**apoB** Apolipoprotein B

**α** alpha

**β** beta

**ABCBII** Bile salt export pump

**ABCG5** ATP binding cassette sub-family G member 5

**ABCG8** ATP binding cassette sub-family G member 1

**g/mL** Gram per milli litre

**α-LPA-1** Apolipoprotein A-1 containing lipoprotein

| | |
|---|---|
| **NF-κB** | Protein complex that controls transcription of DNA cytokine production |
| **TNF-α** | Tumor necrosis factor alpha |
| **NO** | Nitric Oxide |
| **eNOS** | Endothelial Nitric Oxide Synthase |
| **NADPH** | Nicotinamide adenine dinucleotide phosphate |
| **mL/min** | milli Litre per minute |
| **µL** | microlitre |
| **GLIDE** | Docking software develop by Schrodinger |
| **OPLS AA** | Optimized potential for ligand simulation |
| **RMSD** | Root mean square deviation |
| **GOLD** | Docking software develop by the Cambridge Crystallographic Data Centre |
| **DESMOND** | Molecular simulation software develop by Schrodinger |
| **GA** | Genetic algorithm |
| **NaCl** | Sodium chloride |
| **LBFGS** | Limited memory Broyden Fletcher goldfard shanno |
| **RMSF** | Root mean square fluctuation |
| **DMSO** | Dimethyl sulfoxide |
| **L** | Leave |
| **T** | Twig |
| **F** | Fruit |
| **$IC_{50}$** | Measure of how effective the drug is |
| **ZINC 3D** | Free database of commercially available compounds for virtual screening |
| **mRNA** | messenger RNA |

# Chapter 1: Introduction

Cardiovascular disease (CVD) that involves the diseases of the heart and circulatory system remains the leading cause of death in worldwide which affecting almost 4.1 million deaths per year (Nichols *e*t *al*., 2013).

CVD epidemic that has emerge in the developing countries during the past two or three decades contributes a greater share to the global burden of CVD provides less public response even within the effected countries (Mathers & Loncar, 2006). The increase in the rate of CVD is due to the economic transition, industrialization and globalization which change the lifestyle of people in those developing countries which promote heart disease. Over the previous decade or more, the predominance of conventional danger components for atherosclerotic cardiovascular infections has been expanding in the major developing countries, including China and India, with resulting increments in the rates of coronary and cerebrovascular occasions (Celermajer *et al.*, 2012). In Malaysia, the total deaths caused by CVD increased from 32% in 2010 to 36% in 2014 (WHO,2011; WHO,2015). Specific difficulties in tending to the expanding weight of CVD in Malaysia incorporate low spending plans for wellbeing (counting for screening, anticipation, and treatment), and also the training and expertise blend of the wellbeing workforce.

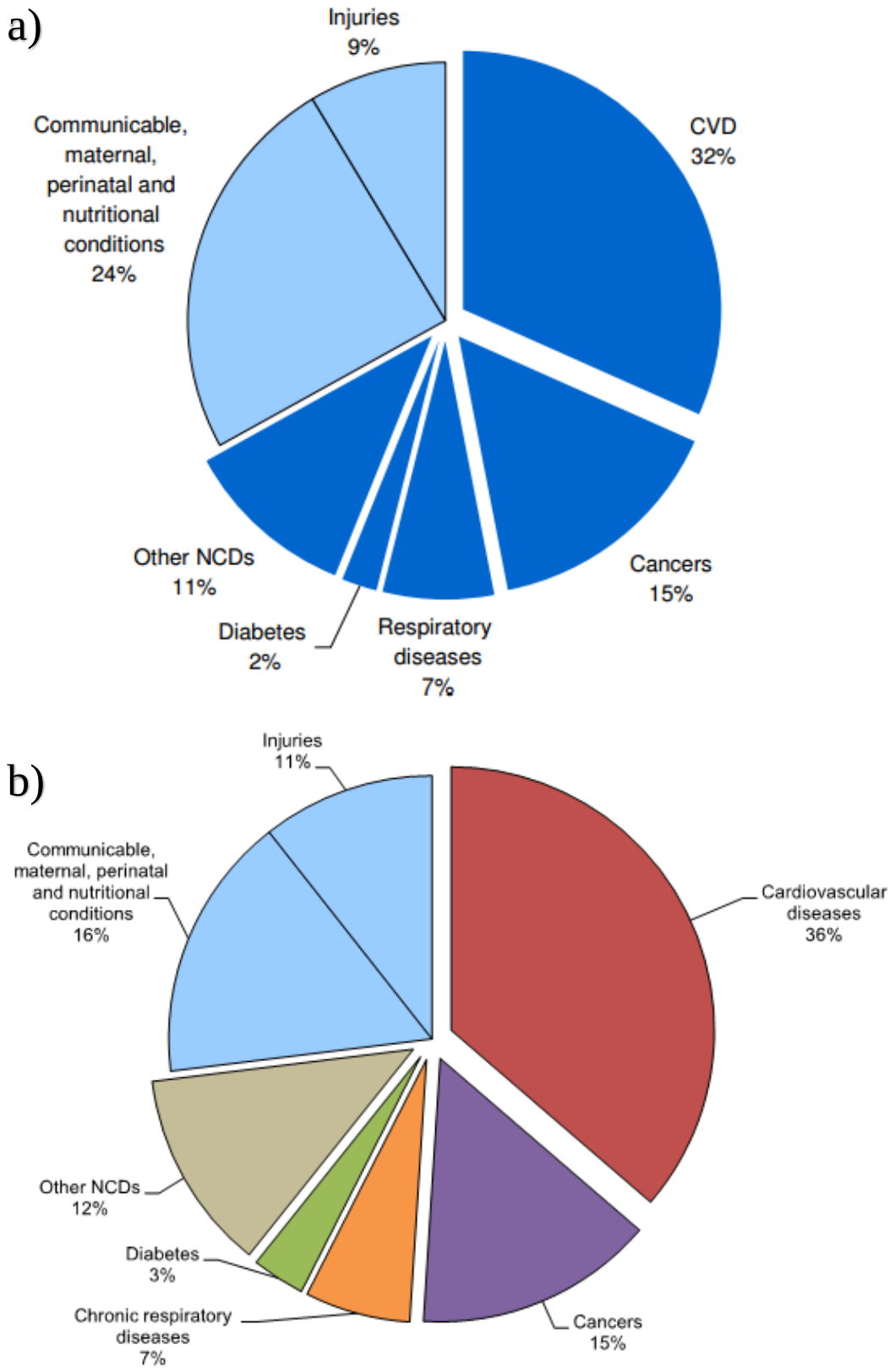


**Figure 1 a) The proportional mortality rates in Malaysia for 2010 b) The proportional mortality rates in Malaysia for 2014 (WHO,2011;WHO,2015)**

Elevated blood cholesterol level especially low-density lipoprotein cholesterol (LDL-C) is correlated with a higher risk of cardiovascular disease events such as heart attack, stroke and heart failure. LDL is also known as a primary carrier of cholesterol, transport cholesterol to cell where it is being used in the cell membrane (Crockett, 1998) and for the synthesis of steroid hormones, vitamin D, and bile acid . Cells take up cholesterol by a process called receptor-mediated endocytosis. LDL binds to a specific LDL-receptor that exposed to the cell surface and is internalized by endocytosis. The endocytic vesicle then pinches into two smaller vesicles; (1) containing free LDL (2) empty receptors. The vesicles which contain LDL fuses with a lysosome to form secondary lysosome. The enzyme of the lysosome will then release free cholesterol to the cytosol. The empty receptors will return to and fuses with the plasma membrane, turning inside out as it does (exocytosis) and later it will be reuse again. The excessive transportation of LDL throughout the human body can cause cholesterol build-up in the arteries. This build up can eventually lead to an arterial blockage that is being known as atherosclerosis. The early stage of atherosclerosis started when atherosclerotic plaque forms when LDLs are accumulated in the arterial intima and become oxidized over time gives rise to the narrowing of arteries, rupture, and stenosis or closure of the lumen, clotting and finally will lead to sudden death if untreated.

High-density lipoprotein cholesterol (HDL-C) is also known as “good cholesterol” because it is shown in several epidemiological studies that high levels of HDL-C are associated with reduced levels of CVD and low-level HDL-C are associated with high risk of CVD . HDL acts as a scavenger, which protects the arteries by removing LDL cholesterol away from the arteries and back to the liver. Cholesterol will then be metabolized and passed from the body.

The progression of CVD will cause serious health condition; therefore, it is important to diagnose these diseases as early as possible. Several tests and diagnosis have been developed over the years including electrocardiogram, echocardiogram, stress test, cardiac catheterization or angiogram, heart scan and magnetic resonance angiography (MRA). But the most effective way is by having healthy ways of lifestyle such as reduced alcohol intake, quit smoking, exercise regularly, reduce stress and having a healthy and balanced diet.

The treatments of CVD are the same for both genders (men and women). Treatments that have been available nowadays may include changing in lifestyle, medication, surgical procedures and rehabilitation.

Lowering the LDL-c levels in the blood has been a major target for research in order to prevent the progression of CVD. Based on this approach numerous drugs have been developed in order to prevent CVD, especially statin. However, some controversial issue arises based on this approach whereby CVD is a multifactorial disease and increase in LDL-c level cannot be solely be blamed as the main factors. Therefore, the research strategies aimed on increasing HDL since HDL is identified as an independent risk factor and it is seem to be promising target in fighting against CVD.

One of the ways to increase HDL-C level in human bloodstream is by inhibition of cholesteryl ester transfer protein (CETP). CETP is a hydrophobic plasma protein that is mainly secreted in the liver and basically travels in the plasma and mainly bound to HDL . It transfers cholesterol esters (CE) and triglycerides (TGs) between HDL and other lipoprotein particles that results in equilibration of lipids in lipoprotein fractions. Hence inhibition of CETP indirectly increases HDL-C levels (Barter *et al,* 2007). Due to this nature, HDL is

rapidly being catabolized and most of the cholesterol are transported through LDL. Therefore by targeting the inhibition of CETP has become an attractive strategy to reduce the CVD.

One of the novel strategies has led to the discovery of novel CETP inhibitors torcetrapib which successfully inhibits CETP activity. However, torcetrapib caused controversy against its clinical trials which increased blood pressure and mortality rate (Barter,2009). Due to this problem, all the clinical trials that are associated with torcetrapib are terminated. This does not cause researcher to give up finding new drugs that can inhibit CETP and more studies and techniques have been implemented in searching for the potent inhibitor of CETP.

Investigation into unexplored natural product is essential in the quest to discover novel therapies for CVD. *Garcinia atroviridis* is used in traditional Malaysian folklore medicine as a cholesterol-lowering agent and yet there is no evidence that shows this plant would directly inhibits CETP. Therefore the ultimate purpose of this work is to study the inhibitory interaction between CETP and *Garcinia* plant species and to gain more detailed information of what compound that can inhibit CETP. The interaction between compound of interest and CETP activity are studied using molecular docking and dynamic simulation, which offer a possibility to examine detailed knowledge on an atomic scale. The obtained results can be used in the future for the development of new inhibitor agents against the progression of CVD.

## 1.1 Aims and Objective

The aim of this research was to evaluate the potential Malaysian rainforest plants that may possess inhibitory activity against Cholesteryl Ester Transfer Protein (CETP) and further analysis of the inhibitory activity of the compound using in-silico approach.

The objectives include:

1) To collect and identify potential Malaysian Rainforest plant.
2) To study the inhibitory interaction between CETP and *Garcinia* species in order to have an idea of what compound that can inhibit CETP.
3) To evaluate the kinetic properties of compound of interest and CETP.
4) To prove the presence of HCA in UNMC 78F ethanol extract.
5) To study the interaction between compound of interest with CETP using molecular docking and dynamic simulation.
6) To study the Structural Activity Relationship (SAR) of HCA analogues through molecular docking.

# Chapter 2: Literature Review

## 2.1 Prevalence of cardiovascular diseases

Cardiovascular disease (CVD) includes a wide range of disorders; diseases of the vasculature, diseases of myocardium, diseases of hearts electrical circuit and congenital heart disease and are among the leading cause of death in most western countries. CVD become a global burden to the economies especially most of the money are invested to the prevention of CVD and treatment of CVD. Besides, incapacity of works might be affecting the economics since the increasing rates of death due to CVD before the age of 65. Based on Nichols *et al.,* (2013), it accounts 680,000 deaths each year in Europe making it the main cause of death before 65 years of age.

Atherosclerosis is the most important cause for CVD and it is a multifactorial disease. Atherosclerosis is a disease in which the arteries narrow down due to the formation of atherosclerotic plaque. This will eventually blocks the oxygenated blood flow to the tissues. This may lead to ischemia, a condition that is lack of oxygen in the blood or myocardial infarction (heart attack), which then might cause death. The development of atherosclerosis might take years to progress and has usually proceeded far before the first symptom appears. Therefore it is important to focus on different treatment and prevention strategies to reduce the risk of CVD.

### 2.1.1 Cardiovascular diseases in general

CVD disease is a term that refers to more than one disease in circulatory system which includes heart and blood vessel. There are 6 types of cardiovascular disease; 1) ischemic heart disease; 2) cerebrovascular disease; 3) peripheral vascular disease; 4) heart failure; 5) rheumatic heart disease and 6) congenital heart disease (WHO, 2016).

There are many risk factors that may attribute to the development of CVD and can be divided into modifiable risk factors and non-modifiable risk factor. The modifiable risk factors includes hypertension or high blood pressure, usage of tobacco, raised in blood glucose levels or diabetes, physical inactivity, unhealthy food consumption, raised in the level of blood cholesterol and overweight or obesity (Barnes, 2013). In addition to modifiable risk factor, there are some risk factor that cannot be altered such as age, gender and family history of CVD (Hobbs, 2004).

The most important risk factor is the raised cholesterol in blood circulation which attribute to over one third of ischemic heart disease in the world (Birtcher and Ballantyne,2004) . The general guidelines to identified those with high risk of developing CVD is those who has LDL-C of less than 2.0 mmol/L (Reiner *et al.,* 2011) .

It is important to have proper risk assessment to validate whether the people are in which category of CVD; low risk, intermediate risk or high risk individual. Cardiovascular risk assessment is beneficial especially to primary health care providers in order to detect patient in order to provide proper treatment. Several studies have also shown that the benefits of risk assessment are maximized when it is directly communicated to the patient and the patients are devoted to the prescribed therapy (Cooney *et al.,* 2009; Grover *et al.,* 2007; Grover *et al.,* 2007; Ebrahim *et al.,* 2011).

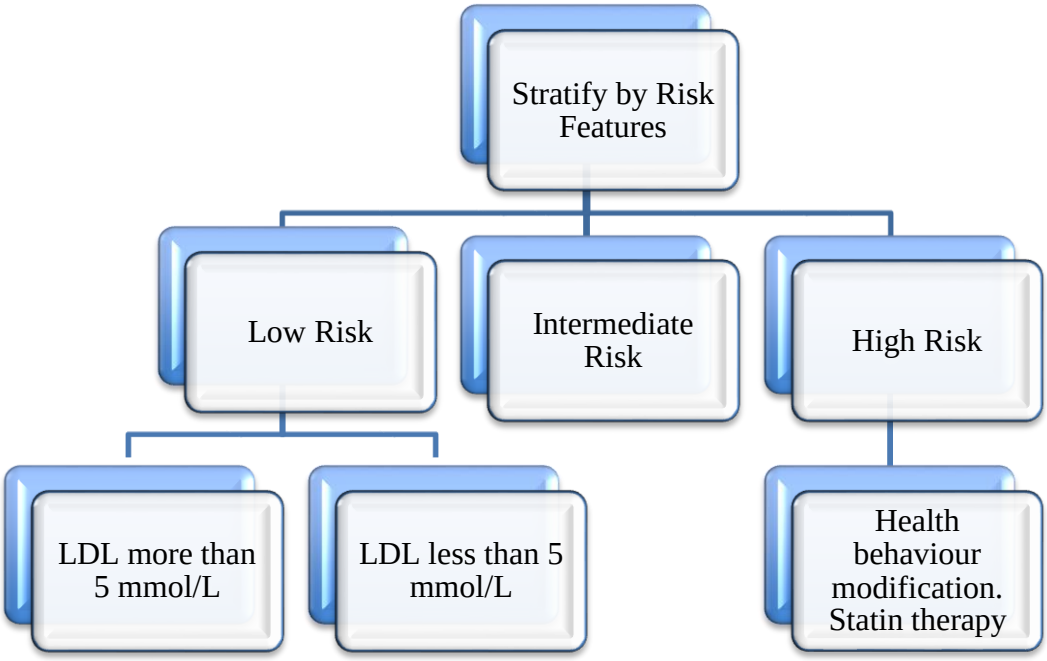


**Figure 2 Risk stratification by Framingham Risk Score and phenotype. Framingham Risk Score is a risk assessment tool for estimating a patient's 10 year risk of developing cardiovascular disease**. (Anderson et al., 2013).

Over the past decade, statins or 3-hydroxy-3-methyl-glutaryl coenzyme A (HMG-CoA) inhibitor have appear to be a primary therapy and it is also shown to reduce the level of CVD by 25% to 35% by lowering the LDL level (Baigent *et al.*,2010). Statin acts as an inhibitor of 3-hydroxy-3-methylglutaryl coenzyme A reductase (HMGCR), the enzymes which are responsible in catalyzing the rate-limiting step of cholesterol biosynthesis (Medina and Krauss, 2009).

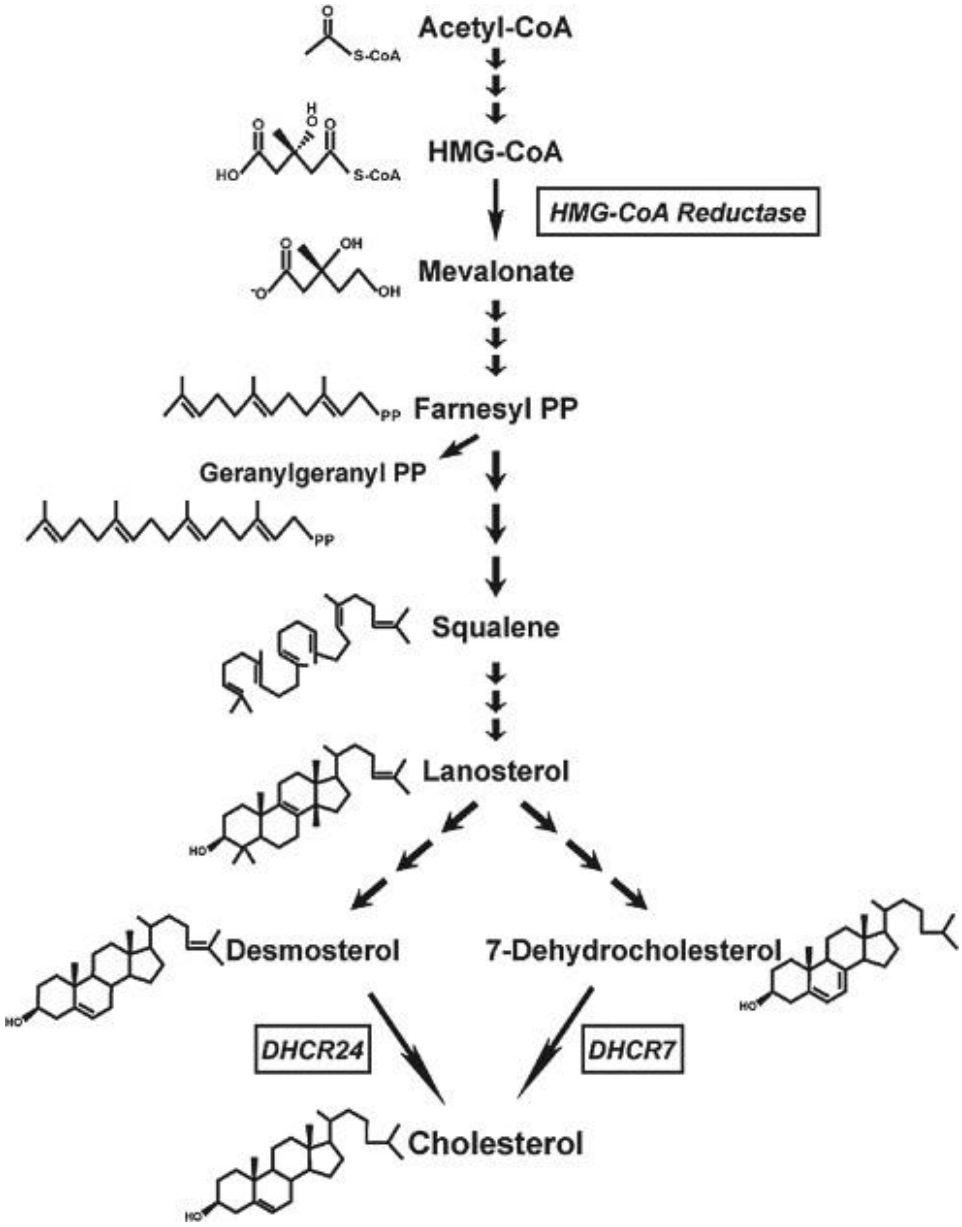


**Figure 3 Cholesterol is the end product of the mevalonate pathway. The initial phase in cholesterol biosynthesis is the generation of a 3-hydroxy-3-methyl-glutaryl CoA (HMG-COA) from acetyl-CoA units. At that point, HMG-CoA is converted to mevalonate by the activity of HMG-CoA reductase on endoplasmic reticulum membrane. This is the main restricting rate response in cholesterol synthesis and becoming the target of statin. Mevalonate is then transformed to isopentenyl pyrophosphate and dimethylallyl pyrophosphate which later producing pyprophosphate and squalene. Production of lanosterol involves the cyclization and oxygenation of squalene. And lastly the cholesterol will be produced when the lanosterol undergoes reduction process (Cortes *et al.*, 2013)**

Statin imitates the HMG-CoA molecule and it competes for the binding to the HMGCR enzyme. This inhibition blocks the mevalonate pathway which is one of the cholesterol producing precursor. Statin alters the conformation of the enzyme when it binds to its active sites which further prevents the enzymes to attain their own functional structure (Corsini *et al,* 1999). This will then lead to the increase in the number of hepatic LDL-receptor which determines the decline in the circulation of LDL and its precursor such as IDL (intermediate density lipoprotein) and VLDL (very low density lipoprotein) (Sehayek *et al.,* 1994). The decrease in LDL-C by statins are dose-dependent study on statin indicate that statins does gives rise to 'pleiotropic effect' such as improving endothelial function, enhancing the stability of atherosclerotic plaques, decreasing oxidative stress and inflammation and an inhibiting the thrombogenic response (Davignon, 2004) .

Statin has remained as the first-line therapy for managing the high level of low-density lipoprotein (LDL) cholesterol in the blood of patient that have been diagnosed with CVD. Since atherosclerosis is a multifactorial disease and the current medication is not enough to prevent the progression of CVD, the therapies concerning to increase HDL-C level has to be improved.

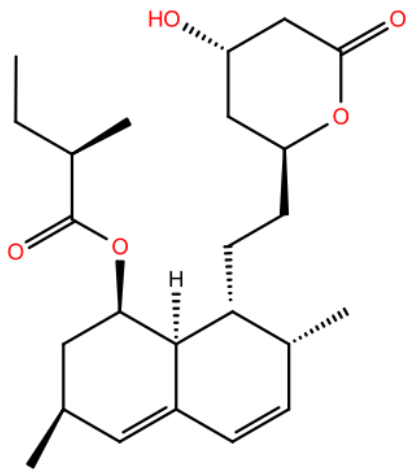


**LOVASTATIN**

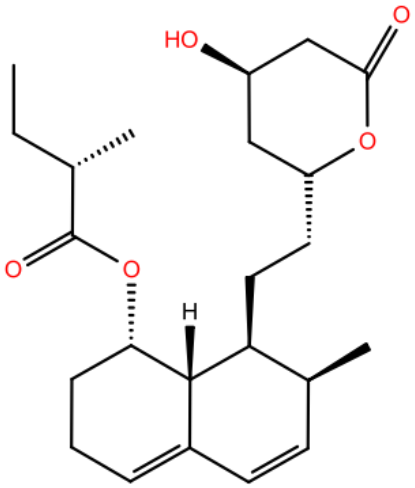


**MEVASTATIN**

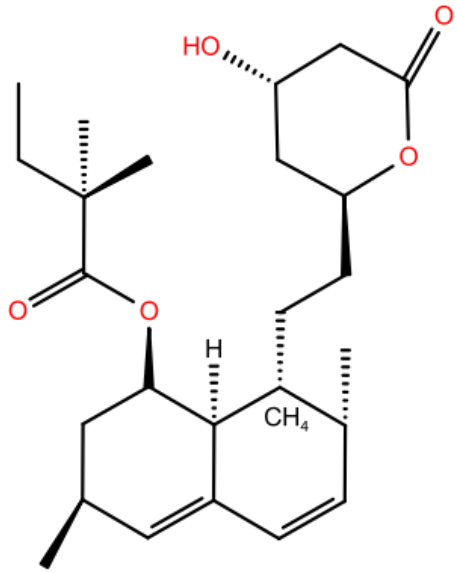


**SIMVASTATIN**

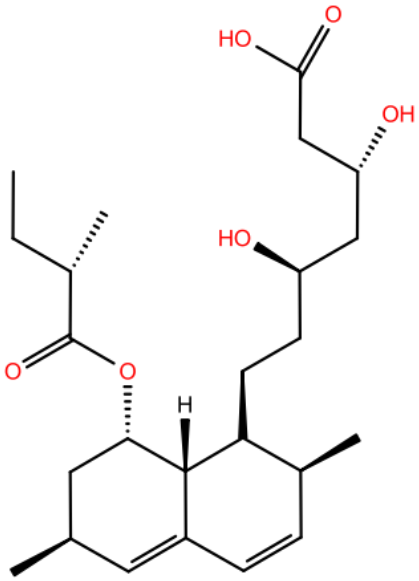


**PRAVASTATIN**

**Figure 4 Various chemical structures of statin**

The use of niacin (nicotinic acid:Vitamin B3), cholesterylamine and fibrates has been use in clinical trials in order to increase HDL-C levels (Boden *et al,* 2011). Niacin acts by inhibits the secretion of VLDL particles, increase lipoprotein lipase activity and decrease triglyceride levels and it has been proven to increase HDL-C levels by 15% to 35% (Taylor *et al.*, 2004). Gemfibrozil, belongs to group of drugs known as fibrates that has been tested, shown an

increase in HDL-C levels by 10-15% (Frick *et al.,* 1987) via the hepatic expression of the main HDL apoliproteins A-I and A-II (apoA-1 and ApoA-II) (Staels *et al.,* 1998; Kumar *et al.,* 2013). The results from these clinical trials are promising but yet more therapies need to be developed. One of which the alternative strategy is to increase the HDL-C level is by focusing into inhibition of CETP.

Health behaviour intervention remains the keystone of any disease prevention which also includes the prevention of CVD (Stuart-Shor *et al.,* 2012; Prochaska and Prochaska, 2013). Data from the INTERHEART study revealed that, in addition to the traditional risk factors which are abnormal lipids, hypertension and diabetes, abdominal obesity, dietary patterns, alcohol consumption, physical inactivity, psychosocial factors and smoking are considered as modifiable risk factors for both sexes and all ages worldwide (Yusuf *et al.,* 2004) .

Nutritional therapy is the most essential elements of the health behavior interventions and its objective is to improve lipid profile and reduce the risk of CVD. Nutritional therapy is also being used in a weight management program. In order to maintain healthy body weight, a balance diet provides all the essential nutrition which balance out the calories intake and number of calories that is being used or "burns-off". Sufficient physical exercise also contributes in the prevention of CVD. Several study has presented the benefits of routine exercise in maintaining healthy lifestyle and prevention of CVD (Thompson *et al.,* 2003; Myers, 2003) .

Psychological factors which includes stress is also modifiable risk factors for CVD. Stress management is important, not only to reduce risk of CVD but to optimize the quality of life. The INTERHEART study revealed that stress is one of the risk factor in the development of

CVD which shows patients with depression have a worse prognosis (Yusuf *et al.,* 2004). Smoking cessation or quitting smoking is the process of discontinuing the addiction of tobacco smoking. This is important in the health behaviour intervention as smoking caused detrimental effects on lipid profiles (Khurana *et al.,* 2000). Based on Ambrose & Barua (2004), there is a linear and dose-dependent correlation between the number of cigarettes smoked per day and the increase in CVD risk. Several pharmacological treatment has been developed to help people to quit smoking includes nicotine-based medicine, transdermal nicotine patch, nicotine gum, nicotine lozenge, nicotine nasal spray, nicotine inhalant, bupropion and vernicline (Schmelzle *et al.,* 2008). Not only the development of treatment, help support services also being offered by expert in order to boost the chance of quitting smoking (Hughes, 2003).

## 2.2 Atherosclerosis

### 2.2.1 Pathogenesis of atherosclerosis

Atherosclerosis is a multifactorial disease which caused by genetic and environmental factors. Basically the names of atherosclerosis derives from Greek words “sclerosis” which means hardening and “athere” bring the meaning of gruel (accumulation of lipid).

The evolution of atherosclerosis starting from arterial wall lesions which is centered by accumulation of lipids and followed by inflammatory response. The changes of the development of atherosclerosis are concisely being described in the next paragraph.

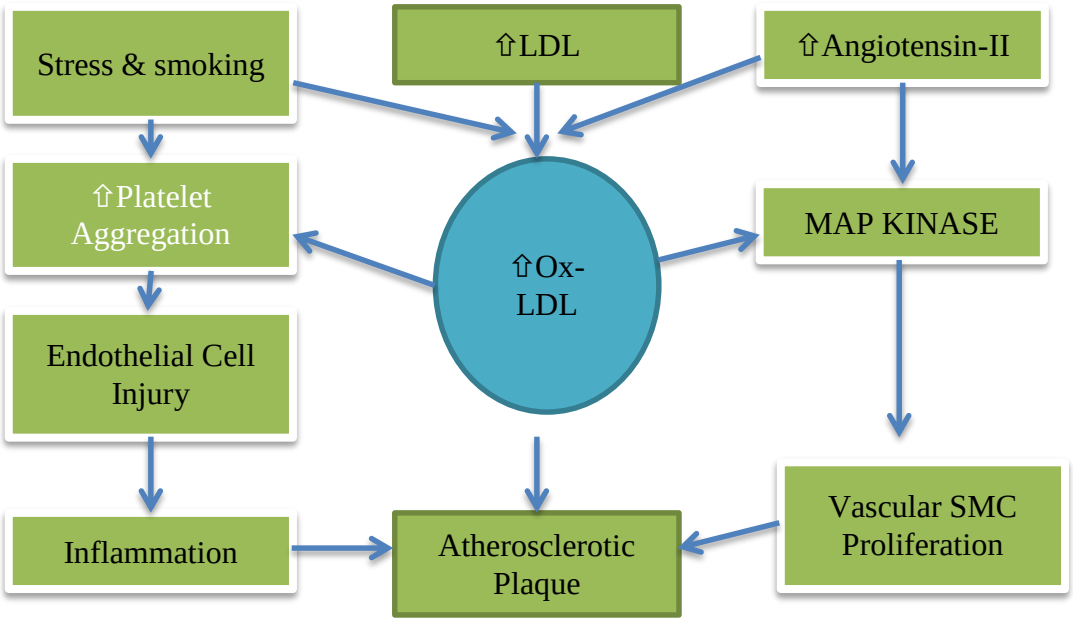


**Figure 5 Schematic diagram of the development of atherosclerotic plaque. This diagram shows the involvement of oxidized low density lipoprotein (Ox-LDL), endothelial cell injury and proliferation of vascular smooth muscle cells (SMC). MAP in this diagram refer to mitogen activated protein** (Singh *et al.*, 2002)

### 2.2.1.1 Early Fatty Streak Development

The normal artery contains three layers, the innermost layer named as intima consists of an extracellular connective tissue matrix which is covered by monolayer endothelial cell. The middle layer, named as media, contains resident smooth muscle cells (SMC) and the outer layer named as adventitia consists of fibroblasts and mast cells. The initial step occurs when the level of LDL leaves the blood increases and enter intima, accumulation will occur. The important event in the initiation of atherosclerotic lesion is the endothelial injury which will activated the inflammatory cascade.

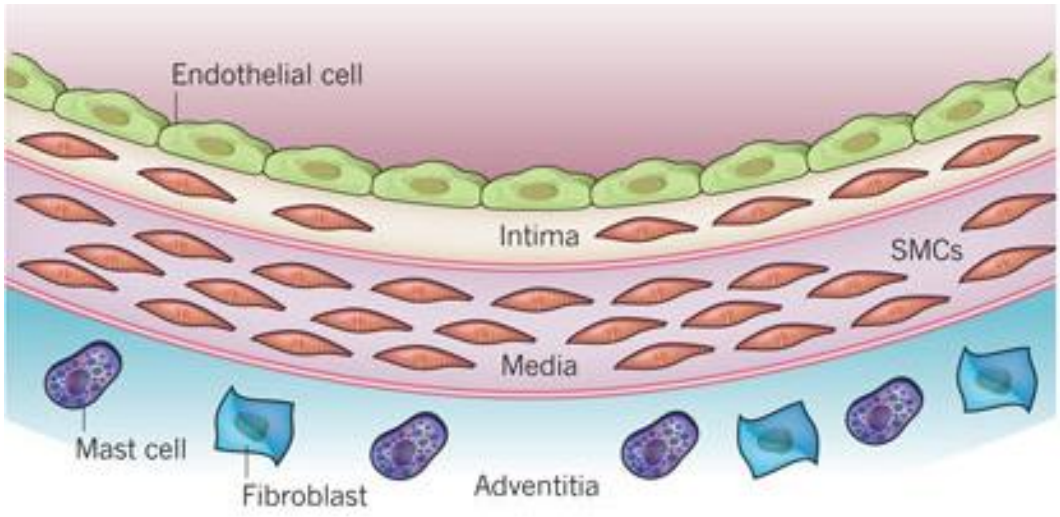


**Figure 6 Three layers of coronary artery** (Libby *et al.*, 2011)

The inflammatory cascade of atherosclerosis initiated when the expression of adhesive protein (vascular cell adhesion molecules [VCAM-1]) increases the recruitment of monocytes and T-cells as response to the endothelial injury. Monocyte chemo attractant protein (MCP-1) also being released by leukocytes which amplify the inflammatory cascade by recruiting more leukocytes, activates leukocytes in the middle layer of artery named as media which cause proliferation of smooth muscle cells.

Once monocytes have attached to the endothelium, chemokines will be produced in the underlying intima. In order to stimulate the migration through the endothelial surface into the media, activated matrix metalloproteinase (MMP) also being release to degrade the connective tissue matrix .

Upon entering the intima, monocytes differentiate into macrophages by the local release of macrophage colony stimulating factor (MCSF) and express at high level of scavenger receptors and toll like receptor. The scavenger receptor that is being expressed by macrophages on their plasma membrane uptake the oxidized LDL that is accumulate in the inside of blood vessel wall and develop into foam cells. Toll like receptors (TLR) promotes atherogenesis through the interruption of endothelial cell integrity and normally initiate the inflammatory responses by producing inflammatory cytokines proteases and cytotoxic radical molecules (Tobias & Curtiss, 2007). The onset of atherosclerosis is believed to start when the lipid accumulation is described as confluent extracellular lipid pools and decreasing in cellularity of extracellular lipid cores (Insull, 2009).

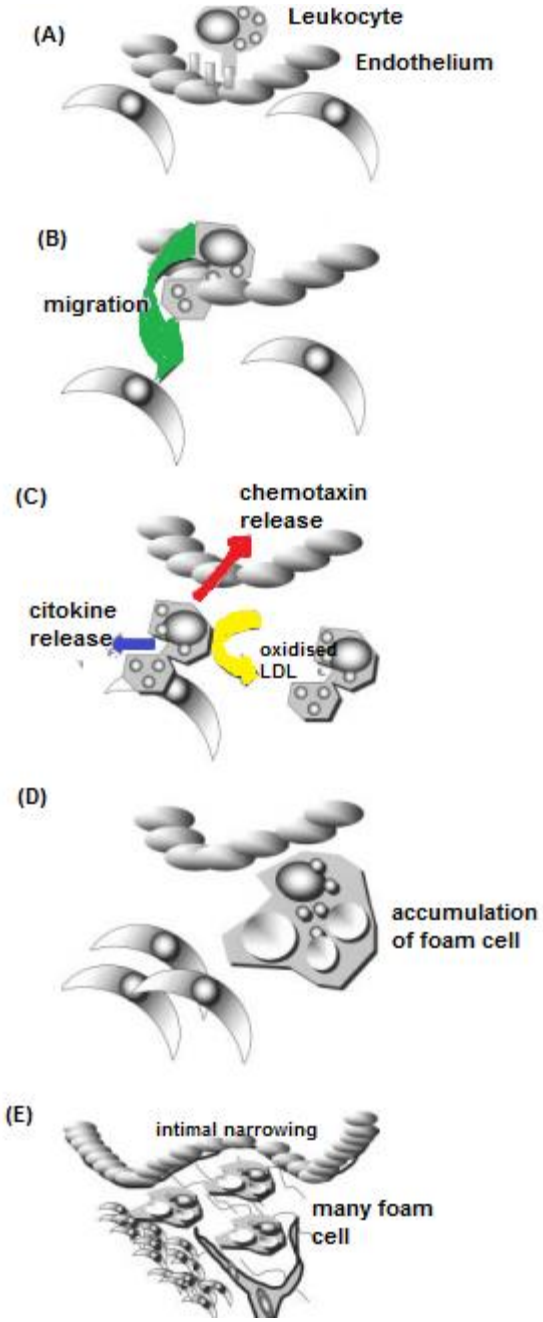


**Figure 7 Series of lesion development (A) The expression of VCAM-1 (adhesive protein) causing the leucocytes to adhere to endothelium as the initial stage of atherosclerosis (B) Leucocytes migrate to the endothelial barrier and begin to accumulate (C) Macrophages releases cytokines and cross the barrier from endothelial surface into media of the vessel (D) Accumulation of foam cells indicates clinical prognosis of atherosclerosis progression (E) Advanced stage of atherosclerosis in which it needs medical intervention whereby it can be characterized by intimal narrowing, many foam cells, neovascularization and flow limiting narrowing.** (Crowther, 2005)

### 2.2.1.2 Progressive atherosclerotic lesions.

Early fibroatheroma occurs as results of pathologic intimal thickening. The accumulation of numerous number of cells, TLR which are also activated the inflammatory cells and other natural cells in the arteries may cause early fibroatheroma. Plaque that is rich with smooth muscle cells excrete proteoglycan will cause lipid binding and further accumulation of extracellular lipid. Some factors may contribute to the apoptotic death of macrophages and SMC which later provokes more serious inflammation (Bentzon *et al.*, 2014).

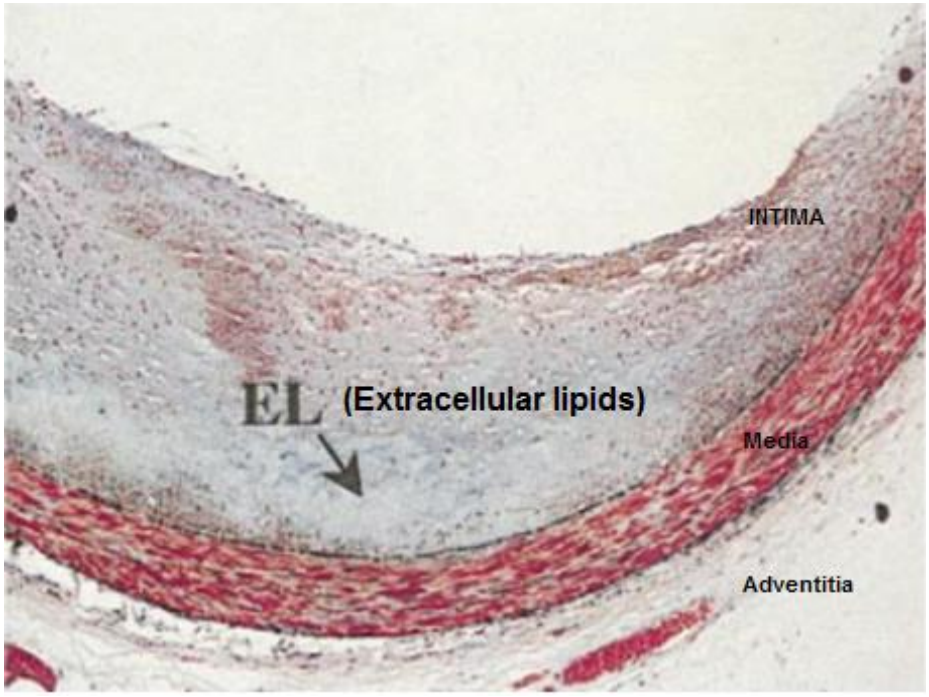


**Figure 8 Intimal Thickening, EL indicates extracellular lipids. Intimal thickening or also known as intermediate lesion is characterized by non-apparent of true necrosis, no cellular debris, some lipid may present in the lesion but scattered. The fibrous cap that is overlying in the lipid region contains lot of smooth muscle cells and proteoglycan. Some scattered macrophages and lymphocytes may likewise be available, however these are generally meager.** (Virmani *et al.*, 2000)

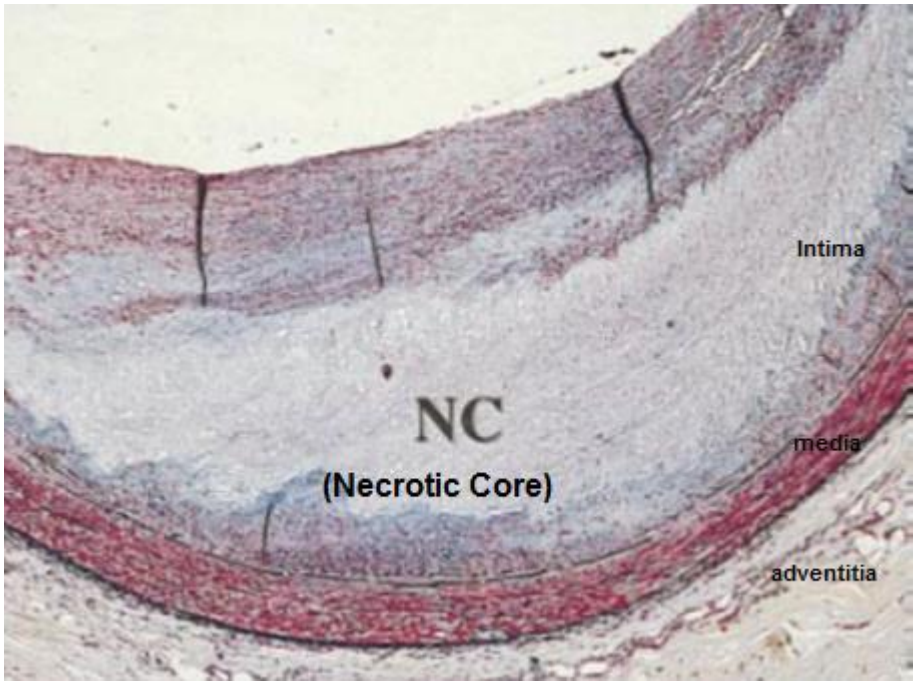


**Figure 9 Early fibroatheroma, NC indicates necrotic core. The more authoritative lesion or also known as fibrous cap atheroma. It is traditionally demonstrates a "genuine" necrotic core which contains cholesteryl ester, free cholesterol, phospholipids and triglycerides. The fibrous cap comprises of smooth muscle cells in a proteoglycan – collagen matrix with a variable number of macrophages and lymphocytes. The media underneath the plague is frequently thin.** (Virmani *et al*., 2000)

Increase accumulation of extracellular lipid may cause early necrosis. This induces the distortion of normal construction of intima until it is fully disrupted. This enlarging pools of lipid-rich necrotic cores takes up 30% to 50% of arterial wall volume (Burke et *al*., 2001). Fibrous cap is made of a layer of fibrous tissue which is found in the intima under the endothelium at the blood interface which forms fibrous plaque lesions.

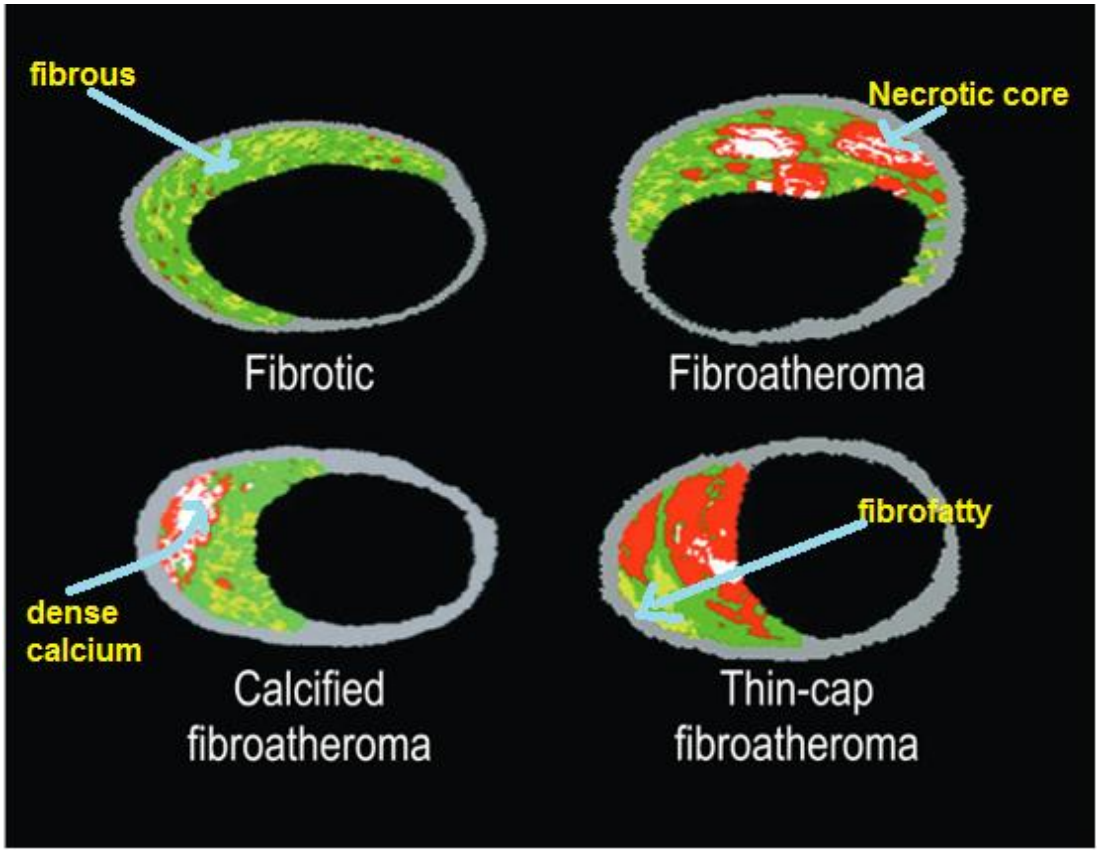


**Figure 10 Examples of coronary lesions via virtual histology. Using the virtual histology, specific color code were assigned for each tissue component, fibroua (dark green), fibrofatty (light green), necrotic core (red) and dense calcium (white)** (García-García *et al*., 2009)

### 2.2.1.3 Thin cap atheroma: A vulnerable plaque

Thin-cap atheroma contain a thin, fibrous cap (less 65μM thick) (Virmani *et al.*,, 2003) and infiltrated by macrophages and lymphocytes. This thin cap fibroatheroma are being called as 'vulnerable plaque' due to the thickness which indicates instability and susceptible to rupture (Virmani *et al.*, 2003). This lesion having the potential to become thrombogenic and produces a thrombus which extends into the arterial lumen (Muller & Tofler, 1992).

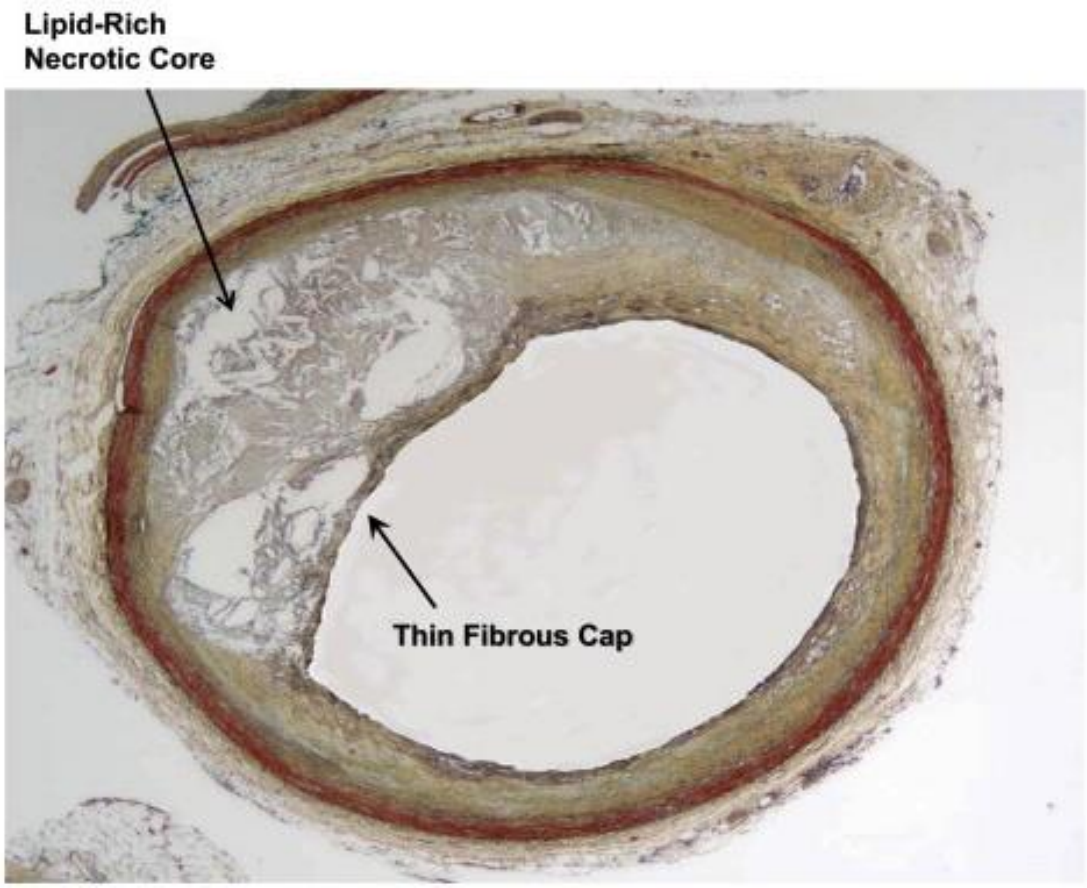


**Figure 11 Illustration of Thin-Cap fibroatheroma** (Virmani *et al*., 2000)**.**

This plaque may cause enlargement and might grow into media and adventitia and distort them. Intramural haematoma might be develop which is cause by a spontaneous rupture of new vasa vasorum (fragile vessels of endothelium), may leak and produce hemorrhage within the arterial wall which later provokes increased in fibrous tissue (Sundt, 2007).

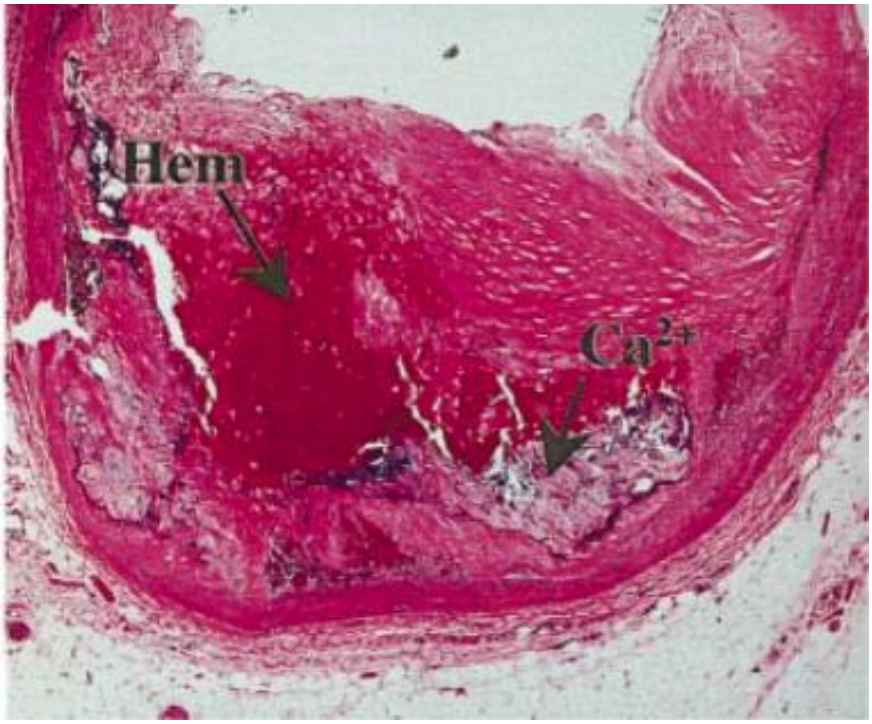


**Figure 12 Fibrous cap atheroma with hemorrhage. This lesion contains red blood cells and fibrin. The fibrous cap is mature and profound inside the intima are territories of calcification.** (Virmani *et al*., 2000)

### 2.2.1.4 Lesion enlargement

The plaque rupture as being described above have the ability to heal silently by forming fibrous tissue, extracellular matrix which consists of proteoglycans, collagen but it is prone to rupture again with the formation of thrombus (Wal & Becker, 1999).

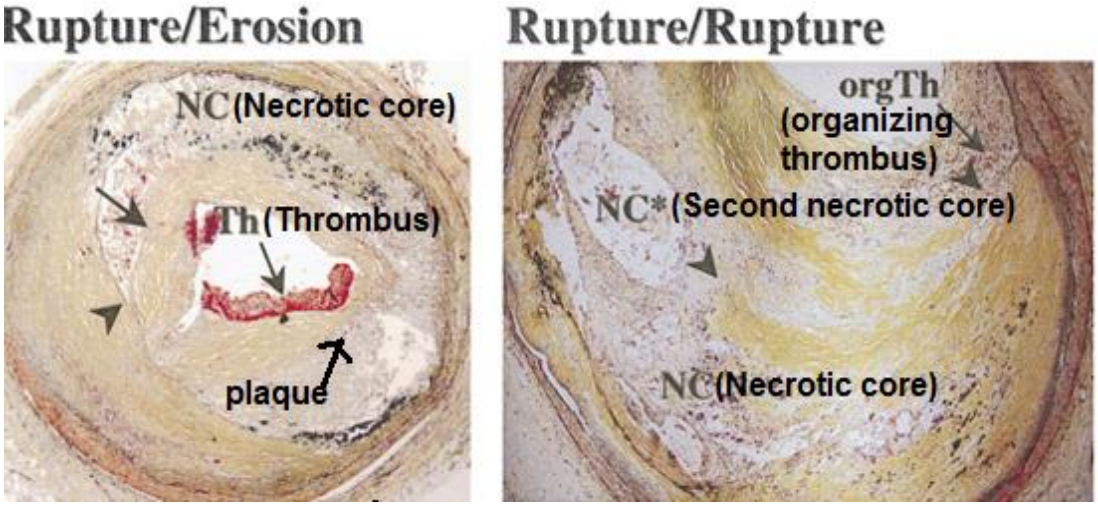


**Figure 13 Illustration of plaque rupture where orgTh is organizing thrombus, NC is necrotic core and Th is acute thrombus. Rupture/Erosion: The past rupture site overlying a necrotic centre is distinguished by the arrowhead, an acute thrombus (Th) from plaque erosion possesses into the lumen. The fibrous cap appears to be thick and the rupture has happened in the centre of the cap. Rupture/Rupture: Repetitive plaque rupture. Multiple rupture site are appeared by arrowheads. NC* indicates the second necrotic centre and an organizing thrombus resulting from the consequent rupture is distinguished by the arrow.** (Virmani *et al*., 2000)

Calcification will occur in the wall of artery may form as small aggregates at first and later as large nodules. These nodules may become sites of thrombosis when it is being exposed due to the plaque rupture. Stenosis (blockage of epicardial coronary vessels) may form due to the increase mass of some plaques and later will cause myocardial ischemia which is the result of oxygenated blood restriction in the heart muscles (Ibañez *et al.*, 2009).

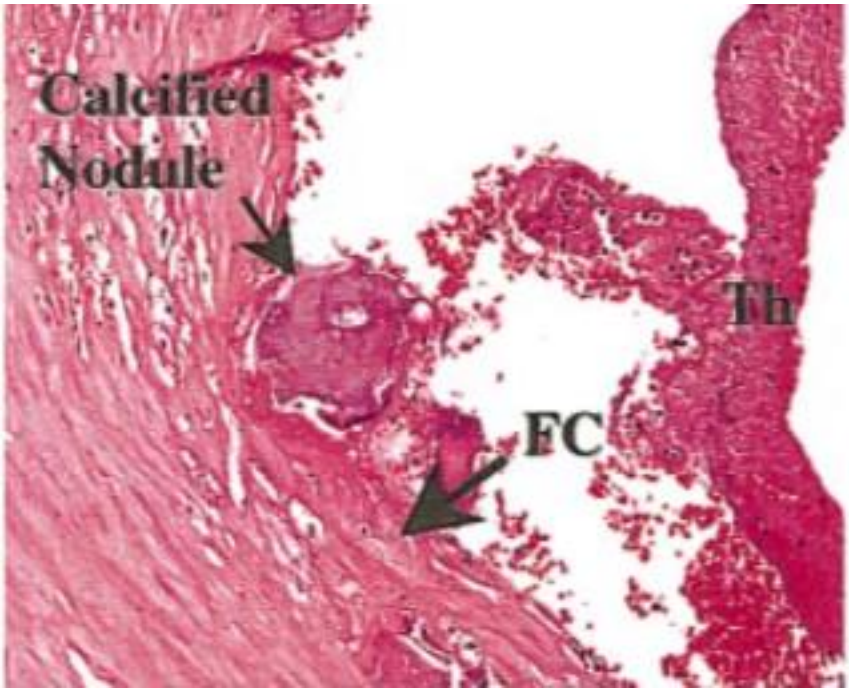


**Figure 14 Calcified nodule, where TH indicates luminal thrombi and FC is thin fibrous cap. Calcified nodules are plaques with luminal thrombi indicating calcific nodules projecting into the lumen through a disrupted thin fibrous cap (FC). There is nonappearance of an endothelium at the site of the thrombus, and inflammatory cells (macrophages, T lymphocytes) are truant.** (Virmani *et al*., 2000)**.**

### 2.2.1.5 Summary of development of atherosclerosis

Atherosclerosis, infrequently called "furring up the arteries," happens when fat (cholesterol) and calcium develop inside the lining of the artery wall, framing a substance called plaque. After some time, the fat and calcium development limits the artery and blocks blood flow through it. The summary of the development of atherosclerosis can be depicted from the figure below.

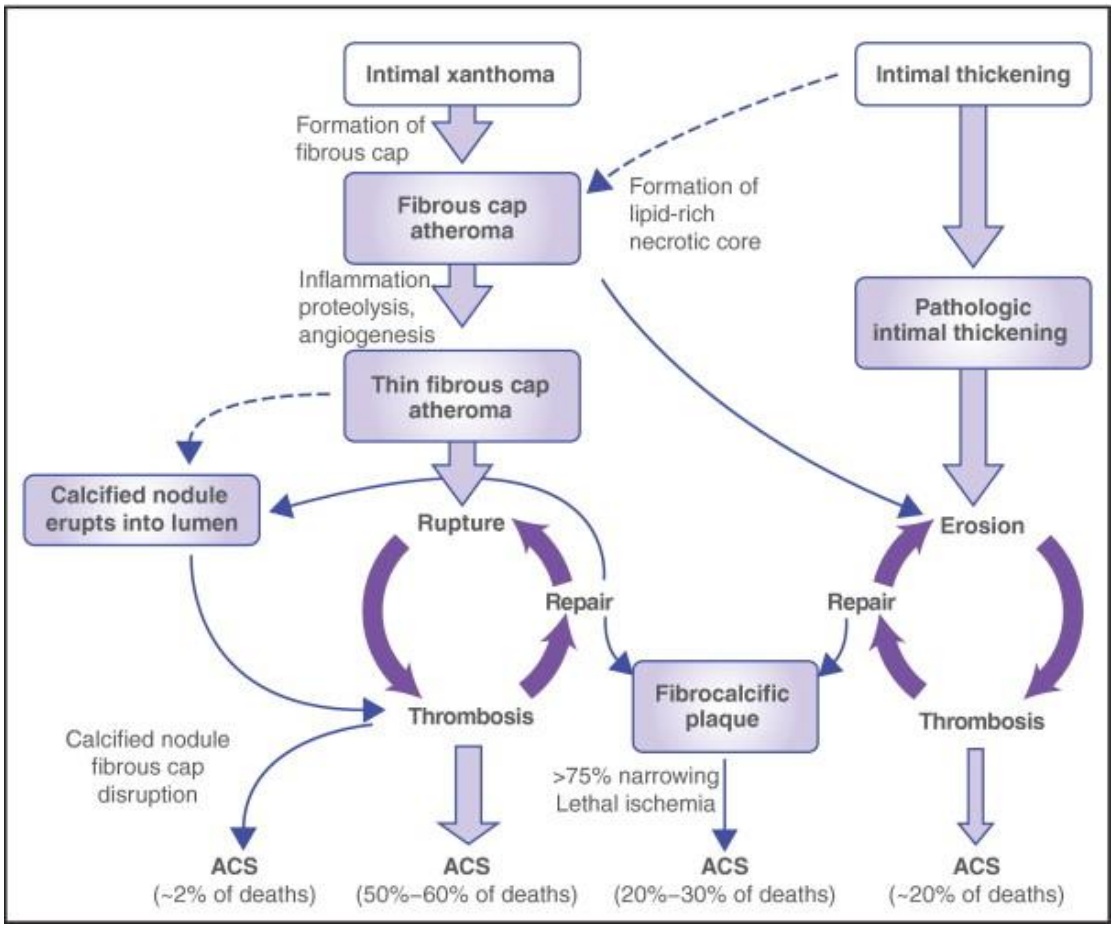


**Figure 15 Schematic diagram of general concepts of the development of atherosclerosis. Atherosclerosis occurs basically from the intimal thickening and intimal xantoma which then leads to the formation of thin fibrous cap atheroma. This will eventually cause rupture or erosion and further development of fibrocalcific plaque. ACS which indicates acute coronary syndrome is a complication due to decrease of blood flow in**

**the coronary arteries which resulting from the formation of thrombosis.** (Virmani *et al.*, 2000)

### 2.2.2 Animal model of atherosclerosis

An animal model has played a major role in the search for new therapies against atherosclerosis. The first breakthrough by Russian Scientist, Alexander Ignatowski in 1908 demonstrated that atherosclerosis can be induced in rabbits by feeding them milk and egg yolks (Konstantinov & Jankovic, 2013). Since this breakthrough, animal models have valuable information regarding diagnosis and therapeutic strategies for atherosclerosis. Several animals models had been used such as mice, rats, guinea pigs, hamsters, avian, swine and non-human primates and there are several advantages, and disadvantages should be taken care of.

**Table 1 Advantages and disadvantages of various animal model of atherosclerosis**

| Species | Advantages | Disadvantages | Sources |
|---|---|---|---|
| **Rabbit** | Expresses Cholesteryl ester transfer protein<br>Cholesterol-sensitive | Forming large foam cells<br>Deficiency in hepatic lipase | Bocan *et al.*, 1993; Nordesgaard and Zilversmit, 1988; Shiomi and Ito, 2009; Buja *et al.*, 2983; Atkinson *et al.*, 1989; Shiomi *et al.*, 1992; Brousseau, 1999 |
| **Pig** | Human-like lipoprotein profiles<br>Moderately cholesterol sensitive on normal diet<br>Large tissue availability due to the size | Expensive<br>No genetic modification available | Skold *et al.*, 1966; Reiser *et al.*, 1959; Koskinas *et al.*, 2010; Gerrity *et al.*, 2001; Prescott *et al.*, 1991; Checovich *et al.*, 1988 |
| **Mice** | Easy to breed<br>Large size of litters<br>Easy for genetic manipulation<br>Low cost<br>Formation of atherosclerosis in short period | Limited tissue availability due to small size<br>No coronary lesions<br>Wild-type strain is relatively atherosclerosis resistant | Yang *et al.*, 2010; Teupser *et al.*, 2006; Smith *et al.*, 2003 |
| **Nonhuman primates** | Develop coronary lesions | Expensive<br>No genetic modification available | Portman and Andrus, 1965; Wolfe *et al.*, 1994; Vesselinovitch *et al.*, 1974; Davis *et al*, 1984; Mott *et al.*, 1992 |

The most widely used animal species that has been used in atherosclerosis research are mouse although there are some limitations. Mice have been used in atherogenesis research due to the ease of making genetic manipulation. Several transgenic mice strains have been develop for atherosclerosis research such as the first genetically mouse with the apoE gene and he two mouse strains that are most as often as possible being utilized as a part of atherosclerosis experimentation are apoE-/ - model and LDL-/ - model (Plump *et al.*, 1992; Zhang *et al*., 1994). Both of these strains are different in their dietary needs for developing atherosclerosis. The development of complex vascular lesion can be induced in $apoE^{-/-}$ by giving normal low-fat rodent chow, and high fat high cholesterol western type diet (WTD), and the lesions develops are comparable to human lesions. A noteworthy hindrance of utilizing this model is that the plasma cholesterol is generally being conveyed by lipoprotein remnants contrasted with LDL that turn into the major carrier of plasma cholesterols in human (Whitman, 2004).

The other most favoured of mice strain for atherosclerosis research is $LDLR^{-/-}$ due to the function of LDLR that influences the uptake of clearance of LDL (Ishibashi *et al*., 1993). The developments of vascular lesions are slow when it is being fed by low-fat chow diet. Despite the limitations of the mice model, the applicability of the mouse findings to human model is to catalog the biological mechanisms of atherogenesis. An exhaustive comprehension of the animal models utilized and complete analysis must be approved so that the information can be extrapolated to people. All in all, animal models for atherosclerosis are important in enhancing our comprehension of cardiovascular disease and developing new pharmacological treatments.

## 2.3 Lipoprotein and Lipid metabolism

Lipoproteins are water soluble particles consists of lipids and proteins and synthesized mainly in the liver and intestines. Lipoproteins aggregate are being classified based on their density when subjected to ultracentrifugation such as chylomicrons (CM), VLDL (very low-density lipoprotein), LDL (low-density lipoprotein) and HDL (high-density lipoprotein) (Chasman *et al*., 2009).

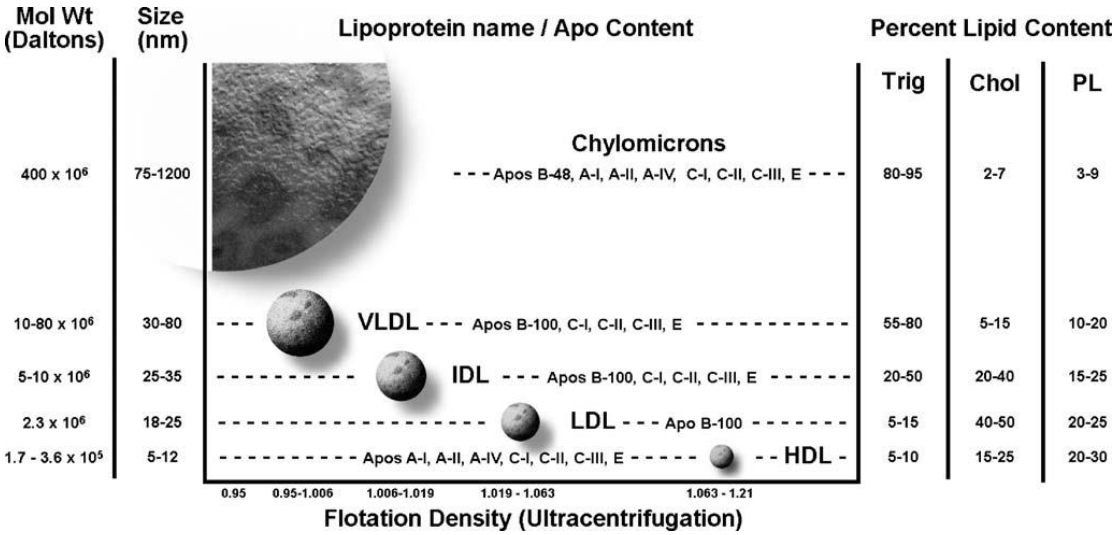


**Figure 16 Major lipoprotein classes and their density** (Saland & Ginsberg, 2007)

The function of lipoproteins as a transporter for hydrophobic triglycerides (TG) and cholesterol in the circulation. Lipoproteins are highly dynamic particles whereby it undergoes constant modification including enzymatic reaction, facilitated and spontaneous lipid transfers, transfers of soluble apolipoprotein and conformational changes of the apolipoproteins in response to the compositional changes (Jonas *et al.*, 1988; Jonas, 2002)

The major routes of metabolism of lipoproteins involves; 1) exogenous pathway which involves in the uptake transportation of dietary lipid from intestine to peripheral tissues 2) Endogenous pathway which involves lipoprotein metabolism that are being synthesized in the liver and 3) reverse cholesterol transport (RCT) involves transportation of the cholesterol

from peripheral tissues back to the liver (Kwiterovich, 2000; Lippi & Guidi, 2000). All of these pathways which are an important target for drugs intervention will be discussed in the next following chapters.

### 2.3.1 Exogenous pathway

Exogenous cholesterol which is secreted from intestinal cells are comprised of dietary uptake. Once the cholesterol is esterified, the cholesterol is being hydrolyzed forming free fatty acids and monoacylglycerols by pancreatic cholesterol ester hydrolase that is being produced by the exocrine pancreas. Free fatty acids and fat-soluble vitamins are then solubilized into micelles and absorbed by enterocytes.

Once in the enterocytes, the free fatty acids underwent re-esterification into cholesterol ester by CoA: cholesterol acyltransferase (ACAT) and assembled with other lipids and apolipoprotein forming chylomicron (CM). CM will be released into the lymphatic system and further into the blood circulation via thoracic duct (Dawson & Rudel, 1999). In the circulation, CM are further hydrolysed forming chylomicron remnants by the help of lipoprotein lipase at the endothelial surface of vessels (Patsch, 1998).

These chylomicron remnants are being discarded from the circulation by chylomicron remnant receptor on the liver which is known as LDL-like receptor protein (Mahley, 1996). If the CM remnants are small enough, it can pass through the endothelial surface of the arterial wall and contribute to atherogenesis by forming plaque formation (Kirchmair *et al.*, 1995).

### 2.3.2 Endogenous pathway

Liver is the primary organ responsible for the synthesis of lipid, which regulates plasma levels and lipid homeostasis and this is the origin of the endogenous lipid at which some of the TG and cholesterol are being synthesized at the liver. Lipid endogenous pathway involves the transportation of lipids from liver to peripheral tissues. The liver synthesizes VLDL which consists of cholesterol and TG and requires apoliprotein B-100 (Gotto *et al.*, 1986). Apoliprotein B-100 contains domains that is responsible for cellular uptake of cholesterol by the LDLR-mediated pathway (Johs *et al*., 2006).

In plasma, VLDL are hydrolyzed into free fatty acid and glycerol by lipoprotein and cofactor, apolipoprotein C-2 (Fielding, 1978; Packard *et al*., 2000). This resulting in the production of VLDL remnants and IDL. IDL undergo alteration with a detachment of the remaining TG and its substitution by cholesterol esters and removal of all the apolipoprotein accept Apo-B. TG in IDL will undergo further hydrogenation forming LDL by hepatic lipase. The removal of LDL is basically by the interaction of apolipoprotein B-100 with LDL receptor. Oxidation of LDL can further transport LDL to macrophage via scavenger receptors, CD36 and SR-A which appear on the surface of macrophage (Kwiterovich, 2000).

### 2.3.3 Reverse Cholesterol Transport

Reverse cholesterol transport (RCT) by which extrahepatic (peripheral) cholesterol is returned to the liver for excretion in the bile and ultimately the feces (Glomset, 1968). RCT involves several steps which are 1) Transportation of cholesterol from peripheral cells to HDL or also known as cholesterol efflux 2) esterification of cholesterol within HDL by enzyme lecithin: cholesterol acyltransferase (LCAT) 3) cholesterol transfer to the apo-B containing lipoproteins 4) remodeling of HDL 5) HDL cholesterol uptake by the liver, kidney and small intestine via lipoprotein receptors.

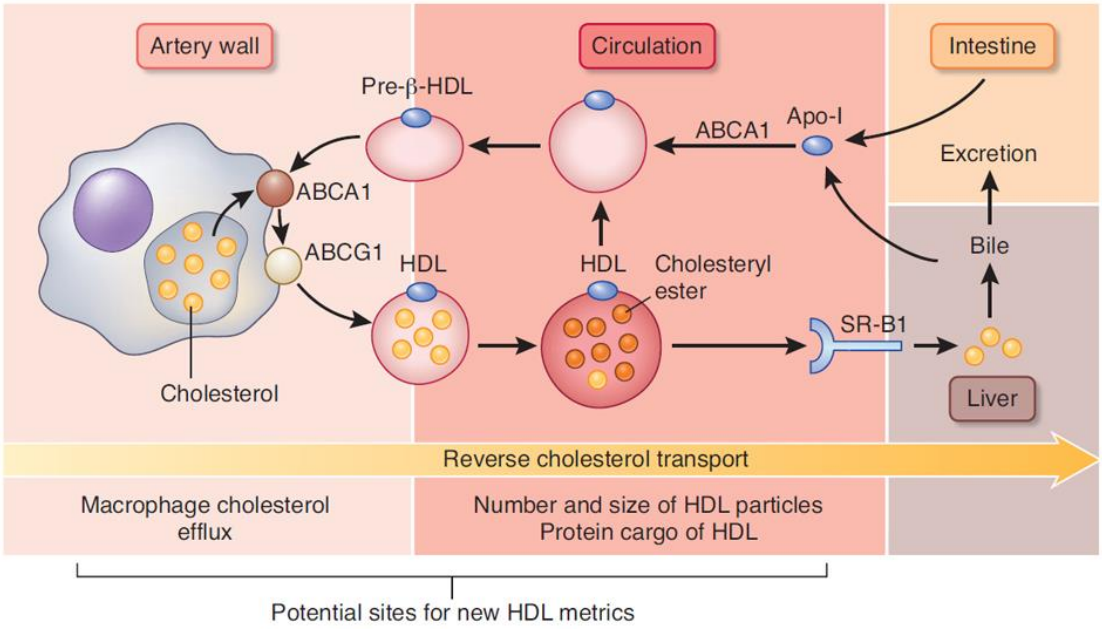


**Figure 17 Overview of reverse cholesterol transport (RCT). The cardioprotective effect of HDL is attributed to its ability to remove excess cholesterol from artery wall macrophages. Two pathways which are being activated when macrophages acquire too much cholesterol involving the membrane ATP cassette reporters; ABCA1 and ABCG1. In the help of lessthin-cholesterol acyltransferase (LCAT) free cholesterol in nascent HDL is converted to cholesteryl ester which will generate a mature HDL particle. HDL will enter the circulation, and it transports back to the liver for excretion in the bile. One membrane protein on hepatocytes, SR-B1 will help to remove the cholesteryl ester from HDL. This will be converted back to cholesterol and bile acid and later will be excreted into the bile for excretion.**(Heinecke, 2011)

#### 2.3.3.1 Step 1: Transportation of cholesterol from peripheral cells to HDL (cholesterol efflux)

Cholesterol that is derived from diets or other by-products synthesis in the liver or intestines is secreted by hepatocytes in the form of apoB-containing lipoprotein in a forward pathway to supply cholesterol to peripheral tissues (Cuchel & Rader, 2006). These lipoproteins are taken up by macrophages forming foam cell (Li & Glass, 2002).

Cholesterol elimination from macrophages involves key regulator, ABC transporter A1 (ABCA1) which helps to efflux forming free cholesterol (Oram & Vaughan, 2006). The binding of lipid pool apolipoprotein A-1 (ApoA-1) to ABCA1 transporter generate multistep process by which phospholipid and cholesterol are transferred to apoA-1 forming discoidal HDL (Hassan *et al*., 2007; Vedhachalam *et al*., 2007).

The second ABCA transporter named as SR-B1 mediates selective uptake of HDL cholesterol by the liver. It collaborates with ABCA-1 by adding cellular lipids to the initial HDL particle forming mature HDL (Barter, 2003).

#### 2.3.3.2 Step 2: Esterification of cholesterol within HDL by enzyme lecithin: cholesterol acyltransferase (LCAT).

Within HDL, LCAT (lecithin – cholesterol acyltransferase) catalyzes the esterification of free cholesterol and phospholipid in HDL ( $\alpha$ -activity) or TG-rich lipoproteins ( $\beta$ -activity) forming cholesterol ester and lysolecithin (Subbaiah *et al.*, 1994). LCAT plays an important role in the maturation of HDL-C from its nascent particles (Zannis *et al.*, 2006).

The function of esterification of cholesterol in HDL is to allows accumulation of free cholesterol and to block reentry of cholesterol into peripheral cells (Yokoyama, 2000).

#### 2.3.3.3 Step 3: Cholesterol transfer to apoB containing lipoprotein

In RCT pathway, CETP balances the redistribution and equilibration of lipoprotein within the plasma compartment. It mediates the transfer of HDL to VLDL and LDL (ApoB containing lipoproteins) in the exchange for TG. CETP is a hydrophobic glycoprotein that consists of 476 amino acids (Tall, 1993).

#### 2.3.3.4 Step 4: Remodeling of HDL

After the transfer mediated by CETP, hepatic lipase, and endothelial lipase reacts to complete the transfer of the remaining CE and TG in the HDL. Hepatic lipase is synthesized by hepatocytes that are secreted and bound to the extracellular matrix of endothelial cells of the liver (Rea *et al.*, 1993).

Hepatic lipase catalyzes the hydrolyzation of TG and phospholipids in VLDL remnants, LDL, and larger $HDL_2$, promoting the remodeling of HDL into its smaller and denser $HDL_3$ particles (Connelly, 1999; Rye *et al.*, 1999).

Hepatic lipase also promotes the attachment of ApoA-1 from HDL particles which will then goes into periphery (Barrans *et al*., 1994; Clay *et al.*, 1992). Hepatic lipase also acts by releasing CE from HDL, which then will lead to the uptake by the liver.

#### 2.3.3.5 Step 5: HDL cholesterol uptake by the liver.

After transportation to the plasma compartment, next step of RCT is mediated by SR-B1 where it transfers cholesterol from macrophages to the liver, SR-B1 is a member of scavenger receptor superfamily of proteins mediates the selective uptake of HDL-C towards the liver (Varban *et al*., 1998).

The last steps of RCT are to eliminate cholesterol from the body. CE is being hydrolysed by neutral CE hydrolase to generate free cholesterol and will further secrete into the bile by the help of ABCBII or bile salt export pump. The function of ABCG5 and ABCG8 also take into accounts as both of these are obligate heterodimers which mediate plant sterols and cholesterol into bile (Yamanashi *et al.*, 2011). These bile products are then being eliminated from the body through intestines.

## 2.4 Role of HDL in atherosclerosis

### 2.4.1 HDL and its anti-atherogenic properties

HDL is the smallest in term of surface area (Stoke's diameter = 5 to 17nm) hence provide the high density (more than 1.063g/mL) among the plasma lipoproteins which consists of several subpopulations which vary in sizes, charges, shape, density and composition of lipids. Apolipoprotein A-1 (Apo A-1) are the predominant HDL proteins, and it has the $\alpha$-electrophoretic mobility when it migrates in agarose gels and this fraction is being labeled as $\alpha$-LpA-I. HDL can also be fractionate by density into $HDL_2$ and $HDL_3$.

The knowledge of anti – atheroprotective of HDL has been established since it is a straightforward process of over-supply of cholesterol to vascular cells and several other mechanisms that are being involved which will be discussed in depth in this chapter.

There several studies indicates that HDL levels are inversely correlated with premature CVD (Barter *et al*., 2007; Gordon *et al*., 1989). HDL does possess anti-atherogenic properties, which have the ability to remove cholesterol from cells which is being described earlier in RCT pathway. The correlation of HDL as anti-atherogenic properties including:

1) Anti-inflammatory activity and antioxidant activity
2) Antithrombotic activity

### 2.4.1.1 Anti-inflammatory and antioxidant action of HDL

Atherosclerosis is an inflammatory disorder that caused by an accumulation of macrophage and T-lymphocytes in the intima. The early stage of the inflammatory response is the adhesion of the monocytes to the endothelium mediated by vascular cell adhesion molecule - 1 (VCAM-1), intercellular adhesion molecule-1 (ICAM-1) and E-selectin (adhesion molecules) (Cullen & Lorkowski, 2005). The monocytes are then being recruited to the subendothelial space by chemokine which is monocyte chemoattractant protein-1 (MCP-1).

Based on some in-vitro studies, HDL inhibits the expression of these molecules (VCAM-1, ICAM-1, E-selectin) by inhibiting endothelial sphingosine kinase; an enzyme that is responsible in the NF-κb pathway and later will activates the expression of the adhesion molecule (Xia *et al.,* 1999). The inhibition of sphingosine kinase has further effect by inhibiting the nuclear translocation of NF- κb (Xia *et al*., 1999).

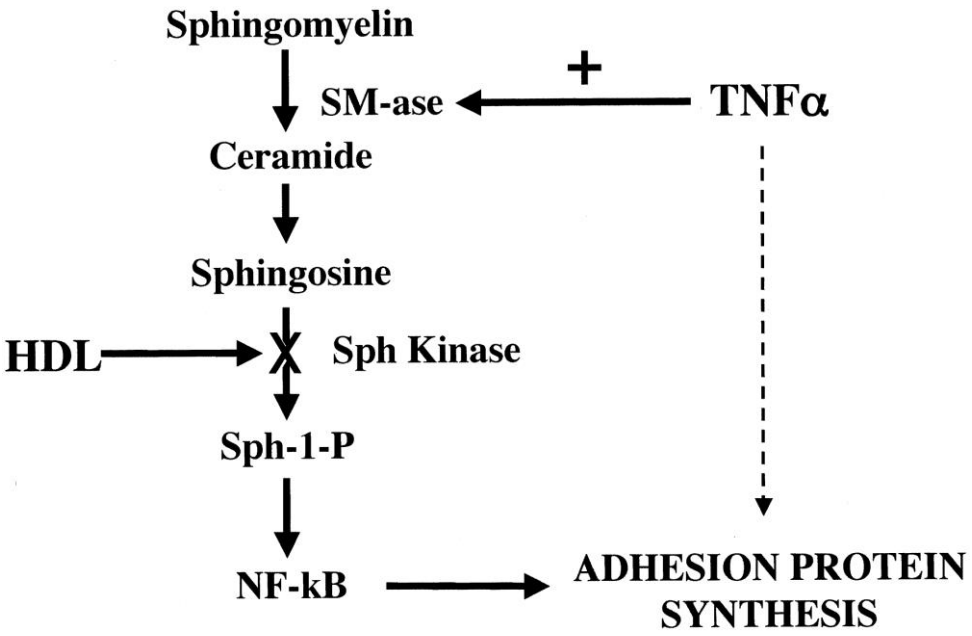


**Figure 18 HDL inhibites the cytokines-induced expression of endothelial cell adhesion molecules by inhibiting sphingosine kinase and hinder formation of adhesion protein synthesis** (Xia *et al.*, 1999)

Due to the inhibition of sphingosine kinase, the reduction of activation of NF-κb may cause a reduction in oxidative stress level as well. This is because NF- κb is being activated by reactive oxygen species and being in an inactive state by low levels of NO (Robbesyn *et al*., 2003). The ability of HDL as an inhibitor of reactive oxygen species causes the synthesis of NO and inhibit the activation of NF- κb may further contribute to the inhibition of the adhesion molecule expression. This mechanism explains the role of HDL as an anti-inflammatory.

HDL also plays their role as anti-atherosclerotic activity by reducing LDL oxidation (Barter *et al*., 2004). Oxidized LDL is known to be the potent inducer for MCP-1 expression during the progression of atherosclerosis plaque. Apo-A1 (apolipoprotein of HDL) has the ability remove lipid hyper oxides from LDL, and the byproducts are then being eliminated by the liver (Barter *et al*., 2004). HDL also contain an enzyme; named as paraoxonase which protects against oxidation of LDL in the artery wall (Mackness *et al.*, 2004).

A study comparing HDL with and without paraoxonase that was being incubated with endothelial cell line together with LDL-C. The results showed that HDL with paraoxonase significantly protect LDL-C from oxidation and the expression of MCP-1 is inhibited (Mackness *et al.*, 2004).

#### 2.4.1.3 Endothelial protection and antithrombotic activity

Endothelium dysfunction or injury towards the endothelium caused by hypertension, diabetes, hypercholesterolemia and smoking is an early step for the development of atherosclerotic lesion. Studies have shown that low HDL-C is associated with endothelial dysfunction (Chan *et al.*, 2001), and high level of HDL-C are associated with improved endothelial dysfunction (Kuvin *et al*., 2002).

The formation of endothelial dysfunction is characterized by decreased bioavailability of NO (nitric oxide) that is essential signaling molecules that induce relaxation in smooth muscle cells (SMC) (Yuhanna *et al*., 2001). Several in-vivo studies have supported this theory of effects of HDL on endothelial function comparing with hypercholaemia patient and non hypercholesterolemia suggesting that patient with hypercholesterolemia appear to have reduce NO bioavailability and when they are subjected for infusion of cholesterol free reconstituted HDL, restoration of endothelial function has been observed (Spieker *et al*., 2002).

The vasodilatory effects of HDL in endothelial cells are mediated by ABCG-1 and also includes 7-oxysterols and cholesterol efflux of cholesterol which improves the development of actives eNOS (endothelial nitric oxide synthase) dimers and results in reduced ROS production (Terasaka *et al.*, 2008). Decreased in cellular production of superoxide also results in inactivation of NO. This eventually makes the bioavailability of NO increased and vasodilation is improved in the presence of HDL. Due to this HDL is proven to reduce the NADPH oxidase activity and expression of its major subunits in endothelial cells (Van *et al*., 2009).

HDL also appears to have antithrombotic activity as the increase production of NO and $PGI_2$ (prostacyclin) which both plays an essential role in inhibiting platelet aggregation (Hassall *et al.*, 1983; Whittle *et al.*, 1980). $PGI_2$ is also produced by endothelium which acts synergically with NO to induce SMC relaxation (Sickle *et al.*, 1986).

Besides NO and $PGI_2$, reduction in PAF production by endothelial cells also contributes to the anti-thrombotic effects of HDL (Sugatani *et al*, 1996). Decrease in PAF production are caused by transportation of PAF acylhydrolase and other enzymes such as LCAT and paraoxonase that would degrade PAF (Forte *et al*., 2002; Satoh *et al.*, 1991).

Another point that would contribute to the antithrombotic activity of HDL is the level of HDL-C are inversely correlated with plasma concentration of VM Willebrand factor; a protein that is important in platelet adhesion and aggregation (Calabresi *et al.*., 2003).

## 2.5 Characteristics of CETP

### 2.5.1 CETP gene and its regulation

The gene for human CETP consists of 25kb of genomic DNA and includes 16 exons (Agellon *et al*., 1990). This gene appear as a single copy of chromosome 16q12-16q21 (Lusis *et al*., 1987). Some of the animal model such as hamster and rabbit shared almost 80 to 96% of amino acid sequence and overall sequence homology that similar to human CETP sequence homology (Drayna *et al*., 1987; Jiang *et al*., 1991; Nagashima *et al*., 1988). That is why rabbit and hamster are commonly being used in CETP research as the subject of in-vivo study.

Genetic variation of CETP also being observed in individual as a major determinant to identify individual that is prone to hyperlipidemia and coronary heart disease (CHD) (de-Grooth *et al*., 2004). Some studies have recorded the effects of CETP polymorphisms on lipid profiles and CETP activity. Based on Ordovas *et al*. (2000), Taq 1B polymorphism at the CETP gene locus correlates to the changes in lipoprotein size, CETP activity, and HDL-C level.

Based on Tall (1993), regulation of CETP gene expression are based on these factors; hormonal, inflammatory and nutritional stimuli. Several sites of the CETP mRNA expressions are liver, kidney, small intestines, spleen, adrenal and adipose tissue (Masucci-Magoulas *et al*., 1995). The presence of CETP gene in adipose tissue shown that it contributes to the CETP activity which causes further reduction of HDL level and an increase in non-HDL-c levels (Zhou *et al*., 2006).

In response to high cholesterol diet, it causing up-regulation of CETP mRNA levels and increase in CETP plasma activity (Jiang *et al*., 1991). Regulation of CETP promoter activity involves SREBP and LXRS where SREBP1a and SREBP-2 stimulate CETP promoter through the interaction of CRE (cholesterol response element), while LXRα/RXRα and LXRβ/RXRβ will activate CETP promoter using DR4 element in a sterol-responsive fashion (Gauthier *et al.*, 1999).

### 2.5.2 Molecular structure of CETP protein

The human CETP contain 476 amino acid residue hydrophobic glycoprotein and its translated mass are about ~ 53kDa, but the mass estimated by SDS-PAGE is 75 kDa (Drayna *et al*., 1987). The cause of the discrepancy between translated molecular mass and SDS-PAGE is due to the N-glycosylation sites at residues 88, 240, 341 and 396 (Tall, 1993).

The crystal structure of CETP was solved in 2007 by using X-Ray crystallography (Qiu *et al*., 2007) PDB id: 20BD. Based on this model, the shape of CETP protein has been described as a boomerang with dimension 135Å X 30Å X 35Å. The overall structure is divided by 4 units:

1) Two terminal at each end of the protein (N- and C- terminal)
2) A central β-sheet that acts as a linker that connects the two terminal and includes six antiparallel strands consist of residues before and after terminal
3) Each terminal contains a highly twisted β-sheet and two helices. Helices are denoted as A and B at N-terminal and A' and B' at C-terminal.
4) Distorted amphipathic helix which is called as helix X that is formed by amino acid GLU465 – SER476 at the C-terminal domain.

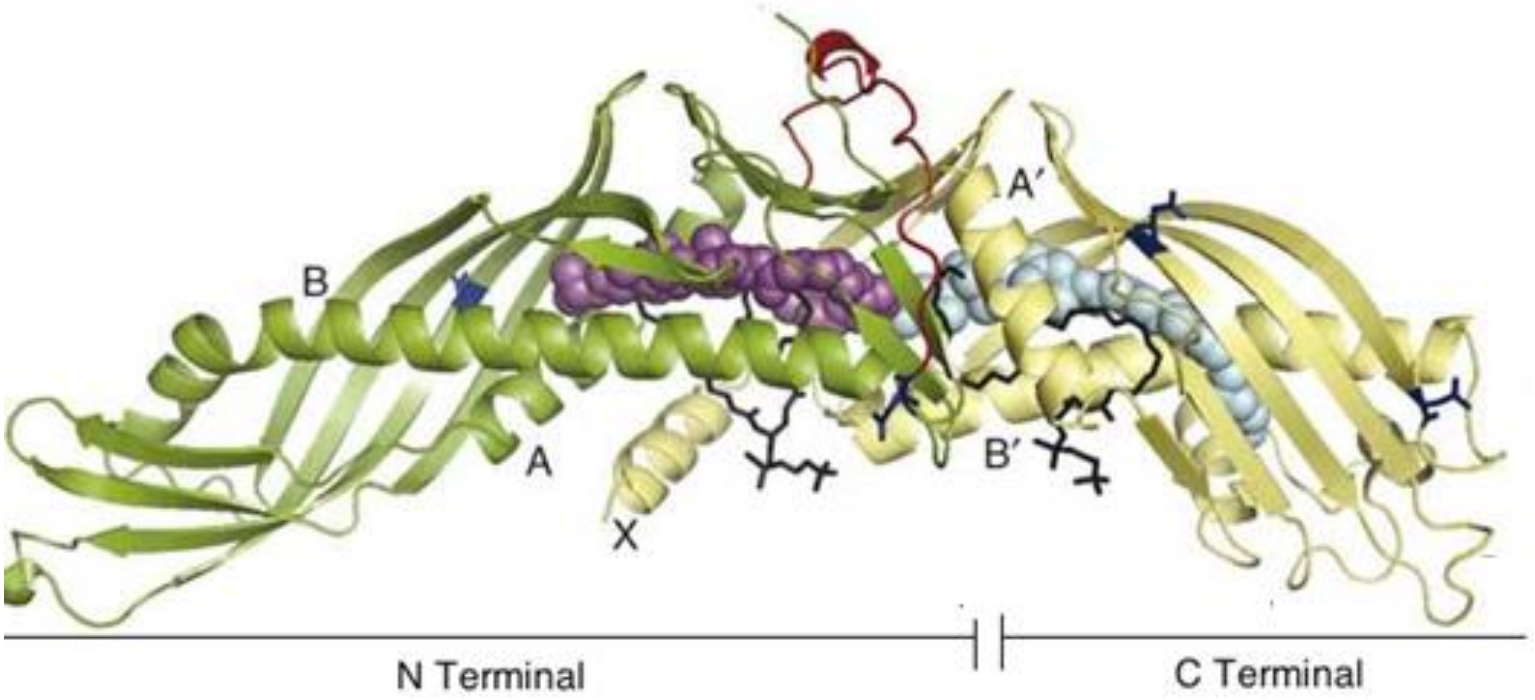


**Figure 19 Crystal structure of CETP using ribbon diagram. Two domains in the structure which are N-terminal (green) and C-terminal (yellow) with linker that is shown in red colour. CE1(magenta) and CE2(cyan) are shown in the middle space of the structure and phospholipids are being labeled as black bonds. Helices A, B, A' ,B' and X are labeled. Helix X belongs to the C-terminal domain but interacts with residues of the N-terminal domain.** (Qiu *et al.*, 2007)

Based on this CETP structure models, revealed that, there are four bound lipid molecules which is being incorporated during protein production. CETP has the 60 Å length of tunnel that contains CE and phospholipid at each of the terminal.

The concave surface of CETP which is consists of N and C terminal openings, helix X and Ω1 flap is the most probable site for lipoprotein binding (Qiu *et al*., 2007). It is hypothesized concept that lipoproteins are likely to be binding at concaved structure compare to other CETP surfaces which are highly glycosylated and do not have proper curvatures to properly binds spherical lipoprotein and does not provide proper access to the tunnel opening.

A biochemical study was done by Bruce *et al*. (1995) demonstrated that CETP has a higher binding affinity towards 10nm diameter nascent discoidal HDL, and this diameter does correspond to the diameter of the concave surface of CETP. The author (Qiu *et al*., 2007), hypothesizes that prior binding of HDL towards CETP surfaces may cause the insertion of Helix X into the bound lipoprotein where this concept is consistent with the role of helix X that facilitates the access of neutral lipid from lipoprotein to CETP tunnel.

### 2.5.3 Function of CETP

CETP is known as the protein that is responsible for the transfer of water insoluble lipids such as CE, TG, and phospholipids to VLDL and LDL (Qiu *et al*., 2007). Two different mechanisms of lipid transfers have been proposed (Morton & Greene, 2003).

The first mechanism which is called as ‘shuttle’ or ‘ping-pong’ mechanism has been consistent with the X-ray crystallography structure that has been resolved by Qiu *et al.* (2007), which shows that overall boomerang shape with a concave surface can bind only one lipoprotein at one time. This structure supports the hypothesis saying that CETP acts as a carrier mechanism. Neutral lipids are accepted by CETP from donor particle to the hydrophobic tunnels. This will then be transported to the aqueous phase and finally being delivered to the lipoprotein acceptor (Tall, 1993).

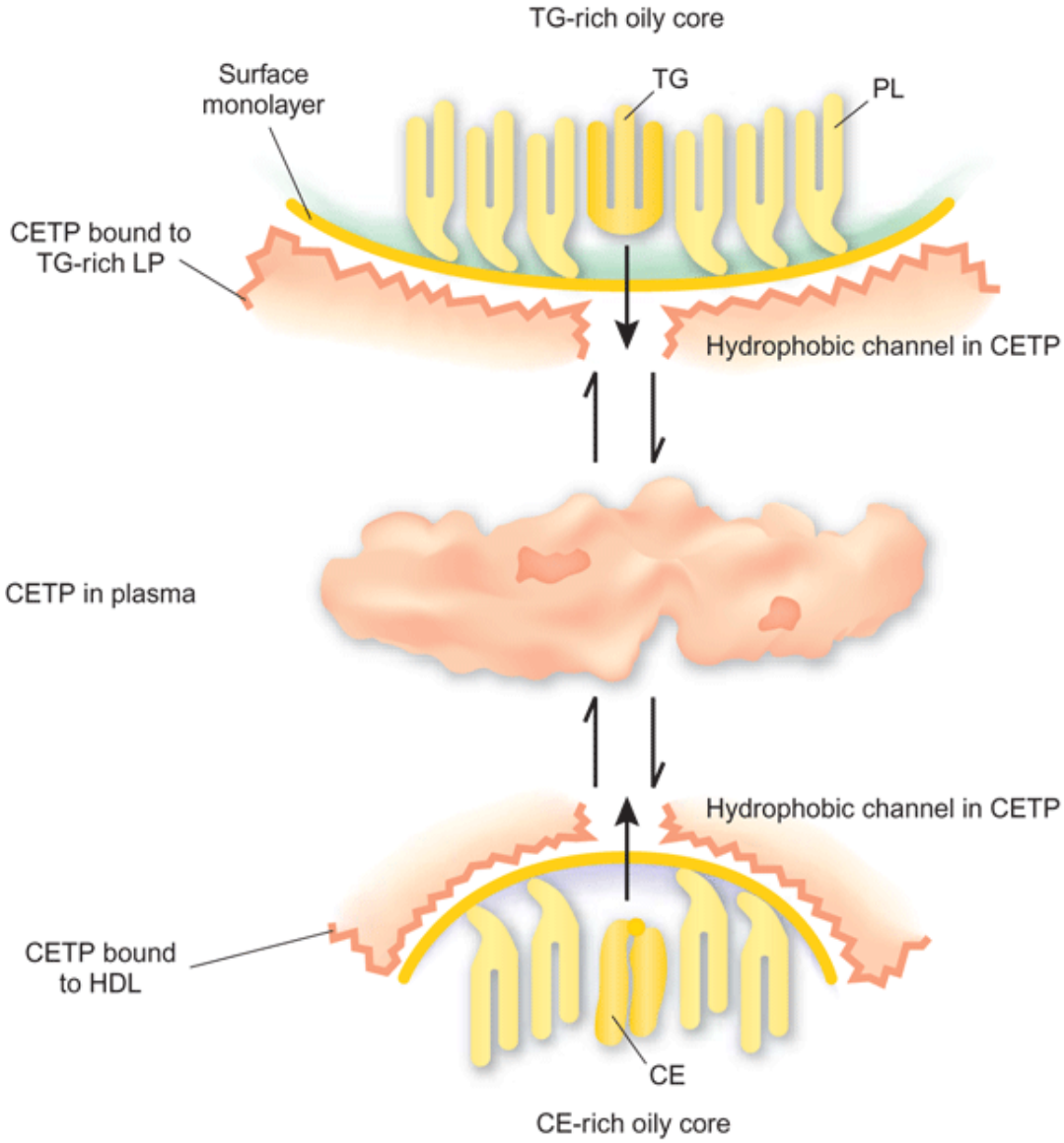


**Figure 20 Basic schematic diagram of CETP function. Middle, CETP in plasma is being describes by its concave surfaces. Top, CETP binds to Triglyceride-rich lipoprotein and will cause triglycerides to be extracted into CETP hydrophobic tunnel and phospholipid will be introduced to protein surfaces. Bottom, CETP binds to HDL and extracting cholesteryl ester from lipoprotein monolayer into the hydrophobic tunnel and introduced phospholipid to protein surfaces. This model showed that CETP can accommodate different sized of spherical lipoprotein and its concave structure by changing its own curvature.**(Hamilton & Deckelbaum, 2007)

This carrier mechanism can occur via homoexchange or heteroexchange (Ko *et al.*, 1994; Morton & Zilversmit, 1983; Serdyuk & Morton, 1999). Homoexchange occurs when there is a bidirectional transfer of the same kind of neutral lipids that is bound, being loaded into the tunnel which results in no net exchange of lipoprotein lipid content (Qiu *et al*., 2007).

Heteroexchange mechanisms is part of RCT mechanism and because of this CETP does plays a crucial role in lipoprotein mechanism (Asztalos *et al.*, 2004). The proposed mechanism of CETP-mediated heteroexchange are as follows:

Step 1: CETP that contains CE will bind into VLDL and releases bound phospholipid (phosphatidylcoline). One or two TG enters the tunnel, and equal amount of CE is transferred into VLDL to create balance.

Step 2: TG bound CETP is then disattached or dissociates from VLDL. This leaves the VLDL particles with a higher CE content.

Step 3: The bound CETP binds to HDL and releases the phosphatidylcholine. One or two TG will enters the tunnel and to create balance, TG is transferred into HDL.

Step 4: The CE-filled CETP dissociates from HDL and this completes the heteroexchange which results in lower CE content in HDL.

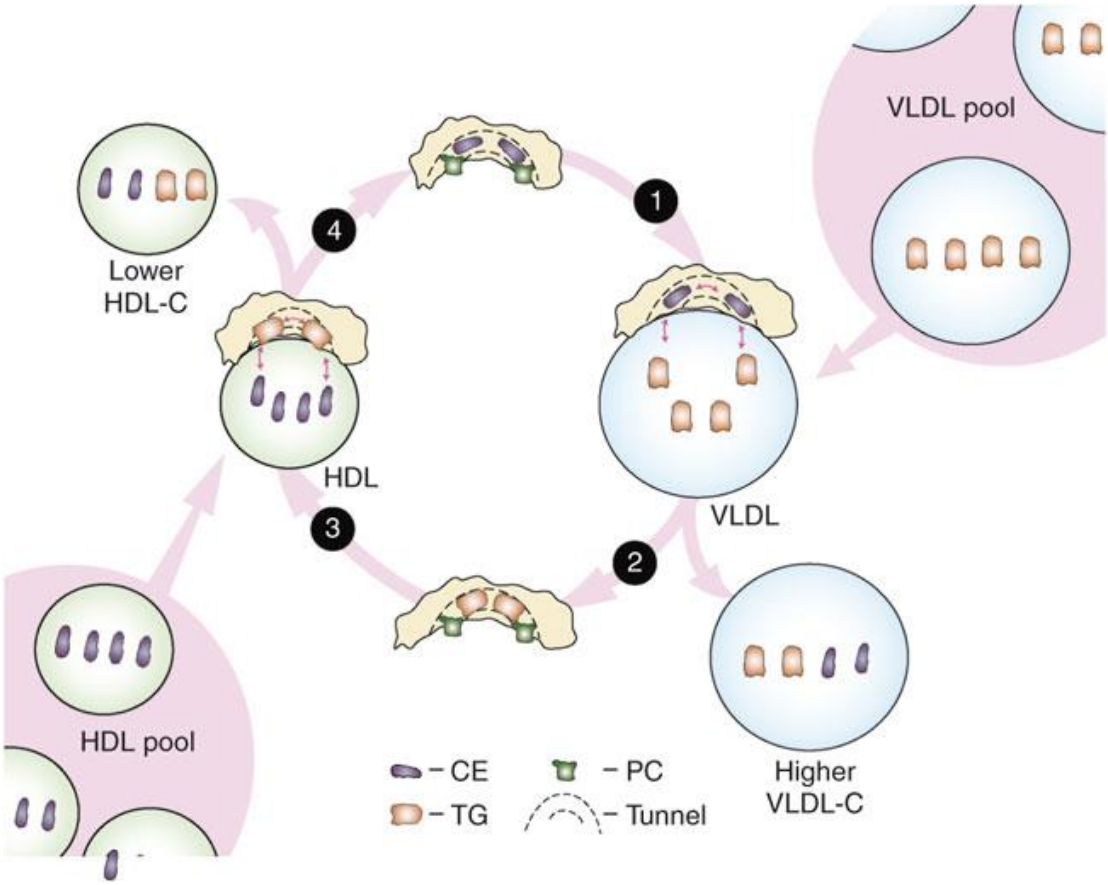


**Figure 21 Proposed mechanism of CETP-mediated heteroexchange. 1) CETP filled with CE binds to VLDL and releases bound phospholipid which also known as phosphatidylcholine, PC. One or two TG enters the hydrophobic tunnel and equal amount of CE is located into VLDL. 2) The TG-bound CETP disengaged from VLDL carrying two phospholipids from the surface, leaving VLDL with higher CE content. 3)The TG bound CETP employs HDL and disengaged the bound phospholipids One or two new CEs enter the tunnel and an equal amount of TG is deposited into HDL.4) The CE filled CETP dissociates from HDL carrying two phospholipids from the surface and accomplish full cycle of heteroexchange which results in lower CE content in HDL.** (Qiu *et al*., 2007)

The depletion of CE in HDL is particularly influenced by TG level (Davidson & Rosenson, 2009). Due to this heteroexchange , RCT routes are mainly through VLDL and LDL and will further taken up to the liver via SR-B1. However, in abnormal at which CETP activity are increased due to the increased of CETP gene expression in peripheral and increase the concentration of lipoprotein acceptor (Tall, 1993). This may cause an increase in the transfer rate of CE to LDL and VLDL, which may cause accumulation in the intima.

In the deficiency of CETP, all the neutral lipid transfer are absent. This means that, in HDL particle the TGs level are reduced, and CE content is increased. Due to the deficiency of CETP and continued activity of LCAT, the size of HDL particles gradually increases and acquire lipoprotein E. This condition provides high-affinity ligand for LDL receptor of the liver, thus removing the increase HDL particles and cholesterol from the tissues (Tall, 1993). Deficient or absent of CETP cause HDL build up and this eventually reduced the amount of cholesterol transfer to LDL and VLDL (Clark *et al*., 2006). The theory of CETP deficiency correlates with reduced risk of atherosclerosis. This cause great interest in CETP inhibition as the alternatives to increase HDL-c levels.

### 2.5.4 The development of CETP inhibitors and its current update

The pathway to inhibit CETP has emerged as an attractive target to elevate HDL-C level as a strategy to reduce the risk of cardiovascular event. In the classic way of understanding the drug inhibition, the analogy that usually being used is that a lock and a key. Drugs act as a competitive inhibitor at which it binds to the active sites, thus blocking the binding of the ligand.

However, in the case of CETP inhibition mechanism, it has been demonstrated that the inhibitors promote CETP-HDL complex formation, which indicates the current inhibitor prevent detachment of CETP-HDL complex and they do not compete with CE and TG in the CETP binding (Masson, 2009). As of these various inhibitory mechanism, further elucidation needs to be done. Understanding the molecular structure and function of CETP together with the inhibitors mechanism of action are important to develop a safe treatment to raise HDL-C treatment.

#### 2.5.4.1 Failed CETP inhibitors: torcetrapib and dalcetrapib

Torcetrapib or also known previously as CP-529414 is a noncompetitive inhibitor and its bind reversible to CETP to form an inactive CETP-HDL complex (Clark *et al.*, 2006; Ranalletta *et al*., 2010). Torcetrapib has nearly entering phase 3 clinical trials but during the phase 2 studies, torcetrapib has cause elevated blood pressure among the tested patient. The failure of torcetrapib is due to is failure to achieve clinical benefit plus the administration of torcetrapib also causing harm. Due to this, in December 2006, torcetrapib phase 3 ILLUMINATE clinical trial was terminated. This termination is because of the significantly

increase the risk of primary combined endpoint of death from coronary heart disease, stroke, myocardial infarction or hospitalization of instable angina (Barter, 2009) that associated with torcetrapib administration although there are significantly increase in HDL and reduce in LDL.

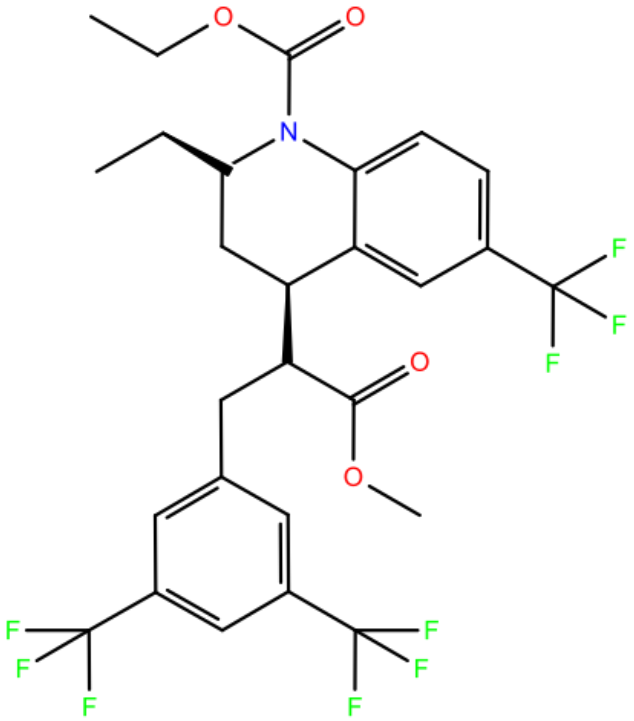


**Figure 22 Chemical structure of Torcetrapib**

The off target outcomes from the administration of torcetrapib are increase in the aldosterone production (Barter *et al.*, 2007) and increase in high blood pressure.

Several in-vitro studies confirmed the upregulation of CYP11B2 (aldosterone synthase) with torcetrapib administration (Forrest *et al*., 2008; Funder, 2010; Hu *et al*., 2009). Theoretically, an excess level of aldosterone promotes sodium retention at the distal renal tubule which results in water retention and an increase in blood pressure (Funder, 2010). Patients that are being diagnosed as hyperaldosteronism shows an increase risk of associated cardiovascular

events such as myocardial infarction, stroke, heart failure, left ventricular hypertrophy and atrial fibrillation (Connell *et al.*, 2008; Milliez *et al.*, 2005).

Dalcetrapib or also known as RO4607381 / JTT-705 is one of the CETP inhibitors that undergoes clinical trial phase III. Dalcetrapib is a less potent inhibitor with its IC50 >1000nm (Ranalletta *et al.*, 2010). Dalcetrapib phase III trial was terminated since it failed to show meaningful or significant clinical outcome although there are no off-target being observed although HDL-C were elevated by 30% (Schwartz *et al.*, 2009).

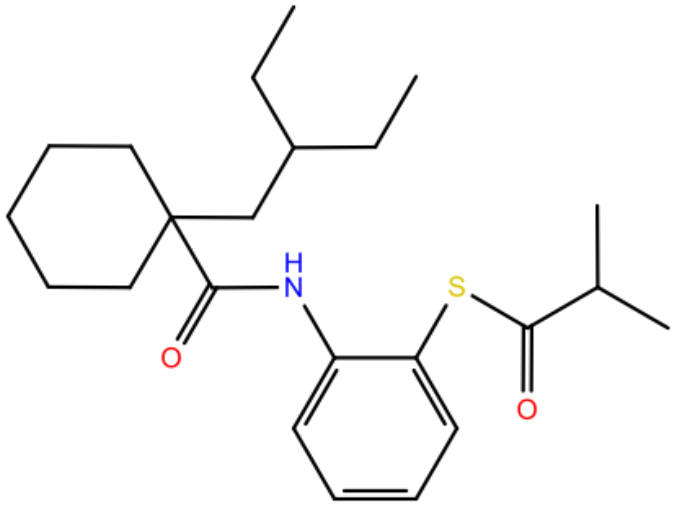


**Figure 23 Chemical structure of Dalcetrapib**

### 2.5.4.2 Ongoing Phase 3 clinical trial of CETP inhibitors: Anacetrapib and evacetrapib

Anacetrapib or MK-0859 has the almost similar IC50 with torcetrapib (IC50:21nM) which also results in the increase of HDL and reduce the atherogenic lipoprotein (Bloomfield *et al.*, 2009). The highly potent CETP inhibitor is evacetrapib (LY2482585) with $IC_{50}$ 5nM has just entered phase 3 clinical trial (Cao *et al.*, 2011).

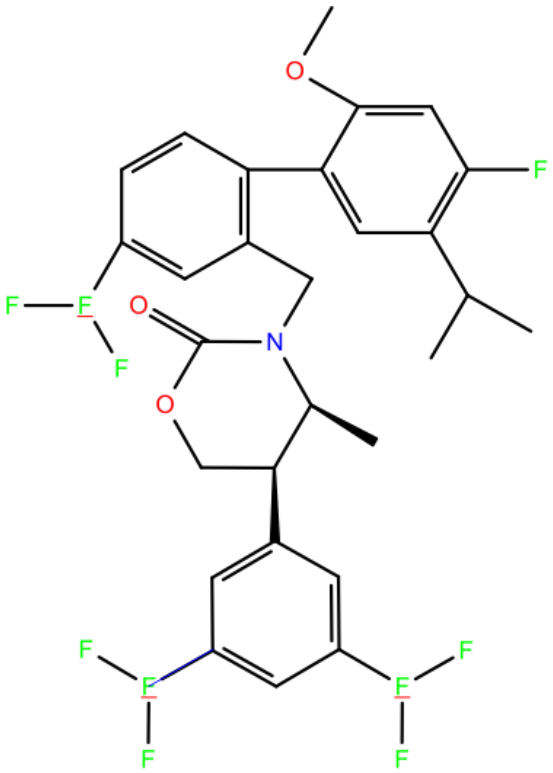


**Figure 24 Chemical structure of anacetrapib**

Unlike torcetrapib, anacetrapib and evacetrapib did not exacerbate any off target outcomes. Both of these inhibitors exhibited a neutral level of blood pressure, neutral level of aldosterone synthesis and it does increase HDL-C. Due to the failures of torcetrapib and dalcetrapib, both anacetrapib and evacetrapib are still under investigation to evaluate any possible side effects. The ongoing REVEAL (Randomized Evaluation of the effects of anacetrapib through lipid modification) trial of anacetrapib is studying the possible outcomes

where 30 000 patients with atherothrombotic cardiovascular disease will be randomized to anacetrapib or placebo administration and will be followed for 4 to 5 years. This study will evaluate the outcomes such as coronary death, myocardial infarction or coronary revascularization (University of Oxford, 2012).

Evacetrapib also just recently entering phase 3 clinical trial in the ACCELERATE (A study of Evacetrapib in High Risk Vascular Disease) where approximately 11000 patients were appointed in a randomized placebo-controlled study of evacetrapib. This study is estimated to complete in 2015 where several possible outcomes are being evaluated such as cardiovascular death, stroke, myocardial infarction, coronary revascularization or hospitalization for unstable angina (Eli Lilly and Company, 2012).

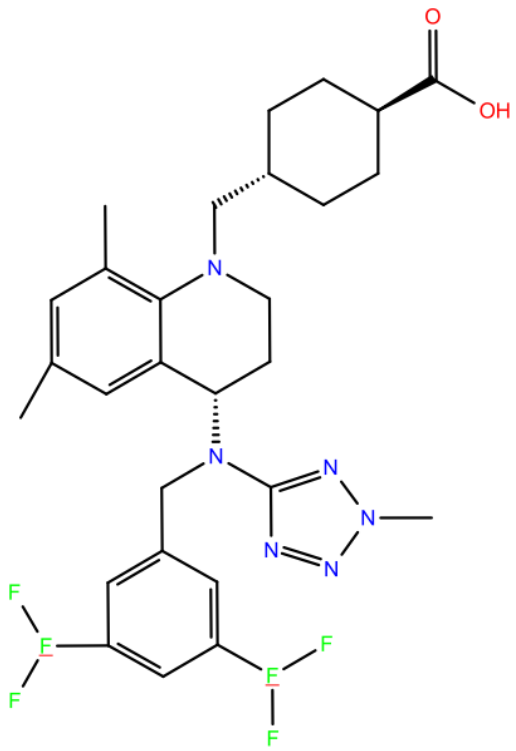


**Figure 25 Chemical structure of evacetrapib**

## 2.6 Selection of *Garcinia atroviridis*

*Garcinia atroviridis Griff ex T anders* of the Guttiferae family are also known as ‘ asam gelugor’ or ‘asam keping’ among Malaysian. It is a medium-sized fruit tree that grows wild throughout Peninsula Malaysia and are also being cultivated commercially in northern of Malaysia due to it’s economic and medicinal value (Burkill *et al.*, 1966).

*Garcinia atroviridis* is a tree that can grow up to 20m and it has orange-yellow depressed globosed fruit with 7 to 10cm diameter. The fruit is usually being sun dried for consumption which is later being called as ‘asam keping’ and are usually being used for seasoning purposes such as dressing fish, curries and sour relish *(Mackeen et al*., 2002).

The young leaves are usually being used as “ulam” which is later being cooked or consumed raw as a salad (Mackeen *et al*., 2000). Some of the Malay recipe uses *Garcinia atroviridis* in steam fish in order to delay early spoilage. *Garcinia atroviridis* also being used as postpartum medication agent, treating ear and throat infection, cough, dandruff and some stomach-ached during pregnancy (Amran *et al.*, 2009). Some of the *post-partum* medication that is being used is making juice from the leaves for women during confinement and lotion that is made from the fruit and vinegar, and this lotion will be applied upon abdomen of women during confinement (Amran *et al.*, 2009).

Several phytochemical studies have successfully isolate some of the compounds from *Garcinia atroviridis* such as garcinia acid and its lactone from fruit rinds, flavonoids, 4-methylhydroatrovirinone, atrovirinone, atrovirisidone in roots and atroviridine from stem

bark (Kosin *et al.*, 1998; Mackeen *et al.*, 2002; Permana *et al*., 2001; Dharma *et al.*, 2005; Tan *et al*., 2013).

*Garcinia atroviridis* also demonstrates a wide range of pharmacological effects such as anti-inflammatory, antiplatelet, antioxidant, antithrombotic action and anti-allergic effects (Mackeen *et al*., 2000). Some studies also successfully reduce blood pressure in rats by using *Garcinia atroviridis* extracts (Amran *et al*., 2009).

From the beginning of human civilization, medicinal plant natural product have been used due to its therapeutic value. It undergoes design, synthesis, semi-synthesis to create potent medicinal agents. The search for biologically active constituents which is from natural product based on traditional use or folklore medicine is still relevant as these plants have the potential to produce pharmacologically active constituent to treat certain diseases.

# Chapter 3: Experimental methods

## 3.1 Sample preparation

### 3.1.1 Plant Collection

The leaves of *Garcinia parvifolia* were collected from the lowland dipterocarp, Sungai Congkak Reserve Forest in Malaysia. The forest is located at 3º 12.930'N, 101º 53.022'E with the altitude ranging from 120m – 1265m above the sea level (Ng & Mariam, 2009) . A voucher specimen (UNMC45L) was deposited at the Herbarium of The University of Nottingham, Malaysia Campus. L are denoted as leaves.

The Leaves (L), twigs (T) and fruit (F) of *Garcinia atroviridis* were obtained from Bukit Ekspo, Universiti Putra Malaysia, Serdang around November 2011 and the voucher specimen named as UNMC78L, UNMC78T and UNMC78F were deposited at The University of Nottingham Malaysia campus.

### 3.1.2 Plant extraction

The plant material for UNMC 45L, UNMC 78L, UNMC 78T and UNMC 78F were dried at the atmospheric temperature (~30 ˚C) and shaded from sunlight for 1 month.

The dried plant were pulverised into smaller parts and subjected to maceration for over 3 days by using sequential gradient extraction of different polarity of solvents starting with hexane, ethyl acetate and ethanol. Solvents were removed after 3 days of maceration by using distillation under reduced pressure at 40˚C and later the crude extracts were pooled together for every and each specific solvent and this procedure were repeated for three times. All the extracts were dried in desiccators until it is concentrated. The residues obtained were designated as aqueous extracts and stored at -20˚C until assayed.

## 3.2 CETP drug screening assay

### 3.2.1 Sample preparation

**Extracts** The extracts were prepared by dissolving in DMSO solvent in order to make stock solutions .The stock solutions were subjected to vortex and sonication when there was difficulty in dissolving. Subsequent serial dilutions were made to the required concentrations using distilled deionized water. The final concentration of DMSO was adjusted to 0.1%.

**Chemical** The analytical standard (+)- Garcinia acid was purchased from sigma Aldrich and it was further being diluted with DMSO until the final concentration of 1% DMSO.

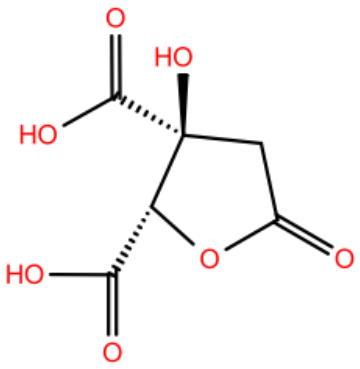


**Figure 26 Structure of Garcinia acid**

### 3.2.2 Principle of the inhibitory assay

The CETP inhibitor drug screening kit (BioVision, Mountain View, CA, USA) uses donor molecule containing a fluorescent self-quenched neutral lipid, which is transferred to an acceptor molecule in the presence of the CETP (rabbit serum). The lipid transfers of donor molecule to the acceptor molecule mediated by CETP will results in an increase of fluorescent intensity. Whereas, in the present of the inhibitor will hinder the lipid transfer and therefore will cause the decrease in fluorescent intensity.

### 3.2.3 Determination of CETP inhibitory activity

To assess the percentage inhibition of the crude extracts towards CETP, fluorescence bioassay was carried out by using the CETP Drug Screening Kit (#k602-100, BioVision, Mountain View, CA, USA). The procedures of the assay can be described briefly as follows: 50 µl of the inhibitors were added, followed by 3 µl of rabbit serum. Then the master mix which is being provided in the assay kit (10 µl of Donor Molecule, 10 µl of Acceptor Molecule and 20 µl of CETP buffer) was added, mixed well and the volume was completed to 203 µl with the provided assay buffer. The mixture was subjected to incubation for 1 hour at 37°C, and the fluorescence intensity was measured by using fluorescence plate reader (Varioscan Flash, ThermoScientific) at Excitation wavelength of 465 nm and Emission wavelength at 535 nm. The percentage inhibition of the extracts towards CETP was determined by comparing the activity of CETP in the presence and absence of the tested compound. As a background, negative control lacking of rabbit serum was being used. Positive controls were tested in order to see the degree of inhibition by 0.1% DMSO, and CETP was not being affected by DMSO. All the measurements were carried out in triplicate. The percentage inhibition of the extracts towards CETP activity was calculated as follows:

$$\text{Percentage Inhibition} = \left(1 - \left[\frac{\text{sample read} - \text{blank read}}{\text{Positive control read} - \text{Negative control read}}\right]\right) \text{x } 100$$

## 3.3 Enzyme kinetic assay

Same procedure as 3.2.3 except that the readings were collected for 60 minutes at every 1 minutes interval.

## 3.4 Phytochemical screening

Several tests were performed to confirm the presence of secondary metabolites: alkaloid, flavonoid, saponin, tannin, steroid, terpenoid and phytosterol.

Phytochemical analysis of plant extracts for active compound was carried on according to Igbinosa *et al.*, 2009; Savithramma & Rao, 2011; Tiwari *et al.*, 2011. All of the test were carried out in triplicate.

### 3.4.1 Detection of alkaloids

0.5g of the extracts were dissolved individually in 10ml of dilute Hydrochloric acid and filtered. Two tests (Wagner's Test and Dragendroff's Test) were performed in order to confirm the presence of alkaloids in the extracts.

#### 3.4.1.1 Wagner's Test

2ml of the filtrates were treated with Wagner's reagent (Iodine in Potassium Iodide). Formation of brown/ reddish precipitate indicates the presence of alkaloids.

#### 3.4.1.2 Dragendroff's Test

2ml of the filtrates were treated with Dragendroff's reagent (solution of Potassium Bismuth Iodide). Formation of red precipitate indicates the presence of alkaloids.

### 3.4.2 Detection of flavonoids

0.5g of the extracts were subjected to two types of flavonoids testing which are (Alkaline reagent test and Lead acetate test) in order to confirm the presence of flavonoids in the extracts.

#### 3.4.2.1 Alkaline Reagent Test

0.5g of the extracts were treated with few drops of 0.5M sodium hydroxide solution. Formation of intense yellow colour, which becomes colourless on addition of 1ml of dilute sulphuric acid, indicates the presence of flavonoids.

#### 3.4.2.2 Lead acetate Test

0.5g of the extracts were treated with few drops of lead acetate solution. Formation of yellow colour precipitate indicates the presence of flavonoids.

### 3.4.3 Detection of saponins

0.5g of the extracts were subjected to two types of saponin testing which are (Froth test and Foam Test) in order to confirm the presence of saponins in the extracts.

#### 3.4.3.1 Froth test

0.5g of the extracts were diluted with distilled water to 20 ml and this was shaken in a graduated cylinder for 15 minutes. Formation of 1 cm layer of foam indicates the presence of saponins.

#### 3.4.3.2 Foam test

0.5g of the extracts was shaken with 2 ml of water. If foam produced persists for 10 minutes it indicates the presence of saponins.

### 3.4.4 Detection of tannins (Gelatin Test)

0.5g of the extracts were added to 1% gelatin solution which contains sodium chloride. Formation of white precipitate indicates the presences of tannins.

### 3.4.5 Detection of steroid/ terpenoid (Salkowski's Test)

0.5g of the extracts were treated with chloroform and filtered. 2ml of the filtrates were treated with few drops of concentrated Sulphuric Acid, shaken and allowed to stand. The appearance of golden yellow colour indicates the presence of terpenoid. The presence of blue or green interface corresponds to the presence of steroid.

### 3.4.6 Detection of phytosterols (Libermann Buchard's Test)

0.5g of the extracts were treated with chloroform and filtered. The filtrates were treated with few drops of acetic anhydride, boiled for 15 minutes and cooled. 1ml of concentrated sulphuric acid was added. Formation of brown ring at the junction indicates the presence of phytosterols.

## 3.5 Statistical Analysis:

The results of three independent experiments were obtained and the values were presented as mean ± standard deviation (SD). One-way analysis of variance (ANOVA) test were applied to analyse P value. P-values less than 0.05 were considered as statistically significant. All statistical analyses were performed by using GraphPad Prism 5.0 (GraphPad Software Inc., San Diego, CA).

## 3.6 Verification of HCA content in crude extract of UNMC 78F

### 3.6.1 Verification using FTIR spectrophotometry method

The FTIR spectra from ethanol extracts were generated by 100 FTIR PelkinElmer (USA). Prior to the sample loading, the stage was cleaned and blanked. A drop of concentrated crude extract was placed on the reading spot and scanned. The absorbance peaks were produced with a resolution of 4 $m^{-1}$ (4000–500 $cm^{-1}$) and averaged 32 scans. The spectra were analyzed by baseline correction and attenuated total reflectance (ATR) to directly investigate the chemical composition of smooth surfaces and undisturbed state of various materials in the sample (Schmitt and Flemming, 1996). Each samples were triplicated and the best results selected for functional groups verification.

### 3.6.2 Verification using HPLC method

(-) Garcinia Acid ($C_6H_6O_7$) from Sigma Aldrich were taken as reference standard. The high-performance liquid chromatography system used in this study was from Agilent (1260 Infinity Series, 1260 Quad Pump) with C18 RP column 4.6 x 150 mm. The system consists of Rheodyne injector with sample loop of 20 µL, OpenLab CDS (Chem station edition) software. In the present study, attempts were made based on HPLC methodology from the existing protocol (Gogoi *et al.*, 2014).

The mobile phase used was HPLC grade (Millipore) water and the HPLC method was carried out taking a series of different (-)- HCA concentrations with final preeminent flow rate of 1.0 ml/min. Detection was done by Dual λ absorbance detector at a wavelength of 210 nm and sample eluted was 20 µL for 8 minutes at 58/8 bar Quart pump and 25 º C of column temperature. Prior to injection to the HPLC system, all the samples and the standards were filtered through membrane filters of pore size 0.45 µm. As water has been used in this study,

to maintain the efficiency and column life after completion of the experiment it is purged several times with methanol.

## 3.7 Molecular docking using GLIDE

### 3.7.1 Overview of docking methodology

The docking methodology that was being used in this project is based on GLIDE (grid-based ligand docking with energetics) that was being implemented together with Schrodinger suite. GLIDE uses a hierarchical filter to search the best position with the active site of the protein. The GLIDE algorithm is based on the systematic search of conformations, positions, orientations of a ligand in the protein active site using the funnel type approach (Friesner *et al*., 2004).

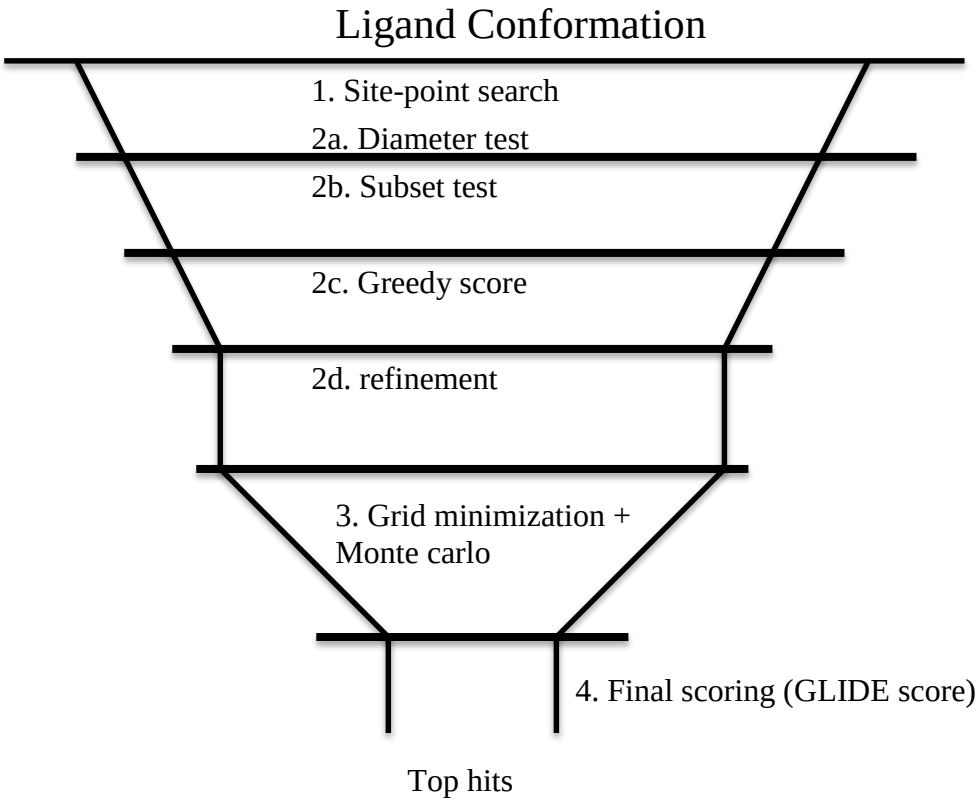


**Figure 27 GLIDE docking hierarchy using the 'funnel' theory** (Friesner *et al*., 2004)

The docking scoring were carried out using GLIDE Score function where GLIDE energy was being used to predict binding affinity.

Small numbers of best-refined poses were passed on the following stage in the hierarchical energy minimization on OPLS-AA van der waals and electrostatic grids for the protein. The best poses were chosen and subjected to Monte Carlo simulations and it will be rescored using GlideScore function.

GLIDEscore can be defined below:

**GScore = 0.065 * vdW + 0.120 * Coul + Lipo + HB + Metal +BuryP + RotB + Site**

Where,

**vdW** = van der Waals energies

**Coul** = represents Coulomb energy

**Lipo** = hydrophobic term

**HB** = hydrogen bonding term

**Metal** = anionic interactions with metal cations

**BuryP** = buried polar group

**RotB** = frozen rotable bond

**Site** = polar but non hydrogen bonding atoms that exist in hydrophobic region

### 3.7.2 Ligand structure preparation

All the compounds were constructed using 2D-sketcher using the Schrodinger graphical user interface Maestro 8.5. The illustration in 2D-sketcher can be converted into 3D structure when it is being exported into the workspace (Friesner *et al.*, 2004).

### 3.7.3 Protein structure preparation

A typical PDB protein complex structure can be downloaded from the Research Collaborator from the Research Collaborator for Structural Bioinformatic (RCSB) website (http://www.rcsb.org). The PDB identification (PDB ID) for CETP are 2OBD (native protein) and 2EWS (torcetrapib attached). The PDB structures for CETP were corrected using protein preparation wizard that can be found in Maestro. The structures were prepared for docking with the protein preparation wizard using the following default steps: assigning bond orders, adding hydrogens, treating metals, creating disulfide bonds, converting selenomethionines, deleting waters, assigning H-bond network, structure minimization in vacuum up to 0.3 Å RMSD by using OPLS_2005 force field. After preprocessing and preparation steps, the H-bonds were further optimized. All waters molecules and additional ligands were deleted from the structure.

### 3.7.4 Receptor Grid Generation

Ligand docking jobs cannot be performed until grids are fully generated. The set up of grid generation can be done from the Receptor Grid Generation drop-down menu from maestro. The grid size can be determined from the position and the size of the active site. The maximum available grid size was 36 x 36 x 36 $Å^3$ outer box and 14 x 14 x 14 $Å^3$ inner box. The force field that is being used for grid generation was OPLS_2005 force field.

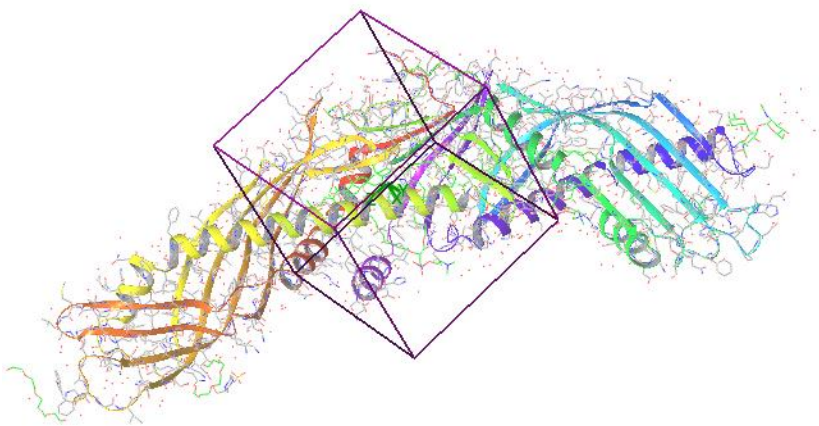

**Figure 28 The image of 2OBD protein in ribbon diagram format. The purple colour box indicates the grid box that was being generated before the docking procedure begun.**

### 3.7.5 Docking protocol

Molecular docking using Glide that was being developed by Schrodinger (Glide,2014) was performed to investigate the binding mode between the active site of CETP and prepared ligands. The docking ligands were treated flexibly, and the prepared protein was held rigidly during the docking procedure. The conformations are further refined via Monte Carlo sampling of pose conformations. There were 20 poses being collected.

### 3.7.6 Confirmation of docking using GOLD suites

In order to validate the docking poses, GOLD suites were being employed to dock the ligands of interest with CETP (PDB ID: 2OBD). GOLD uses a Genetic algorithm for searching binding space and ligand conformational space and it employs matching of pharmacophore points to generate ligand poses (Verdonk *et al.*, 2003). GOLD uses several scoring functions, which includes GoldScore, ChemScore, ASP and ChemPLP.

The protein and ligands were first being prepared in Maestro interface and the ligands were docked into the active sites using GOLD suites. Binding site of CETP was defined as all the residues that are located within 10Å from CE atom in N terminal. The default parameters if GOLD suites was using genetic algorithm (GA) in order to search for the reasonable conformation of ligands. The maximum number of GA runs was set to 10. The total number

of poses available was 10. Based on the three scoring function, chemscore fitness function has been chosen in order to evaluate the docking conformation (Guo *et al.,* 2004)

## 3.8 Molecular Dynamic Study using Desmond

### 3.8.1 Overview of Molecular Dynamic methodology

Molecular dynamic (MD) simulations is best to describe molecular motions of a system based on time and space using applied force fields. This technique gives virtual understandings into the atomic fluctuations but it is mainly based on the applied force fields, electrostatic interactions and motion assimilation through distinct time frame.

Three basic stages for MD simulation contains:

1) setup

2) equilibrium

3) run.

In the setup stage, the protein were inserted with water, soaking the protein into the membrane and also soaking the protein-membrane complex into a box of water. The system underwent energy minimization and heated gradually to the desired temperature for simulation and later will be equilibrated. In the equilibration stage, the protein heavy atoms were restrained and it will slowly released until the full system was stable and unrestrained. The MD simulation was based on force field method and it was basically obey Newton's second law:

$$F = ma$$

F = net force of an object

m = mass of an object

a = acceleration of an object

### 3.8.2 Molecular Dynamic Simulation protocol

The docking results from GLIDE were subjected to long equilibrium molecular dynamic (MD) simulations by using Desmond **(**Schrödinger Release 2015-1, 2015) with default OPLS_2005 force field.

The ligand-protein complex was embedded in POPC(1-palmitoyl-2-oleoyl-sn-glycer-3-phosphocholine) membrane and solvated with TIP3P water in a periodic orthorhombic box with 10 Å x 10 Å x 10 Å distance through the Desmond system builder which can be found in Maestro interface. In order to maintain the neutrality of the system, sodium and chloride ions were added. 150 mM $Na^{+}Cl^{-}$ were added as well in order to simulate the physiological condition of the system. The final system consisted of 69370 atom.

The system undergoes energy minimization using the Desmond minimizer which can be found in Maestro interface, which uses limited-memory-Broyden-Fletcher-Goldfard-Shanno (LBFGS) and steepest decent algorithms. Simulations were conducted with a constant temperature of 300 K using Nosé-Hoover chain thermostat (Martyna *et al.*, 1992) and Martyna-Tobias-Klein barostat methods Martyna *et al.*, 1994). The simulations were run for 10s and 20ns in total. Long-range electrostatic interaction was calculated using particle mesh Ewald algorithm (Darden *et al.*, 1999). The systems were undergoing default relaxation protocol before the MD simulation.

The system undergoes eight steps MD simulation protocol that involves:

Stage 1: Task

Stage 2: Simulate

Stage 3: Simulate, Berendsen NVT, T=10 K, Small timesteps, and restraints on heavy solute atoms

Stage 4: Simulate, Berendsen NPT, T=10 K, and restraints on heavy solute atoms

Stage 5: solvate_pocket

Stage 6: simulate, Berendsen NPT and restraints on heavy solute atoms

Stage 7: simulate, Berendsen NPT and no restraints

Stage 8: simulate

Trajectories were further analysed using desmonds. All the simulations were evaluated based on system potential energies, calculation of the radius gyration, root mean square (RMSD) and root mean square fluctuation of the protein (RMSF).

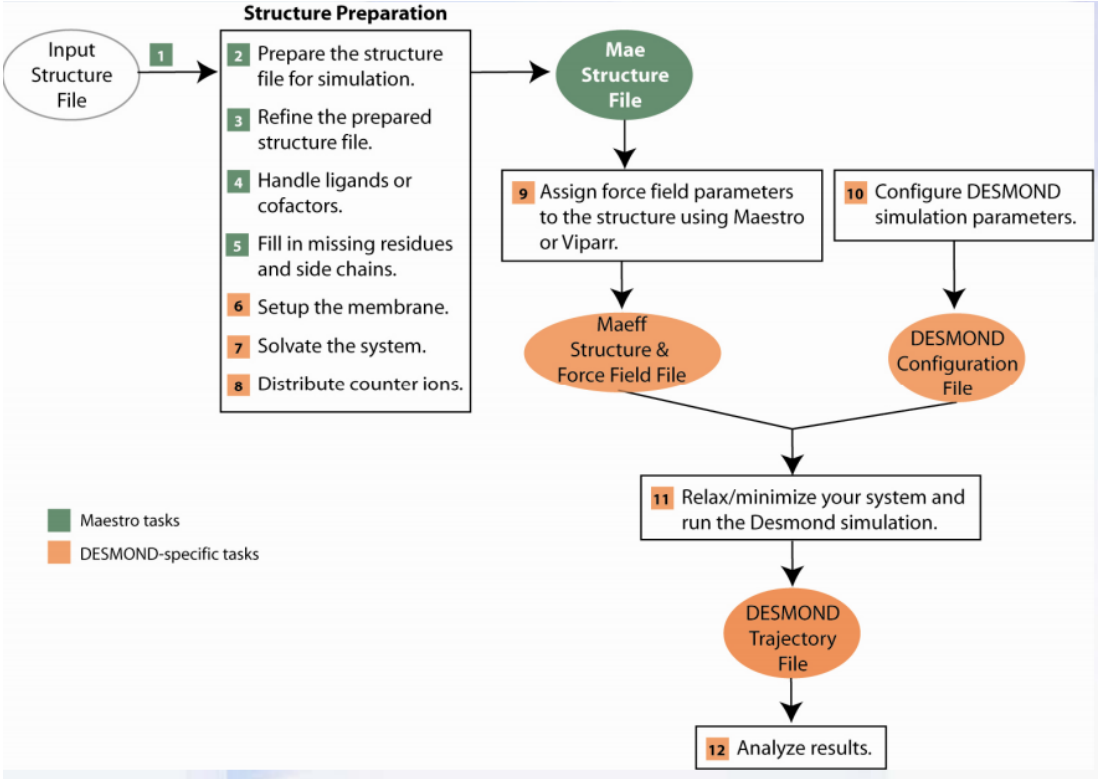


**Figure 29 Flowchart of MD simulation by Desmond**

## 3.9 Virtual Screening and SAR (Structural Activity Relationship) studies of HCA analogues against CETP

### 3.9.1 Preparation of the compound libraries

An analogue is described as a structure that is related to the drug of interest, in which biological and chemical properties might differ. As part of structure-activity relationship study, structural analogs of an initial lead compound are tested. The analogs were retrieved from web-accessible ZINC three-dimensional (3D) (www.zinc-docking.com). Zinc 3D is a database that compiles chemical structures, and it contains 13 million of compound (Irwin & Shoichet, 2005; Irwin *et al.*, 2012).

The compound library that is obtained from ZINC 3D database is further processed with Ligprep module in Maestro interface. A set of 9 ligands were prepared using Ligprep module.

### 3.9.2 Preparation of protein binding sites and targets

The three dimensional structures of CETP are obtained through RCSB website with the PDB ID:2OBD. The PDB structures for CETP were corrected using protein preparation wizard that can be found in Maestro. The structures were prepared for docking with the protein preparation wizard using the following default steps: assigning bond orders, adding hydrogens, treating metals, creating disulfide bonds, converting selenomethionines, deleting waters, assigning H-bond network, structure minimization in vacuum up to 0.3 Å RMSD by using OPLS_2005 force field. After preprocessing and preparation steps, the H-bonds were further optimized. All waters molecules and additional ligands were deleted from the structure. The set up of grid generation can be done from the Receptor Grid Generation drop-down menu from maestro by using OPLS_2005 force field.

### 3.9.3 Docking simulations and ligands ranking

All analogue compounds that were prepared earlier were docked into the binding site using Glide. The Glide SP was employed here to screen all the analogues and a maximum number of poses per ligand was set 100 before it being passed to grid-refinement calculation. One good conformation for each molecule which being ranked by Emodel score where Emodel combines GLIDEScore with non-bonded interaction energy with the internal energy of the generated ligand conformation. All molecules with the highest ranking poses (G-score) were selected for further experimental analysis.

### 3.9.4 CETP assay for the analogs

Chemicals: DL-isocitric acid trisodium salt hydrate, and potassium hydroxycitrate tribasic monohydrate were purchased from Sigma Aldrich, and it was being diluted with 1% DMSO.

In order to assess the percentage inhibition of the analogs towards CETP, a fluorescence bioassay was carried out by using the CETP Drug Screening Kit (#k602-100, BioVision, Mountain View, CA, USA). The procedures of the assay can be described briefly as follows: 50 µl of the inhibitors were added, followed by 3 µl of rabbit serum. Then the master mix which is being provided in the assay kit (10 µl of Donor Molecule, 10 µl of Acceptor Molecule and 20 µl of CETP buffer) was added, mixed well and the volume was completed to 203 µl with the provided assay buffer. The mixture was subjected to incubation for 1 hour at 37 °C, and the fluorescence intensity were measured by using fluorescence plate reader (Varioscan Flash, ThermoScientific) at Excitation wavelength of 465 nm and Emission wavelength at 535 nm. The percentage inhibition of the extracts towards CETP was determined by comparing the activity of CETP in the presence and absence of the tested compound. As a background, negative control lacking rabbit serum was being used. Positive

controls were tested in order to see the degree of inhibition by 0.1% DMSO and CETP were not affected by DMSO. All the measurements were carried out in triplicate. The percentage inhibition of the extracts towards CETP activity was calculated as follows:

$$\text{Percentage Inhibition} = \left(1 - \left[\frac{\text{sample read} - \text{blank read}}{\text{Positive control read} - \text{Negative control read}}\right]\right) \text{x } 100$$

# Chapter 4: Results and Discussion

Secondary metabolites that is being isolated from natural product are often used as medicines (Sung *et al.*, 2004). Up to date, there are several research that has been done in order to identify plants that has the ability to reduce the plasma low lipoprotein level (Amran *et al*., 2009; Khalili *et al*., 2009).

Torcetrapib, is a potent inhibitors for CETP which shows assuring results towards inhibition of CETP activity, increases in HDL-c levels and affect reduced progression of atherosclerosis in animal models (Okamoto *et al.*, 2000). However, during phase 2 of ILLUMINATE study, administration of torcetrapib has caused off target results which are increase in production of aldosterone and elevated blood pressure among tested patient. This considered as failure since it cause higher risk of combined end0point of death from coronary heart disease, stroke, myocardial infarction and hospitalization due to instable angina (Barter, 2009).

This led to the increase interest of research towards other CETP inhibitors especially in natural product. Plants have well documented for their medicinal uses for thousands of years. They have evolved and adapted over millions of years to withstand bacteria, insects, fungi and weather to produce unique, structurally diverse secondary metabolites. Their ethnopharmacological properties have been used as a primary source of medicines for early drug discovery (Butler, 2004). According to World Health Organization (WHO), 80% of people still rely on plant-based traditional medicines for primary health care (Farnsworth *et al.*, 1985) and 80% of 122 plant derived drugs were related to their original ethopharmacological purpose (Fabricant and Farnsworth, 2001). The knowledge associated with traditional medicine (complementary or alternative herbal products) has promoted further investigations of medicinal plants as potential medicines and has led to the isolation

of many natural products that have become well known pharmaceuticals. These explain that plant natural product provides a suitable platform as a candidate for CETP inhibitors. All of the plants that were being chosen for preliminary screening against CETP were chosen due to their ethnopharmacological properties that possess the cholesterol lowering properties. Due to this interest, all of the plants which are UNMC78 and UNMC 45L were chosen and to be tested their potency against CETP activity. Up to date there is no specific protocol that has been developed in search of CETP inhibitors from plant natural products especially that contains crude extracts which is known to possess many secondary metabolites.

## 4.1 Plant collection and identification

*Garcinia atroviridis Griffith ex T. Anderson* plant parts (leaves, twigs and fruits) were collected from Taman Botani, Universiti Putra Malaysia and was identified by botanist in Universiti Putra Malaysia. *Garcinia atroviridis* was deposited in University of Nottingham Malaysia Campus herbarium as UNMC 78 where UNMC 78L was indicated as leaves of *Garcinia atroviridis*, UNMC 78T as twigs of *Garcinia atroviridis* and UNMC 78F as fruit of *Garcinia atroviridis*.

**Figure 30 *Garcinia atroviridis* plant found in Taman Botani, UPM.**

**Figure 31 Young leaves of *Garcinia atroviridis***

**Figure 32 Yellow colour fruit is riped fruit and green colour fruit is unriped fruit.**


**Figure 33 Dried fruit of *Garcinia atroviridis* which is also known as '*asam keping*'.**

The leaves of *Garcinia parvifolia* were collected from the lowland dipterocarp, Sungai Congkak Reserve Forest in Malaysia and a voucher specimen (45L) was deposited at the Herbarium of The University of Nottingham, Malaysia Campus.

**Figure 34 *Garcinia Parvifolia* with unriped fruit**

## 4.2 Extraction Results

### 4.2.1 Extraction Yields

Table 2 represents the yield of extraction for different plant parts of *Garcinia atroviridis* which are leaves, twigs and fruits and leaves parts of *Garcinia parvifolia.* All of these plant parts were extracted using different polarity which ranging from low polarity to high polarity of organic solvent.

**Table 2 Yield of Extraction of *Garcinia atroviridis* and *Garcinia parvifolia.***

| **Scientific name** | **Plant part** | **Code** | **Dried weight (g)** | **Solvent used for extraction (ml)** | **Extracts** | **Percentage yield** |
|---|---|---|---|---|---|---|
| *Garcinia atroviridis* | Leaves | 78L | 1596 | 12784 | Hexane | 9.3 |
| | | | | | Ethyl Acetate | 10.1 |
| | | | | | Ethanol | 13.8 |
| | Twigs | 78T | 1109 | 8872 | Hexane | 8.4 |
| | | | | | Ethyl Acetate | 10.3 |
| | | | | | Ethanol | 12.7 |
| | Fruit | 78F | 865 | 6920 | Hexane | 5.6 |
| | | | | | Ethyl Acetate | 6.1 |
| | | | | | Ethanol | 8.0 |
| *Garcinia parvifolia* | Leaves | 45L | 437 | 3496 | Hexane | 3.4 |
| | | | | | Ethyl Acetate | 4.1 |
| | | | | | Ethanol | 5.0 |

The extraction yield of the plants is highly depending on the solvent polarity which will later determines both quantitatively and qualitatively the extracted compound. Based on the table 2, three solvents with increasing polarity had been used in the maceration process which is Hexane, Ethyl Acetate and Ethanol. The highest percentage yield obtained is from Ethanol extracts of all plant species and the lowest percentage yield is obtained from Hexane extracts of all plant species.

## 4.3 Phytochemical screening of crude extract

In order to understand the possible compounds that might be present in the plant species, various phytochemical screening had been carried out.

In order to predict the presence of alkaloids, flavonoids, saponin, tannin, steroid, terpenoid and phytosterol content in the extracts, phytochemical screening of UNMC 78L, UNMC 78T and UNMC 78F had been carried out and the result can be shown in table below. The results of phytochemical screening of UNMC 45L can be obtained from Wong *et al.* (2012).

**Table 3 Phytochemical screening of UNMC 78T**

| Extracts | Alkaloids | Flavonoids | Saponin | Tannin | Steroid | Terpenoid | Phytosterol |
|---|---|---|---|---|---|---|---|
| Hexane | - | ++ | - | + | ++ | + | ++ |
| Ethyl Acetate | - | - | - | ++ | - | - | + |
| Ethanol | + | - | + | - | + | + | - |

**++ highly present**

**+ slightly present**

**- not present at all**

Based on table 8, more secondary metabolites are present in the Hexane extracts of UNMC 78T compare to the ethyl acetate extracts and ethanol extracts of UNMC 78T. Based on the table above, flavonoids, tannin, steroid, terpenoid and phytosterol present in the hexane extract. For the ethyl acetate extracts, only tannin and phytosterol does present in the extracts. Alkaloid, saponin, steroid and terpenoid were present in the ethanol extracts of UNMC 78T.

**Table 4 Phytochemical Screening of UNMC 78L**

| Extracts | Alkaloids | Flavonoids | Saponin | Tannin | Steroid | Terpenoid | Phytosterol |
|---|---|---|---|---|---|---|---|
| Hexane | - | ++ | - | - | ++ | + | + |
| Ethyl Acetate | - | + | - | ++ | + | ++ | - |
| Ethanol | + | - | + | - | - | - | ++ |

**++ highly present**

**+ slightly present**

**- no present at all**

Positive results of flavonoids, steroid and terpenoid can be seen with the Hexane and Ethyl Acetate extracts of UNMC 78L. Ethyl Acetate extracts of UNMC 78L contains tannins which does not present in both Hexane extracts and ethanol extracts. Phytosterol does presents in both Hexane and Ethanol extracts. Conversely, only the ethanol extracts of UNMC 78L revealed the presence of saponin and alkaloids composition in the screening.

**Table 5 Phytochemical screening of UNMC 78F**

| Extracts | Alkaloids | Flavonoids | Saponin | Tannin | Steroid | Terpenoid | Phytosterol |
|---|---|---|---|---|---|---|---|
| Hexane | - | ++ | - | ++ | - | - | - |
| Ethyl Acetate | - | - | + | + | - | - | - |
| Ethanol | ++ | ++ | + | - | - | - | + |

**++ highly present**

**+ slightly present**

**- not present at all**

The table above (table 10) shown that Ethanol extracts contain alkaloids, flavonoids, saponin and phytosterol while Ethyl acetate extracts slightly contain saponin and tannin. Hexane extracts only contains flavonoids and tannin.

## 4.4 Optimizing and development of Cholesteryl Ester Transfer Protein Assay

### 4.4.1 Development of Cholesteryl Ester Transfer Protein Assay

One of the main objectives of this study is to develop a protocol in order to see the inhibition activity of the crude extracts and other possible inhibitor against CETP activity. The basic principle of the CETP assay is based on fluorometric reading at which it contains donor molecule and acceptor molecule. Donor molecule contains fluorescent self-quenched neutral lipid which will be transferred to acceptor molecule in the present of CETP. The successful transfer will cause increase in the fluorescent intensity value while presence of inhibitor will reduce the fluorescent intensity reading.

There is no literature up-to-date that uses the CETP drug screening kit in natural product research drug discovery. No reference can be made on the optimal conditions that could be used in the experiment. Hence, several attempts on optimization of the assay kit were carried out to establish a new method for this research purpose.

The important parameter in this optimization of assay is the incubation time. This CETP screening assay kit needs to be incubated at certain period of time specifically according to the human basal body temperature which is $37^0$C. Several tests had been done at different incubation times which are 30 minutes, 40 minutes, 50 minutes, 60 minutes and 90 minutes.

It is being reported that 1,3,5-triazines were found to be potent towards CETP (Xia *et al*, 1999). And, in this study to optimize the CETP drug screening kit, 10uM of 1,3,5-triazine had been used to assess the optimal time of reaction.

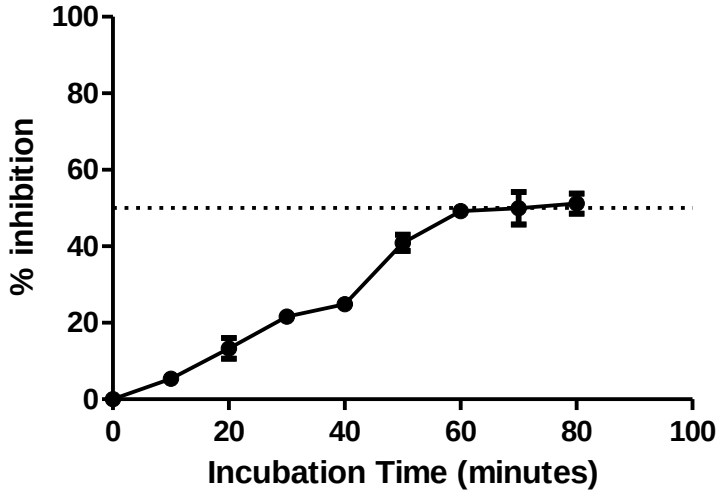


**Figure 35 Different incubation time of 1,3,5-triazine against CETP inhibition. Each point represent the mean ± standard deviation from three different independent experiment (n=3) *P*<0.05.**

Based on the figure 35, the suitable incubation time is 60 minutes and this value correspond towards the $IC_{50}$ of the 1,3,5-triazine (Okamoto *et al*., 2000). Less incubation time might lead to incomplete reaction between the donor molecule and the acceptor molecule. It is important to incubate the samples at the appropriate incubation time as this will produce better accuracy in the percentage of inhibition due to the facts that perfect time taken for incubation will leads to complete reactions of the sample. Besides, prolong incubation time might cause the reaction to be "saturated" which will lead to the loss of activity and the fluorescence intensity reading is not accurate anymore (Foti and Fisher, 2004).

The percentage inhibition of the extracts towards CETP activity was calculated as follows:

$$\text{Percentage Inhibition} = \left(1 - \left[\frac{\text{sample read} - \text{blank read}}{\text{Positive control read} - \text{Negative control read}}\right]\right) \text{x } 100$$

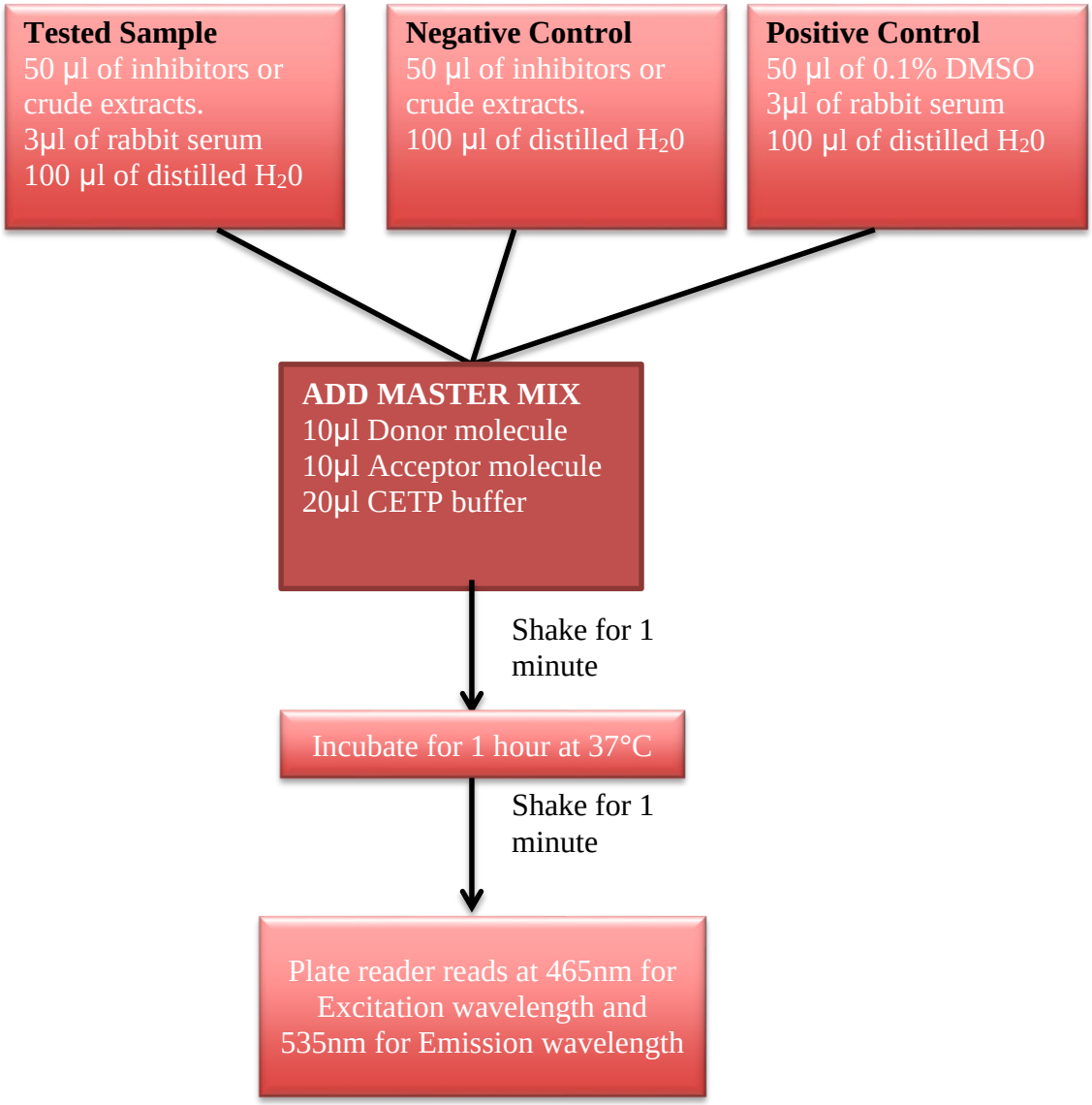


**Figure 36 Summary of CETP assay**

### 4.4.2 CETP inhibitory assay for all plant extracts

After the optimization of CETP has been done, further CETP inhibitory assay being done involving all the extracts of UNMC 78, UNMC 45L and one crystal product that was being isolated from UNMC 45L which is known as clusianone (Wong, 2013). A higher inhibition activity of CETP assay is being indicated by a lower value of $IC_{50}$, is anticipated as an active inhibition. The results are being described below.

#### 4.4.2.1 Inhibition of extracts from UNMC 78T against CETP activity

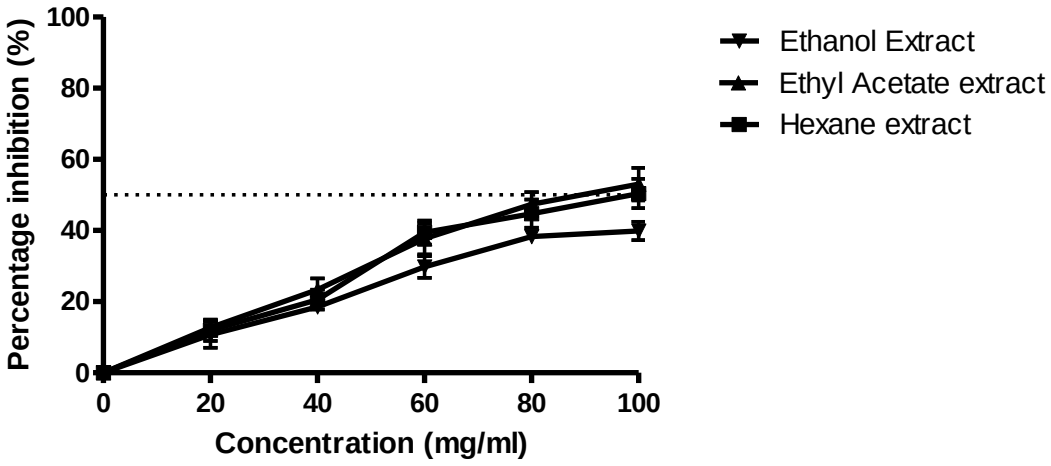


**Figure 37 Percentage inhibition of UNMC 78T against CETP activity. Each points represent the mean ± standard deviation from three independent experiment (n=3) *P*<0.05.**

**Table 6 $IC_{50}$ of UNMC 78T plant extracts**

| Plant Extract UNMC 78T | $IC_{50}$ |
|---|---|
| **Hexane** | 89.67 ± 0.035 mg/ml |
| **Ethyl acetate** | 94.25 ± 0.002 mg/ml |
| **Ethanol** | Cannot be determined |

The three extracts of UNMC 78T with different polarity which are Hexane, Ethyl Acetate and Ethanol were screen to assess their inhibitory effect against CETP activity. The $IC_{50}$ for hexane extract and ethyl acetate extract are 89.67 ± 0.035 mg/ml and 94.25 ± 0.002 mg/ml respectively. These values considered very high since it almost reach 100mg/ml. However, the $IC_{50}$ of ethanol extract of UNMC 78T cannot be determined at the concentration studied.

This reveals that extraction by using both low polarity and intermediate polarity solvents were the best in extracting the secondary metabolites from UNMC 78T that are actively inhibits CETP activity. In agreement with earlier results of UNMC 78T, hexane and ethyl acetate have been generally described as most suitable solvents for extraction that recover flavonoids and phytosterol. These phytochemicals have been investigated and they does have the properties as a cardioprotective effects (Cook & Samman, 1996; Testai *et al.*, 2013; Yoshida & Niki, 2003).

#### 4.4.2.2 Inhibition of extracts from UNMC 78L against CETP activity

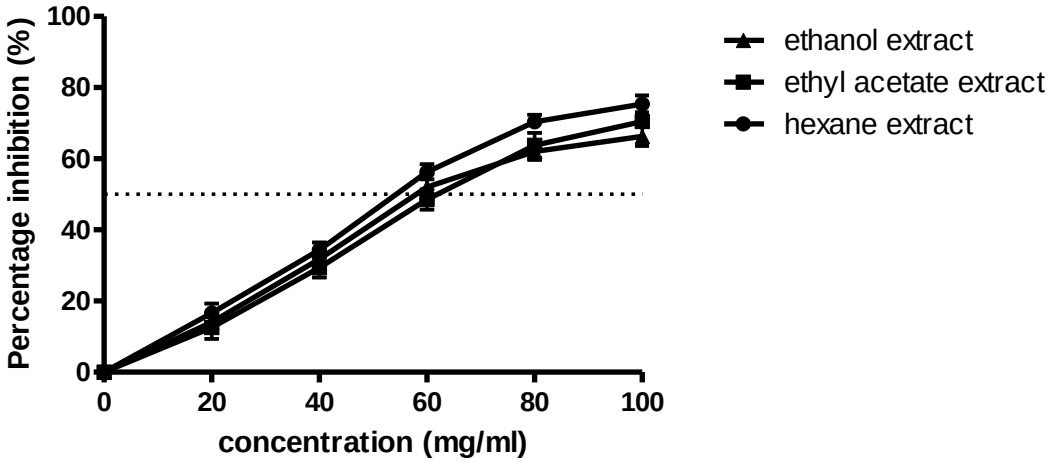


**Figure 38 Percentage inhibition of UNMC 78L against CETP activity. Each point represent the mean ± standard deviation from three independent experiment (n=3) *P*<0.05.**

**Table 7 $IC_{50}$ of UNMC 78L plant extracts**

| Plant Extract UNMC 78L | $IC_{50}$ |
|---|---|
| **Hexane** | 54.83 ± 0.027 mg/ml |
| **Ethyl acetate** | 59.01 ± 0.003 mg/ml |
| **Ethanol** | 62.47 ± 0.005 mg/ml |

All of the plant extracts of UNMC 78L, which are Hexane and Ethyl Acetate, and Ethanol undergoes screening to detect its inhibitory effect against CETP. Hexane extracts show the highest potency compared to the other extracts followed by Ethyl Acetate extract and Ethanol extract shows the lowest potency among other extracts. The $IC_{50}$ for all the extracts are presented in the table above. All of the extracts

shows a gradual increase in the percentage of inhibition as the concentration of the extract increases.

Percentage inhibition of UNMC 78L against CETP activity does produce the same percentage inhibition trend as UNMC 78T where the most potent extracts is hexane extracts and least potent is ethanol extracts. Based on the analysis of $IC_{50,}$ small differences of the value of $IC_{50}$ can be observed between the three extracts with different polarity. The higher potency of hexane extracts and ethyl acetate extracts is due to the present of flavonoids, steroids and terpenoids in the extracts and these phytochemicals might present as an active ingredient that acts towards inhibition of CETP activity.

#### 4.4.2.3 Inhibition of extracts from UNMC 78F against CETP activity

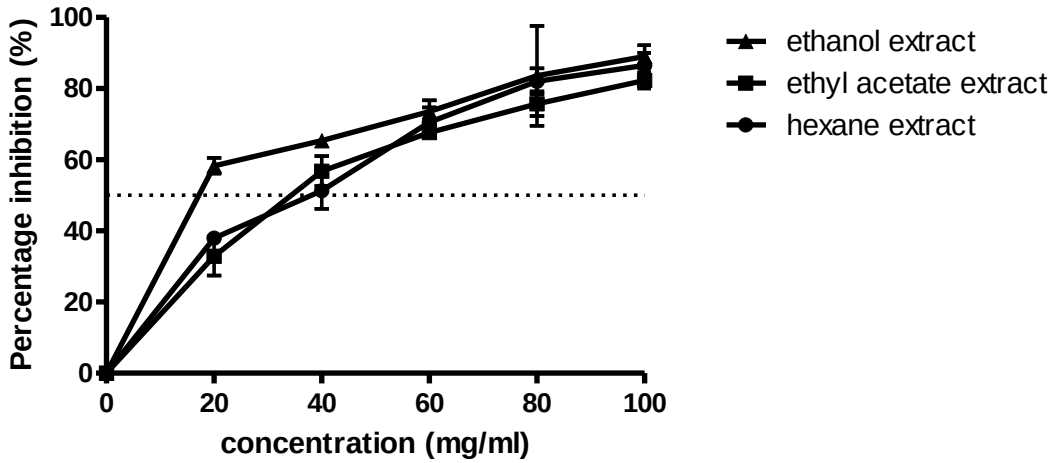


**Figure 39 Percentage inhibition of UNMC 78F against CETP activity. Each point represent the mean ± standard deviation from three independent experiment (n=3) $p<0.05$.**

**Table 8 $IC_{50}$ of UNMC 78F plant extracts**

| Plant Extract UNMC 78F | $IC_{50}$ |
|---|---|
| **Hexane** | 41.23 ± 0.007 mg/ml |
| **Ethyl acetate** | 35.79 ± 0.003 mg/ml |
| **Ethanol** | 19.28 ± 0.021 mg/ml |

Three extracts of UNMC 78F were initially screened on the inhibitory effects towards CETP activity. $IC_{50}$ values were determined and being listed in the table 8. Among these three extracts, ethanol extracts of UNMC 78F appeared to be more potent compared with hexane extract and ethyl acetate extract. This finding gives some interesting insight since the values obtained for the percentage inhibition of ethanol extracts from UNMC 78F is considered to be very potent compared to the other extracts of different plant parts of UNMC 78 because less amount of ethanol extracts of UNMC 78F is needed to obtain 50 percent effect. Thus, therapeutic preparations of drugs will reflect the potency.

In the present works, UNMC 78F shows a remarkable effects against the CETP activity. This being indicated by the lowest values of $IC_{50}$ compared to other extracts. This findings suggest that extraction using high polarity solvent is the most effective way in extracting the active secondary metabolites from UNMC 78F. This results is well supported by other studies which suggest the important bioactive compound that present in UNMC 78F which is Hydroxycitric acid (HCA) are being extracted by using higher polarity solvents (Lewis, 1965).

#### 4.4.2.4 Inhibition of extracts from UNMC 45L against CETP activity

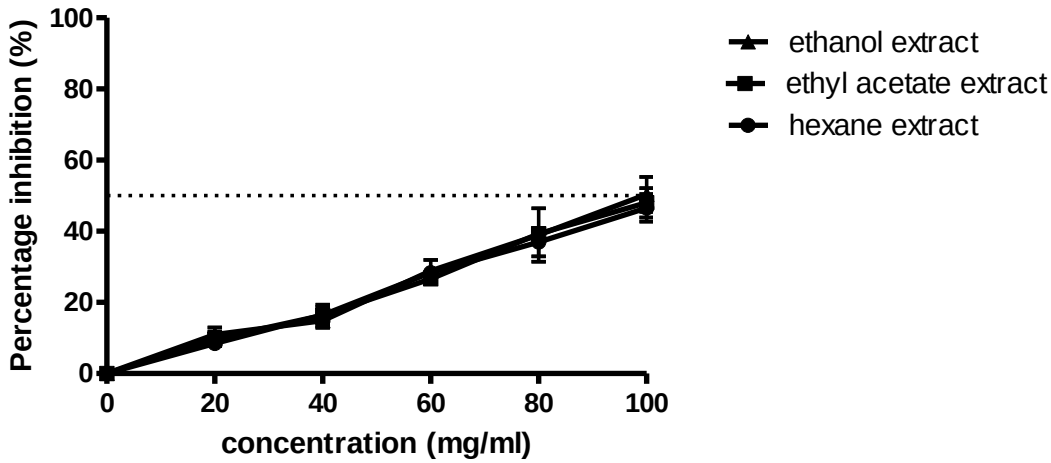


**Figure 40 Percentage inhibition of UNMC 45L against CETP activity. Each point represent the mean ± standard deviation from three independent experiment (n=3) $p<0.05$.**

**Table 9 $IC_{50}$ of UNMC 45L plant extracts**

| Plant Extract UNMC 45L | $IC_{50}$ |
|---|---|
| **Hexane** | 97.35 ± 0.0045 mg/ml |
| **Ethyl acetate** | 98.72 ± 0.0032 mg/ml |
| **Ethanol** | 96.24 ± 0.0028 mg/ml |

Based on the figure 40, all of the UNMC 45L crude extract exhibit minimal inhibitory effect since all of the extracts have the almost similar $IC_{50}$ values and these value cannot be determined as potent compared to crude extracts from UNMC 78 plant species. This is because the values obtained for the $IC_{50}$ is almost 100mg/ml and this values considered very high. The higher the $IC_{50}$ values, the less potent the extracts is. The $IC_{50}$ values of the plant extracts can be summarized above.

Preliminary screening of UNMC 45L shows that all of the extracts can inhibit CETP however, the results are not that potent compared to UNMC 78. The lowest value of $IC_{50}$ is

ethanol extracts followed by hexane extracts and ethyl acetate. This might be due to the presence of certain secondary metabolites that are being extracted via hexane, ethyl acetate and ethanol extracts from UNMC 45L is not highly active in the inhibition of CETP activity. Although same solvents is being used as in previous extraction of UNMC 78T, UNMC 78L and UNMC 78F but different activity is being observed due to specific compounds that might present in one species and not in other species.

#### 4.4.2.5 Inhibition of Clusianone (Pure compound isolated from UNMC 45L) against CETP activity

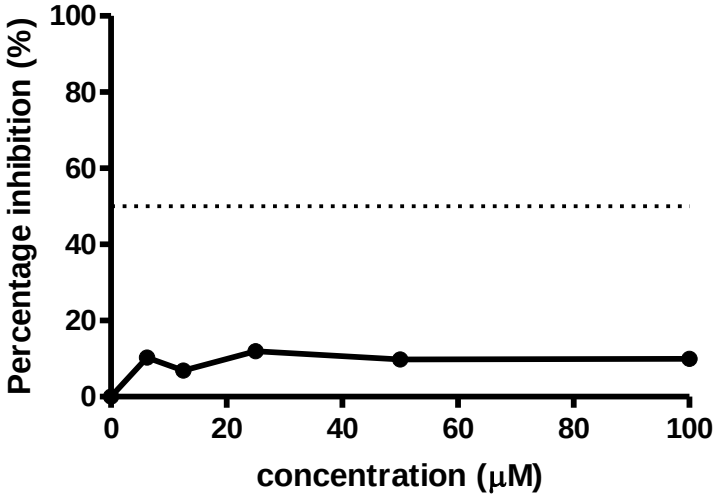


**Figure 41 Percentage inhibition of clusianone against CETP activity. Each point represent the mean ± standard deviation from three independent experiment (n=3) *P*<0.05.**

Clusianone, a pure crystal compound found in hexane extracts of UNMC 45L (Wong, 2013) had been tested for CETP inhibition. Large numbers of polyisoprenylated benzophenone have been isolated from Guttiferae (Clusiaseae) family and clusianone and its derivatives are considered as polyisoprenylated benzophenone. Several studies have proven that benzophenone and its derivatives does have important bioactivity such as anti lipogenic, anti-cancer, anti-oxidant, anti-inflammatory, and anti-ulcer (Kumar *et al.*, 2013; K. Yoshida *et al*., 2005). Due to this interesting bioactivity, it is important to see the efficiency of clusianone tested against CETP activity.

Various concentration had been used to see the effect against CETP. However, no effective inhibition can be seen from lowest to the highest concentration of clusianone and the

percentage inhibition does not reach 50% inhibition. Due to this reason, IC50 of clusianone against CETP inhibition cannot be determined. The results obtained are quite disappointing as the $IC_{50}$ of clusianone cannot be determined. From this observation, clusianone is not an effective inhibitor towards CETP at this range of concentration. However, final conclusion cannot be drawn based on these ranges of concentration, as there are some limitations. The possible reason is it that clusianone might target specific protein to react since it does not inhibit CETP in this amount but possible to inhibit HMG-CoA reductase with this range of concentration (Wong,2013).

**4.4.2.6 Inhibition of Hydroxycitric Acid against CETP activity.**

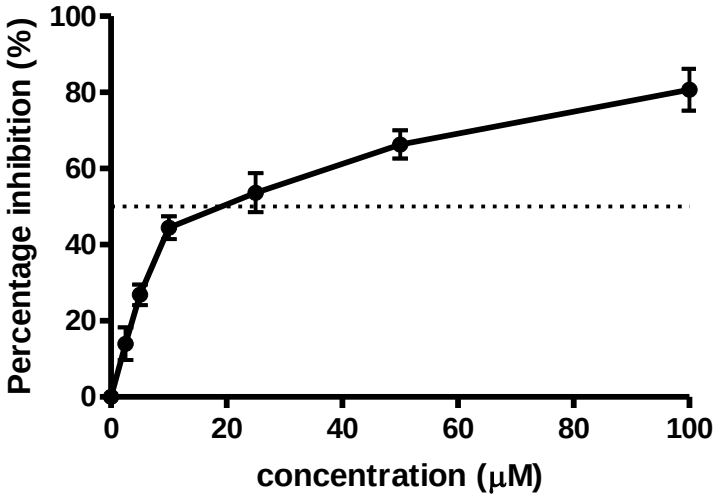


**Figure 42 Percentage inhibition of Hydroxycitric acid (HCA) against CETP activity. Each point represents the mean ± standard deviation from three independent experiment (n=3) *P*<0.05.**

This study was initiated after we discovered the highest inhibition of crude fruit rind extracts of *Garcinia atroviridis* against CETP activity via the CETP inhibitory assay. Based on several literatures (Jena *et al*, 2002, Hobbs, 1994), HCA is the principal compound that acts as a potent inhibitor of ATP citrate lyase which catalyzes the extramitochondrial cleavage of citrate to oxaloacetate and acetyl-CoA: citrate + ATP + CoA acetyl-CoA + ADP + Pi + oxaloacetate (Daikuhara *et al*., 1968). The inhibition of this reaction limits the availability of acetyl-CoA units required for fatty acid synthesis and lipogenesis during a lipogenic diet, that is, a diet high in lipids (Sullivan *et al*., 1972). Extensive animal studies indicated that (-)-HCA suppresses the fatty acid synthesis, lipogenesis, food intake, and induced weight loss (Sullivan *et al.*, 1972). Several studies have confirmed that HCA does not bring short term and long term bad effect. One of the studies uses variable time length which is 4 to 30 days

and doses taken are from 150mg to 1500mg of pure compound but no one has ever reported about toxicity of HCA (Leonhardt *et al.,* 2004; Leonhardt *et al.,* 2001; Rao & Sakariah, 1988) Several form of readily available product that contains HCA can be found commercially such as Regulator®**,** Citrin K® and SuperCitrimax® (Preuss *et al.*, 2006)**.** Based on this, the initial assumption is HCA is also responsible for inhibiting the CETP activity.

Based on the CETP inhibitory assay that was being graphed in figure 42, the $IC_{50}$ of HCA inhibition against CETP is 20.07 ± 0.05 μM. This value indicates that HCA is a potent inhibitor towards CETP activity. From this assay, HCA has been identified as a potential inhibitor for CETP. This significant results for CETP inhibition is important and need to be further validated in series of in-silico techniques which are being discussed later in this chapter.

## 4.5 Determination of enzyme reaction: Designing and Optimizing enzyme kinetics assay

### 4.5.1 Kinetic properties of HCA against CETP activity

Every inhibitor might have different inhibitory mechanisms against the protein of interest (Copeland, 2000). There are four main types of inhibition; competitive inhibition, non-competitive inhibition or mixed, uncompetitive inhibition and mechanism-based inactivation or also being called as suicide mechanism. This study is important to assess the inhibitory mechanism of HCA against CETP. Only kinetic study of HCA has been carried out since it shows the highest inhibition rates.

In order to evaluate the mechanism of inhibition between CETP and HCA, enzyme kinetic study was being done. However, there are no reported kinetic assay procedures has been done by using the assay kit. The same assay kit that was being used in the screening assay was also use in this experiment and the same protocols had been applied except that the readings were taken every 1 minute interval during the 60 minutes incubation period.

The kinetic assay is being done based on Michealis Menten equation in order to determine the Km value and the maximum reaction rate which is Vmax using Lineweaver-Burke plot.

$$\mathrm{Vo} = \frac{\mathrm{Vmax}\,[\mathrm{s}]}{\mathrm{Km} + [\mathrm{s}]}$$

The type of inhibition with the values of Ki can be determine from Lineweaver-Burke plot or double reciprocal plot. This is important to know the properties of the inhibitors and the mechanism of reaction between the inhibitors and the protein in order to know the effectiveness of the inhibitor.

Several concentrations have been tested to see their kinetic properties every 1-minute interval for 60 minutes duration.

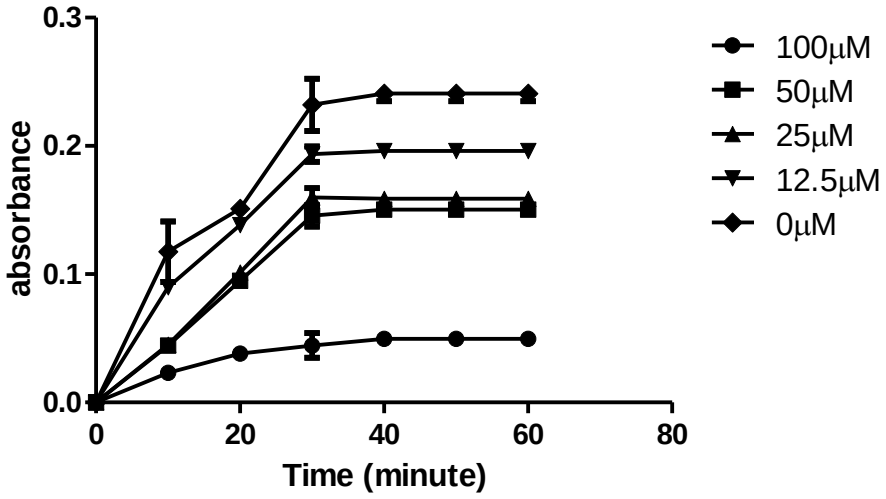


**Figure 43 Progress curve for kinetic assay of HCA against CETP. Each point represents the mean ± standard deviation from three independent experiment (n=3) *P*<0.05.**

Progress curve from figure 45 shows that as the time passed by the absorbance increase resulting in the formation of the by product. But when it started to reach 30 minutes, the absorbance remains constant which indicates that the maximum incubation times has taken place.

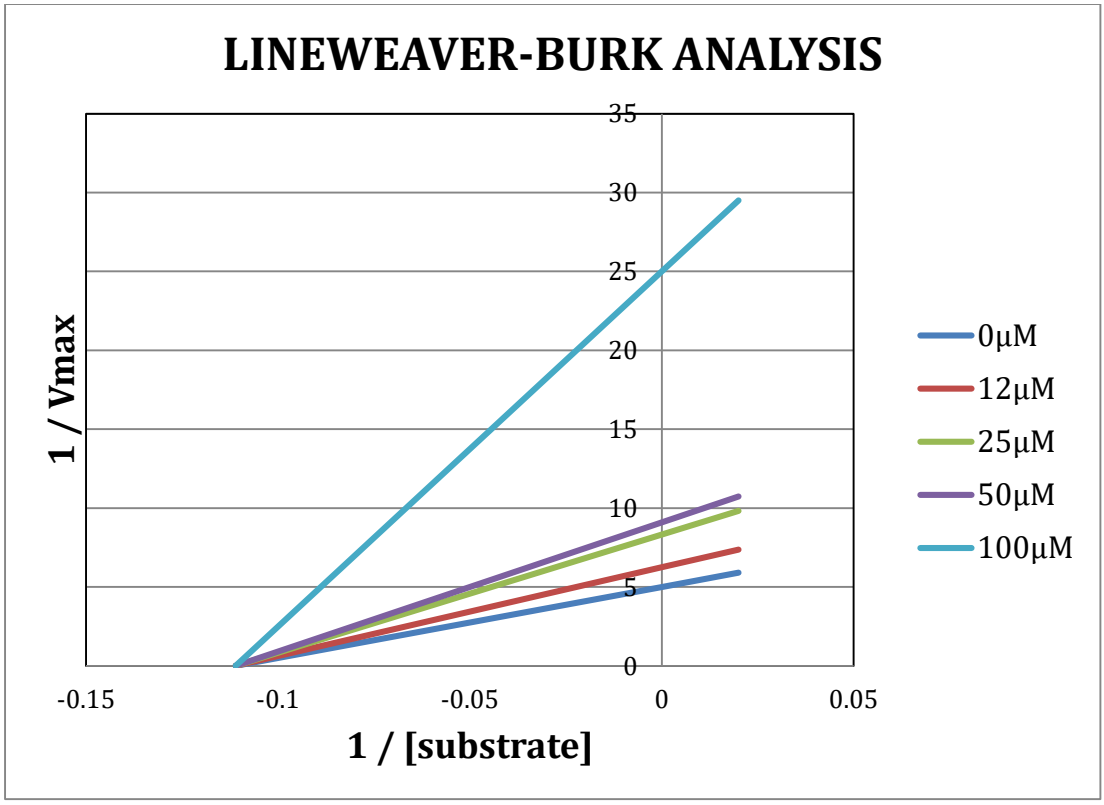


**Figure 44 Lineweaver-burk analysis of HCA inhibition kinetic assay.**

Further analysis by using Michaelis-Menten equation through the double reciprocal plots or Lineweaver-burk analysis in figure 44, suggested that HCA is a non-competitive inhibitor against CETP. Noncompetitive inhibitor or allosteric inhibition is an inhibitor which binds to enzymes regardless of substrate binding. This can be seen in the Lineweaver-Burk plot in figure 44, whereby the Km is unchanged for every substrate concentration and the Vmax which is the slope is increased when the concentration of the inhibitor increase. The mechanism of action of HCA is the same as that torcetrapib, where it has been proven to be non-competitive inhibitor through traditional biochemical method (Clark *et al.*, 2006). The results obtain from enzyme kinetic assay can be used as a supporting data for molecular modeling experiment which later can predict the specific interaction of the inhibitor and the active site.

## 4.5 Validation of HCA presence in ethanol crude extracts of UNMC 78F

### 4.5.1 Validation by using FTIR method

The spectra of the *G. atroviridis* fruit rind (UNMC 78F) macerated with ethanol solvent provide a number of spectral details indicating some similarities with each other. From the FTIR spectra analysis, all significance functional groups were present. The existence of carboxylic acid, esters and hydroxyl group indicated high probabilities of the HCA content in the concentrated crude extract of *G. atroviridis* fruit rind (UNMC 78F) (Jena *et al*., 2002). The absorbance peaks of the spectra and data can be seen in Figure 45 and Table 10, respectively.

#### 4.5.1.1 Hydroxyl (OH) bands

The OH stretch value for ethanol extracts of UNMC 78F were fitted within the range 3550 $cm^{-1}$ to 3200 $cm^{-1}$. The O-H band value in ethanol extracts of UNMC 78F is 3405.17 $cm^{-1}$ (Figure 45). However, it can be seen that the OH band spectra were broad and less peaky, this may due to different signal arise from vibrations of molecules, as the identification of hydroxyl and carboxyl group require O-H stretch. This situation leads to broadening and overlapping bands of spectra (Schmitt and Flemming, 1996).

#### 4.5.1.2 Carboxyl (COOH) bands

According to the standard IR spectra table, the present of carboxyl group in the sample can be deduced as long as the O-H, C=O and C-O stretch lie in between the value of 3200 $cm^{-1}$ – 2500 $cm^{-1}$ , 1725 $cm^{-1}$ – 1700 $cm^{-1}$ and 1300 $cm^{-1}$-1000 $cm^{-1}$, respectively. The C=O stretch of carboxyl group depicted sharply at 1720.52 $cm^{-1}$ for the sample macerated in ethanol extracts of UNMC 78F. The C-O stretch were shown at 1200.27 $cm^{-1}$ and 1062.1 $cm^{-}$1. Both values

fall in C-O stretch standard range, which arise the probability one of the value is specific to the carboxyl group. It is proven that the range below 1500 $cm^{-1}$ can be very specific for a substance or for different types of substitution. This range is frequently referred to as the "fingerprint region" of a spectrum (Diem, 1994; Urban, 1994; Schrader, 1995 *in* Schmitt and Flemming, 1996). Since the C=O and C-O stretch between carboxyl group and esters close in range, the way to detect the presence of the carboxyl groups is by confirming the O-H stretch which is absent in esters. Thus, the O-H stretch must be within the range of 3200 $cm^{-1}$-2500 $cm^{-1}$. From the spectra absorbance peak, O-H stretch mildly depicted at the value 2922.41 $cm^{-1}$ for ethanol extracts. Hence, as the value for O-H, C=O and C-O stretches fall within the standard range, it can be deduced that carboxyl groups exist in the sample.

#### 4.5.1.3 Esters bands

The present of esters can be verified from the C=O and C-O stretch peaks. In this experiment, the spectra absorbance peaks between esters and carboxyl groups resembled within the same range. However, the O-H stretch absorbance peaks that only exist in carboxyl group and two-specific absorbance below 1500 $cm^{-1}$ relatively belong to either one of the groups can be a good inference in verifying their presence, as in FTIR, different forms of vibrations are discriminated, arising from different forces and binding angles of atoms in a molecule. Thus, complex molecules display numerous options of internal vibrations (Schmitt and Flemming, 1996). As in carboxyl groups, the C=O stretch of esters in ethanol extracts fall in between 1730 $cm^{-1}$-1715 $cm^{-1}$. The possible value of absorbance peak for C-O stretch binding in esters, 1199.08 $cm^{-1}$ and 1062.1 $cm^{-}1$ in ethanol extracts. The strong band for both stretches can be good base to conclude the existence of esters in this sample.


**Figure 45 FTIR Absorbance peaks for ethanol extracts of UNMC78F**

**Table 10: Tabulated position of absorbance peaks**

| Vibration | Position (cm-1) | |
|---|---|---|
| | Standard | Sample extracted by ethanol |
| **Alcohols/Hydroxyl** | | |
| O-H stretch | 3550-3220 | 3405.17 |
| **Carboxyl group** | | |
| O-H stretch | 3200-2500 | 2922.41 |
| C=O stretch | 1725-1700 | 1720.52 |
| C-O stretch | 1300-1000 | 1200.27/1062.69 |
| **Esters** | | |
| C=O stretch | 1730-1719 | 1720.52 |
| C-O stretch | 1300-1000 | 1200.27/1062.69 |

### 4.5.2 Validation by using HPLC method

HPLC method has been employed in this chapter in order to validate the presence of HCA in ethanol crude extracts of UNMC 78F. Two chromatogram can be seen in figure 46 and 47. One clearly resolved peak were obtained in each chromatogram where the retention time of HCA in standard is 1.069 minute in figure 46 and the peak obtained from ethanol extracts of UNMC 78F is 1.106 minute in figure 47.

The results were comparable since the peak of the ethanol extracts of UNMC 78F was appeared in the same timescale as the standard. Two small peak also appeared in the crude extract of UNMC 78F in figure 47 indicates that other compound also present in the sample. The results in figure 47 which shows that HCA is the major organic acid that is found in the fruit sample of UNMC 78F since it was resolved as a single peak with no interference from other compound. The identity of HCA peak was confirmed by determination of relative retention time and by spiking with standard HCA. The retention time of HCA in this experiment is also being confirmed by other publication as well (Jayaprakasha and Sakariah, 1998; Ibnusaud *et al.,* 2000; Jena *et al.,* 2002;Jayaprakasha and Sakariah,2002; Asish *et al.,* 2008, Kumar *et al.,* 2013; Upadhyay *et al.,* 2013 ).

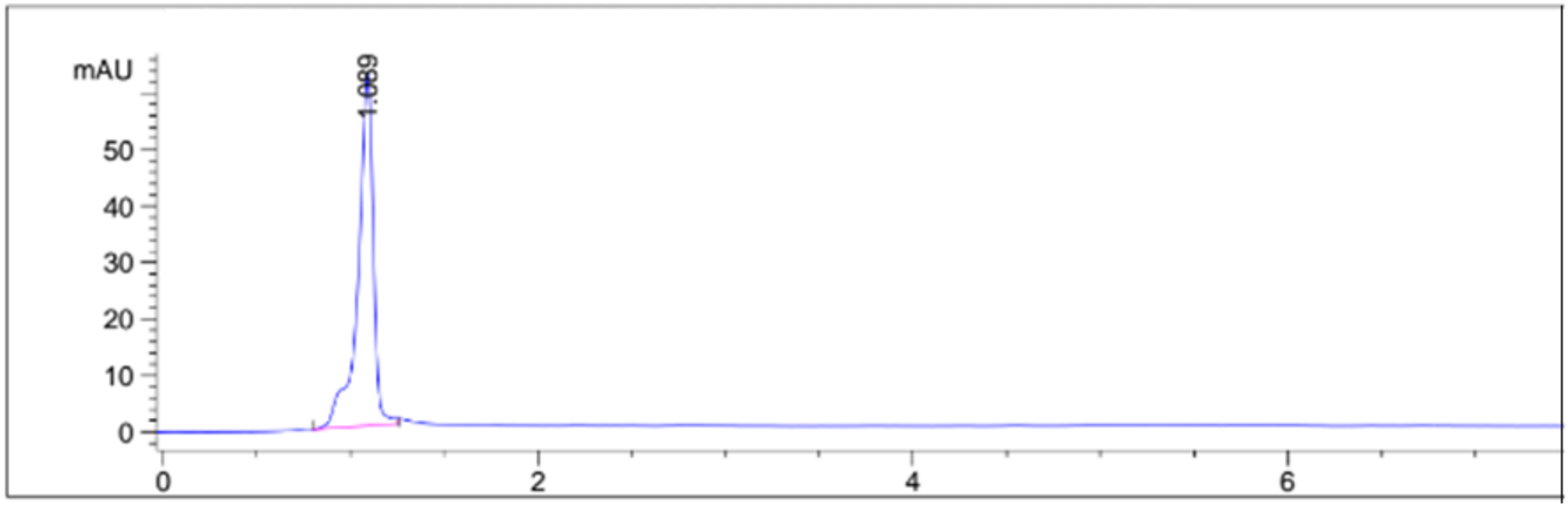


**Figure 46 Chromatogram of HCA standard. The peak can be seen at Rt= 1.089 minute**

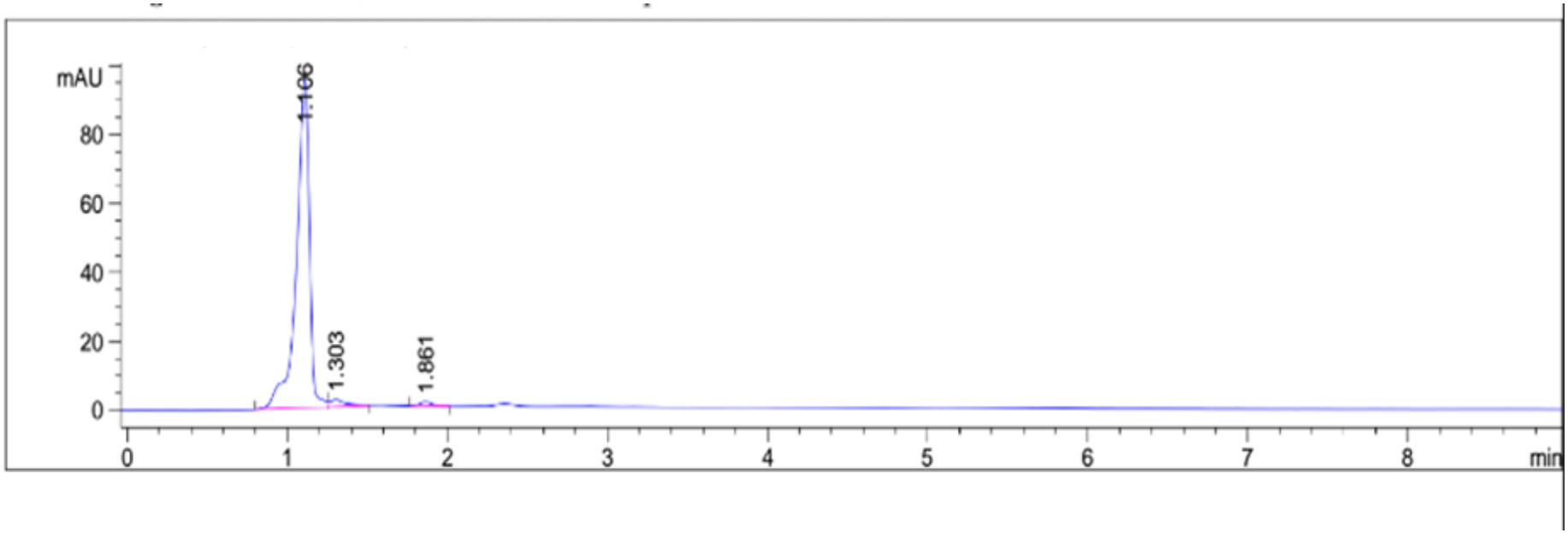


**Figure 47 Chromatogram of ethanol extract of UNMC 78F. The peak can be seen at Rt= 1.166 minutes, 1.303 minutes, 1.861 minutes**

## 4.6 Validation of HCA inhibition using molecular docking study

Molecular modeling has been used in the next part of the thesis in order to validate the screening result and also to see the interaction between the inhibitor and CETP virtually. This study does not aim to find the possible binding poses of HCA but it is to show the most suitable binding sites for HCA. By using GLIDE (Grid-based ligand docking with energetics) molecular docking software which uses hierarchical filter in order to search for the best position of the inhibitor with the active site of the protein. This software is the best in order to search the most probable binding sites of crystal structure of CETP at which HCA would favour to bind at.

Based on the previous study done by Liu *et al.* (2012), crystal structure of torcetrapib bounds to CETP binding site has been obtained and PDB (Protein Data Bank) identification for this structure is 4EWS. Based on this crystal structure, torcetrapib bounds inside the CETP tunnel and this binding site is used as reference for the molecular docking study of HCA against CETP.

**(a)**

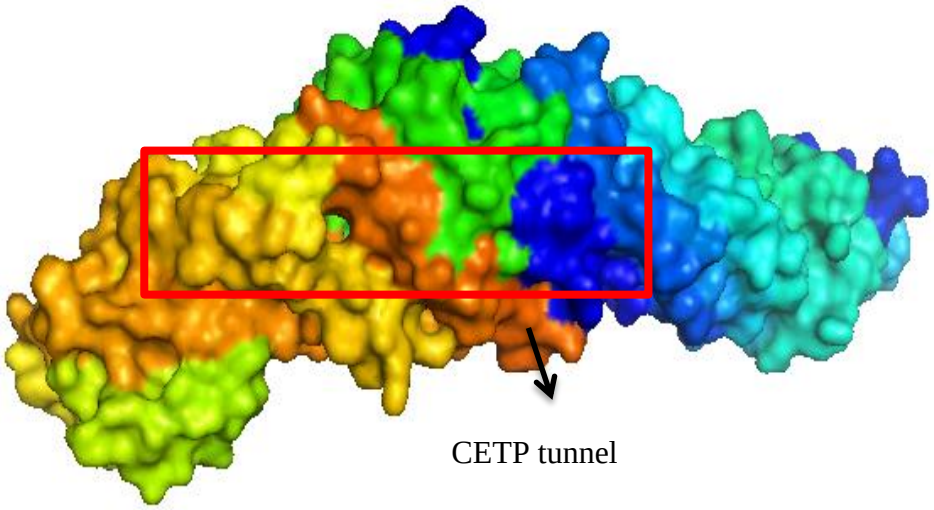


**(b)**

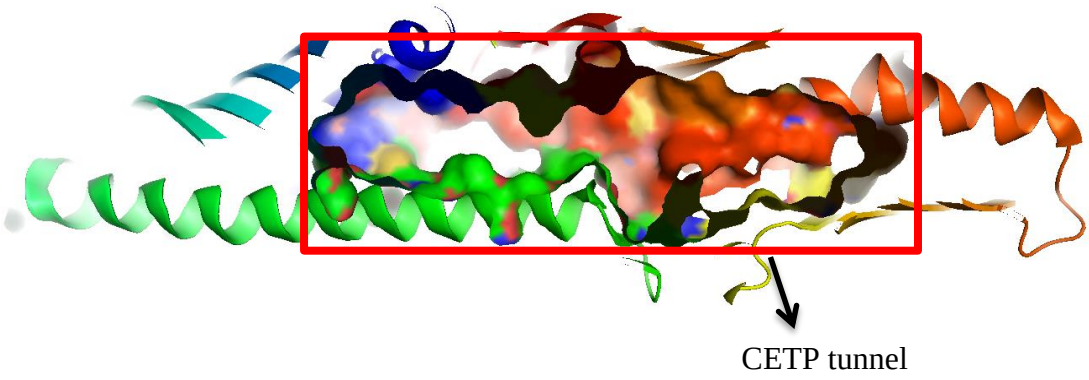


**Figure 48 (a) Image of CETP using solid surface setting in PyMol. (b) Sliced image of CETP where the tunnel is being labelled in red box.**

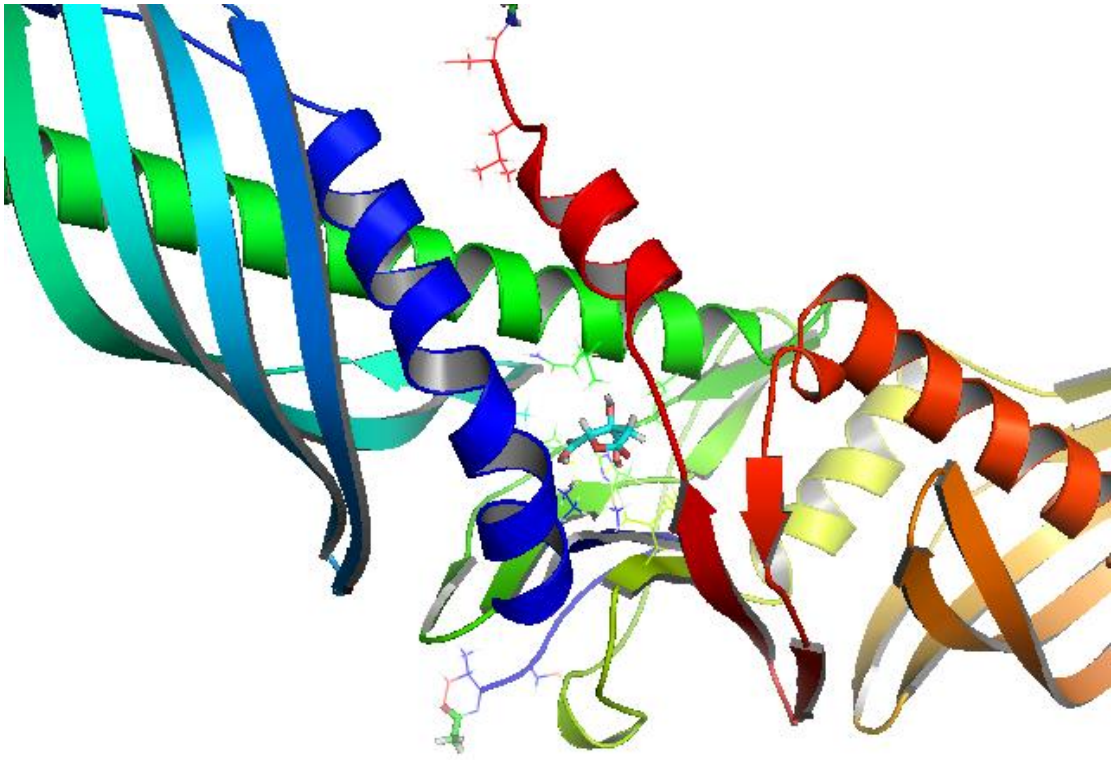

**Figure 49 Ribbon view of docking pose of HCA against CETP. The structure of HCA is indicated as the stick view.**

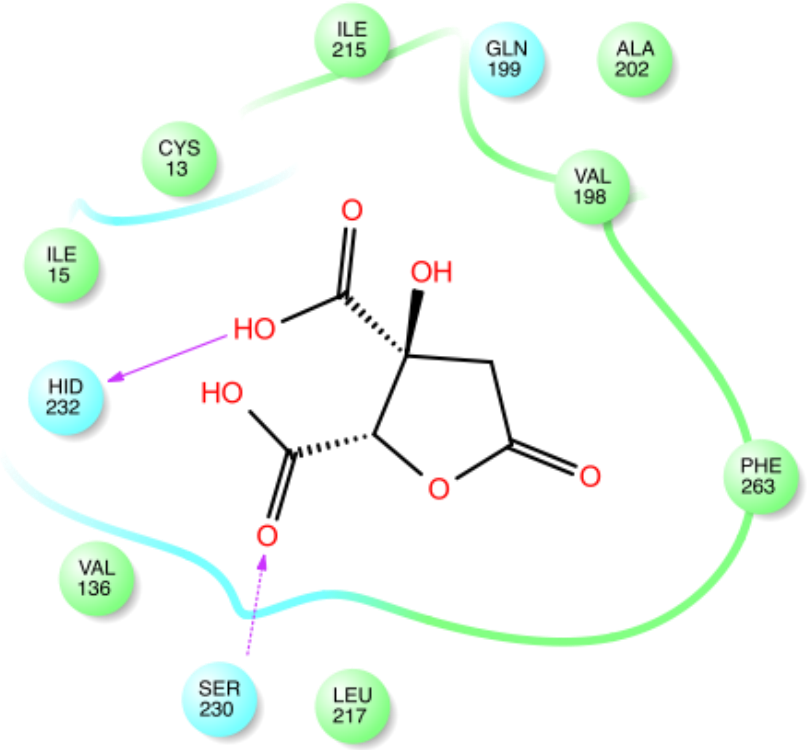


**Figure 50 2D representation of the ligand-receptor interaction between HCA and residue model obtained from docking using Glide showing hydrogen bonds involving backbone atoms (solid purple arrows) and hydrogen bonds involving side-chain atoms (dashed purple arrows). Polar and hydrophobic residues are depicted with light blue and green circles respectively.**

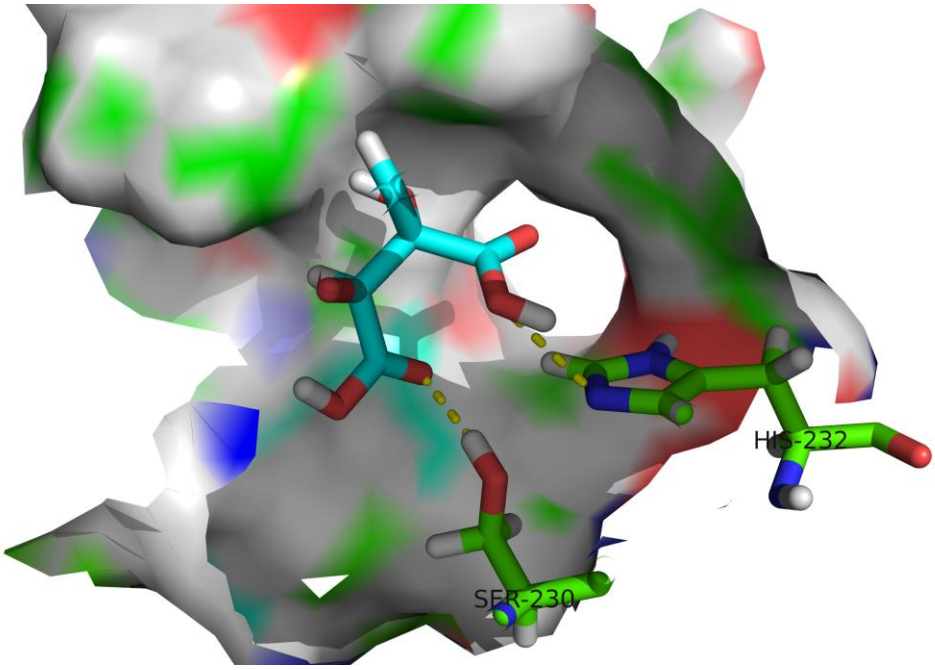


**Figure 51 3D representation of HCA and residues that involve. The yellow dashed line indicated the hydrogen bonding of HCA with HIS232 and SER230.**

Based on the Molecular docking results by using GLIDE, multiple poses has been generated but one best pose has been chosen. The best pose has been taken into account based on the reading of GLIDE gscore and GLIDE emodel. GLIDE gscore is an empirical scoring function that approximates the ligand binding free energy. GLIDE e model is a significant weighting of the force fields components (electrostatic and Van Der Waals energies). GLIDE basically use Emodel in order to choose the best pose of a ligand and will rank the best poses against one another with GLIDE score. So, GLIDE emodel can be summarized as scoring based on GLIDE score, internal ligand strain (External) and Coulomb and Van Der Waals energy.

**Table 11 Docking result of HCA from GLIDE**

| | |
|---|---|
| **GLIDE gscore** | -4.573 |
| **GLIDE emodel** | -31.665 |

The best pose and docking score for molecular docking of HCA to CETP are being summarized in table above. The GLIDE g-score reading is -4.573 and the GLIDE emodel value is -31.665. The GLIDE g-score that is being indicated in table 11 above shows the sum of the individual H-bond scores for H-bonds between the ligand and given residue. The more negative the score the stronger the H-bonding. Based on our results the negative values that was being obtained indicate that the H-bonding between HCA and CETP is strong. Based on this experiment, multiple poses has been generated and GLIDE emodel helps in picking up the 'best' pose of a ligand. The results obtained in this experiment is the best rank among other poses.

Based on figure 51, there are still large space left in the N pocket after HCA binding and C pocket are remain undisturbed. This suggests that HCA entered the tunnel through N-terminal opening. CETP tunnel are hydrophobic in nature and HCA is deeply buried inside the hydrophobic tunnel of N terminal. Based on the ligand receptor interaction figure, HCA is occupying the pocket formed by side chains of PHE263, VAL198, GLN199, ILE215, CYS13, ILE15, HIS232, VAL136, SER230 and LEU217. All of the side chain residues are hydrophobic at which PHE263 are being remarked as hydrophobic neck of the tunnel except for these three residues which are GLN199, SER230, and HIS232 which is a polar residues. Due to this properties, HCA forms hydrogen bonding towards SER230 and HIS232. This hydrogen bonds helps in the stability of the bonding of HCA towards CETP tunnel.

In order to revalidate the producibility of GLIDE docking data, rescoring by using GOLD suites has been implemented. The usage of GOLD has been employed since it is using different scoring matrices and different algorithm. The idea of revalidation of using different

docking software is to see whether HCA does bind to the same site when different docking software has been use. The score that provide the same binding site with the same residue through GOLD suites indicates that the GLIDE data are reproducible. The best Chemscore value obtained is **38.6** and it does shows the same binding site and residues compared to GLIDE results.

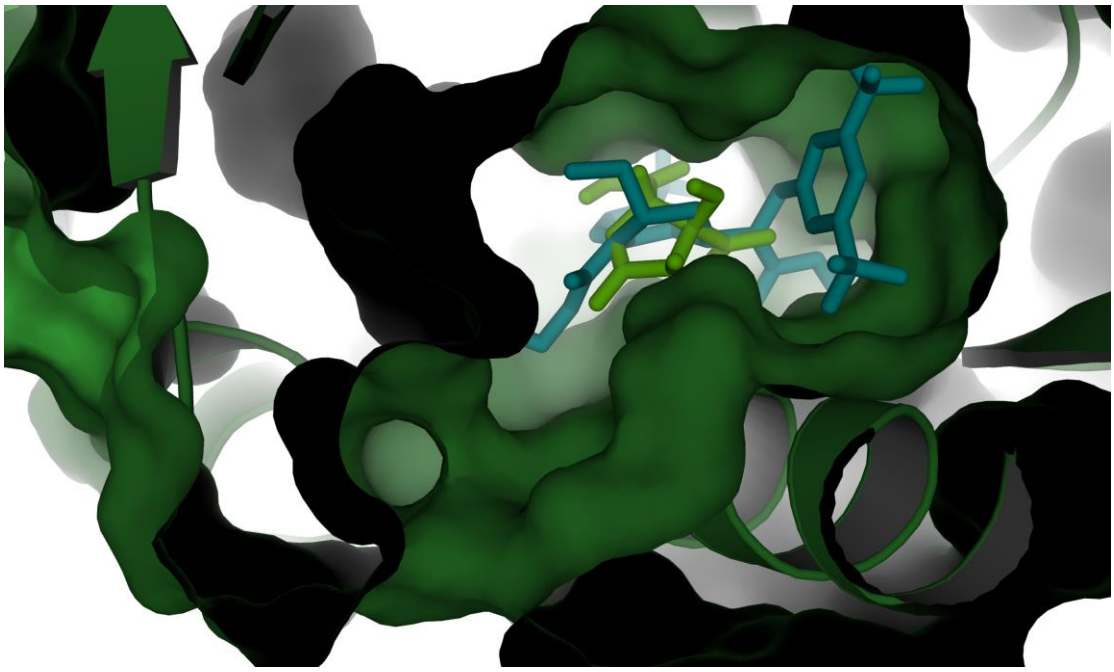

**Figure 52 3D superimposed image of HCA and torcetrapib where blue colour stick indicates torcetrapib and green colour stick is HCA.**

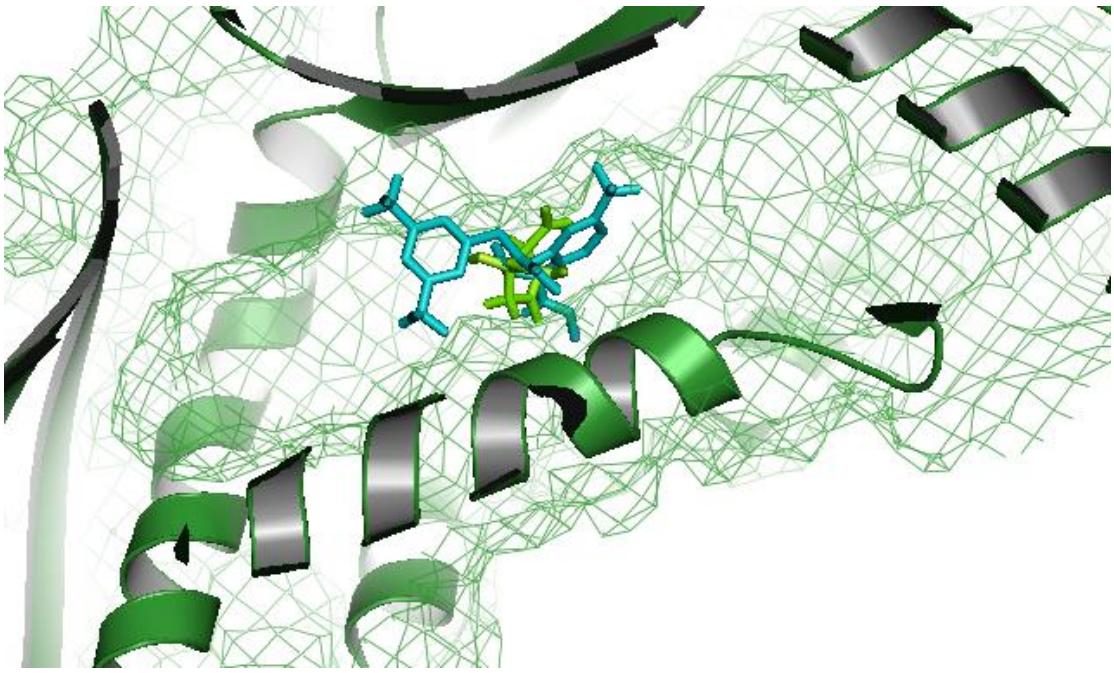

**Figure 53 3D mesh surface of superimposed image of torcetrapib (blue colored stick) and HCA (green colored stick)**

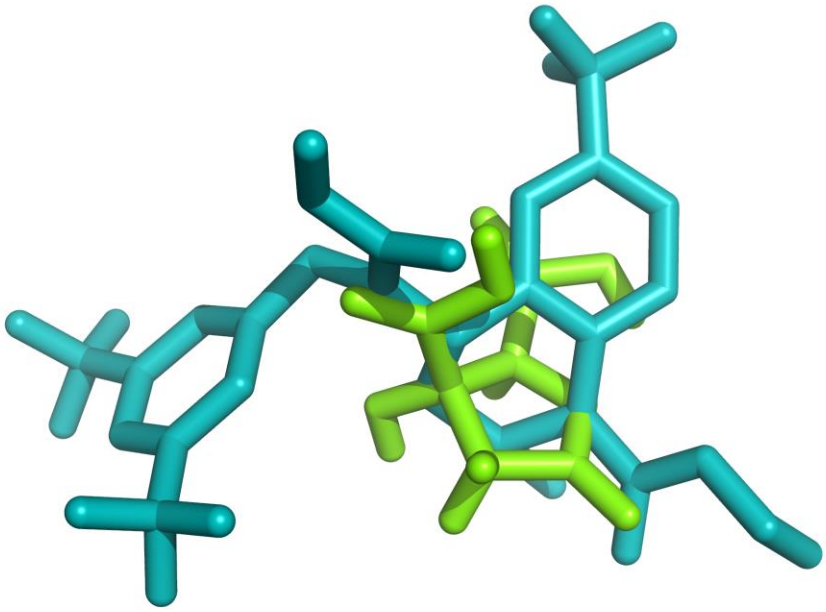

**Figure 54 Enlarged image of superimposed torcetrapib (blue colored stick) and HCA (green colored stick)**

The solved crystallised structure (PDB ID: 4EWS) with known inhibitor, Torcetrapib had been use as reference for its binding site. The structure had been loaded into Pymol and command script 'align' has been used to create superimposed image of Torcetrapib and HCA. Based on figure 52to figure 54, torcetrapib and HCA bounds at the same side although both of them have huge differences in structure. The (Root Mean Square Deviation) RMSD value that is being obtained through alignment is **2.703Å**. The RMSD measures how difference the two ligands which are HCA and torcetrapib. The smaller the values of RMSD indicates how closer and similar the ligands. Based on this result, the value obtained is expected for this structure (Koike *et al.*, 2008).

## 4.7 Molecular dynamic study of HCA inhibition.

Analysis through molecular dynamic study has been done as part of this thesis in order to see the stability of the HCA-CETP complex that is being immersed in explicit water molecules in nanosecond time scale. In this dynamic study, the complex are being tested in equilibrium state at which large scale motions are absent but they are still free to move but not in any specific direction (Zeiske *et al.*, 2016). This is important to see whether the HCA-CETP complex is still bind to each other when the molecular dynamic condition is being applied for the duration of 20ns timescale.

In this work, the interaction between CETP and HCA were studied. The system used is the HCA-CETP complex and MD simulations were performed with 10ns and 20ns. The main purpose for this study is to see the overall stability of the system in nanosecond time scale based on the Root Mean Square Deviation (RMSD) and Root Mean Square Fluctuation (RMSF) that obtained.

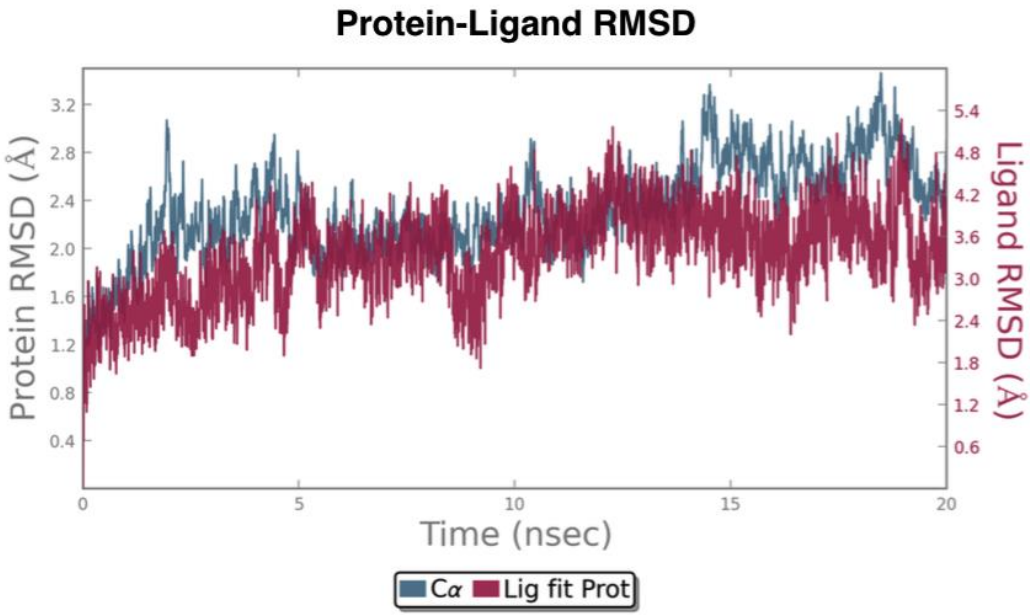


**Figure 55 RMSD value for 20ns simulation run**

Protein RMSD: In figure 55, shows the RMSD values of a protein (left Y-axis). All protein frames are first aligned on the reference frame backbone, and then the RMSD is calculated based on the atom selection in the system. Monitoring the RMSD of the protein can give insights into its structural conformation throughout the simulation. The overall structure of HCA-CETP complex appeared to be equilibrated less than 5ns as deciphered by the plot in figure 45 and figure 46. The backbone net displacement which is measured as α-carbon RMSD reach almost plateau reading after 5ns. The overall RMSD reading are range between 0.8 Å, 2.4 Å and the highest is 3.2 Å. The values seems to stabilize around a fixed value meaning that the system are already being equilibrated. The RMSD values does not fluctuates and seems to stabilize around fixed values which means that the system are fully equilibrated.

Ligand RMSD: Ligand RMSD (right Y-axis) indicates how stable the ligand is with respect to the protein and its binding pocket. In the above plot, 'Lig fit Prot' shows the RMSD of a ligand when the protein-ligand complex is first aligned on the protein backbone of the reference and then the RMSD of the ligand heavy atoms is measured. The values obtained for ligand RMSD are almost similar to the protein RMSD indicates the stability of the HCA

binding.

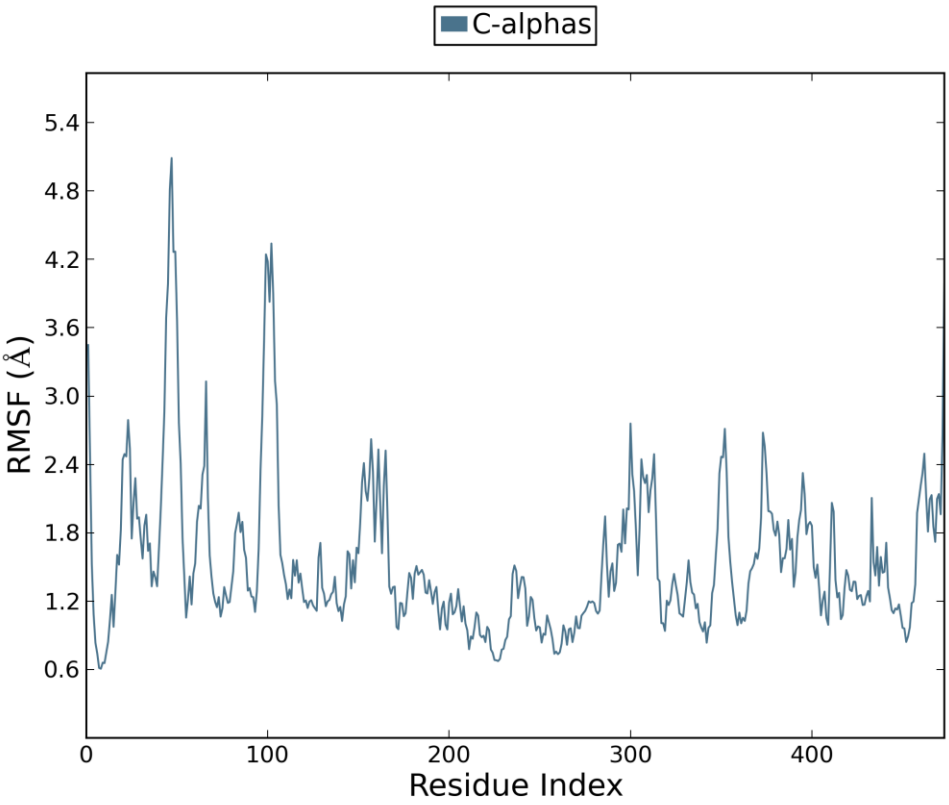


**Figure 56 RMSF value for CETP during 20ns simulation run**

The Root Mean Square Fluctuation (RMSF) analysis is used to characterizing changes along the protein chain throughout the simulation run. On this plot in figure 56, most of the RMSF values for amino acid fluctuates between 1.2 Å to 3 Å, but there is also some amino acid that fluctuates higher than that.

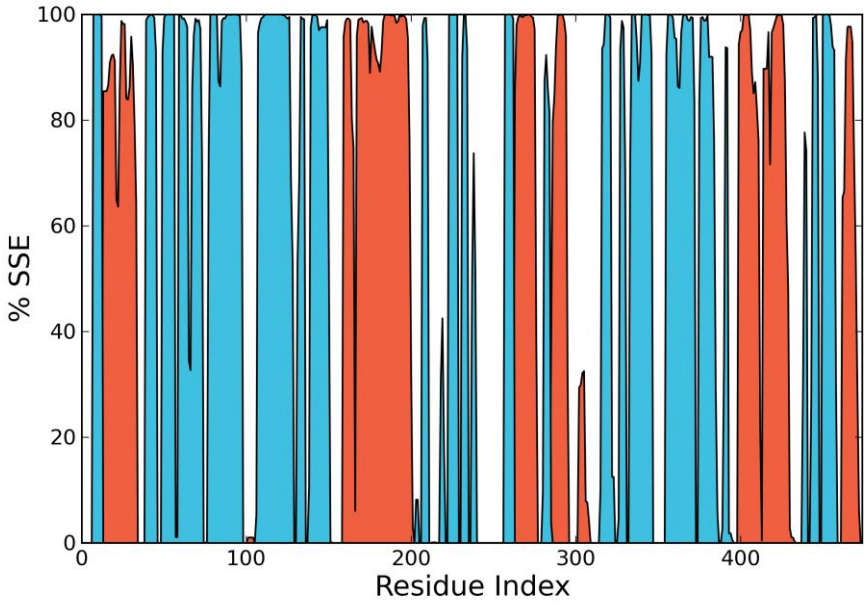


**Figure 57 Histogram of Secondary Structure Element (SSE) for every amino acid residue in CETP during simulation run. The orange region corresponds to the alpha helix and the blue region corresponds to the beta sheets of CETP.**

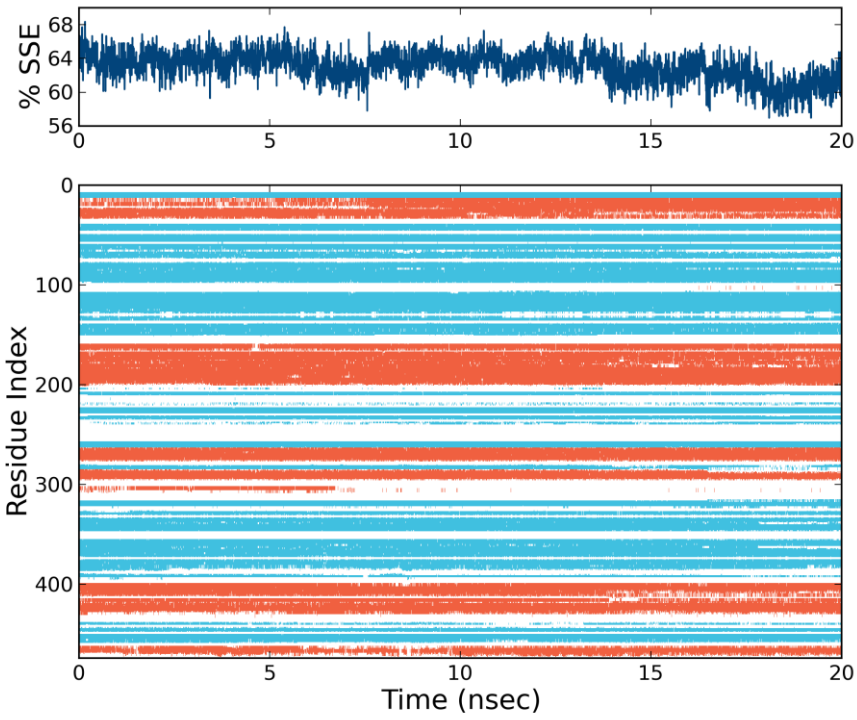


**Figure 58 SSE analysis like alpha helices and beta strands are monitored throughout of the simulation trajectory where top panel shows the percentage of SSE over 20ns simulation time and bottom panel monitors each amino acid residue over time. The blue region corresponds to beta sheets and the orange region corresponds to alpha helix strands of CETP.**

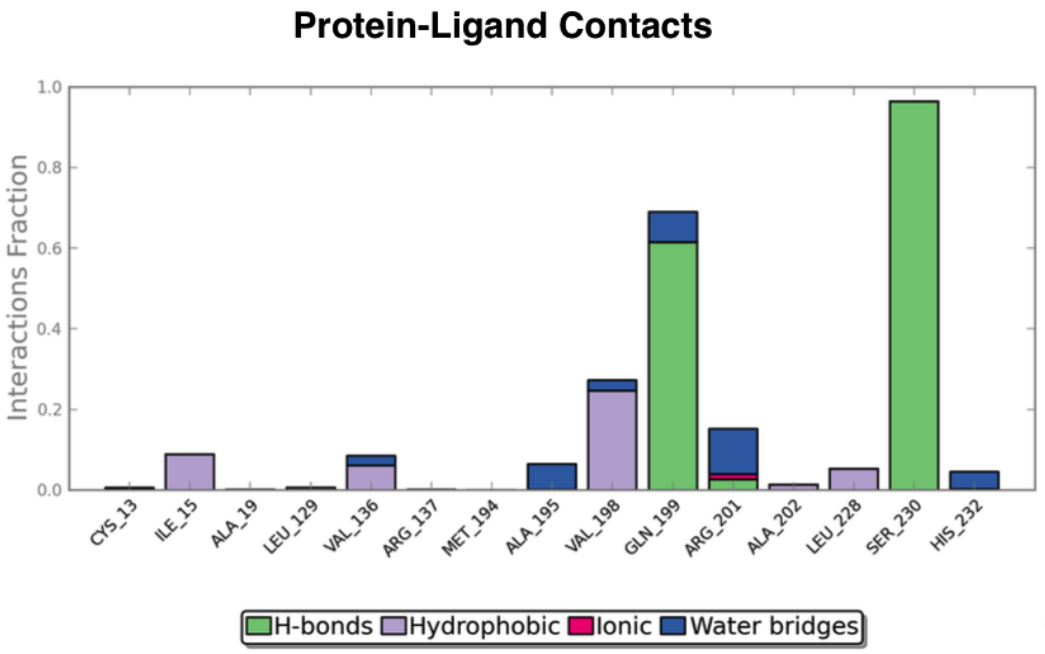


**Figure 59 Protein interaction diagram with the ligand throughout the simulation run. The green, purple, pink and blue indicates hydrogen bonds, hydrophobic bonds, ionic bonds and water bridges, respectively.**

The protein interaction diagram are shown above where the interaction can be categorized into four types such as Hydrogen Bond, Hydrophobic bond, Ionic bond and water bridges. Hydrogen bond can be largely seen on SER 230 and GLN 199. Small traces of hydrogen bond can be seen on ARG 201. Hydrophobic bonds interaction can be seen at residue ILE 15, VAL 136, VAL 198, ALA 202 and LEU 228. Small traces of ionic interaction can be seen at ARG 201. Water bridges interaction can be seen at residue VAL 136, ALA 195, VAL 198, ARG 201 and HIS 232.

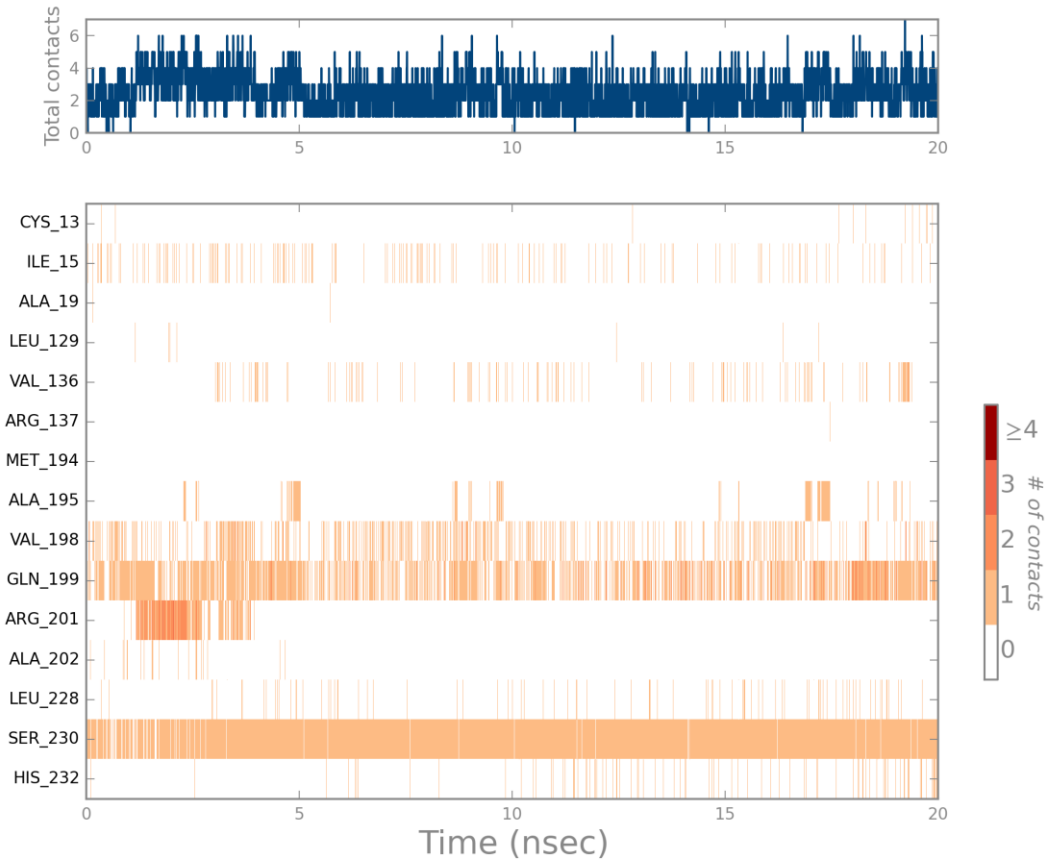


**Figure 60 Summary of interactions between residues over 20ns simulation run. There is a total of 6 contacts that has been made throughout the 20ns simulation run and this can be seen on the top panel of the figure. The X values of the bottom panel of the figures indicates the time taken for the overall simulation run and the Y values shows the residues that is involves. The values in the middles corresponds to the number of contacts based on the colour intensity.**

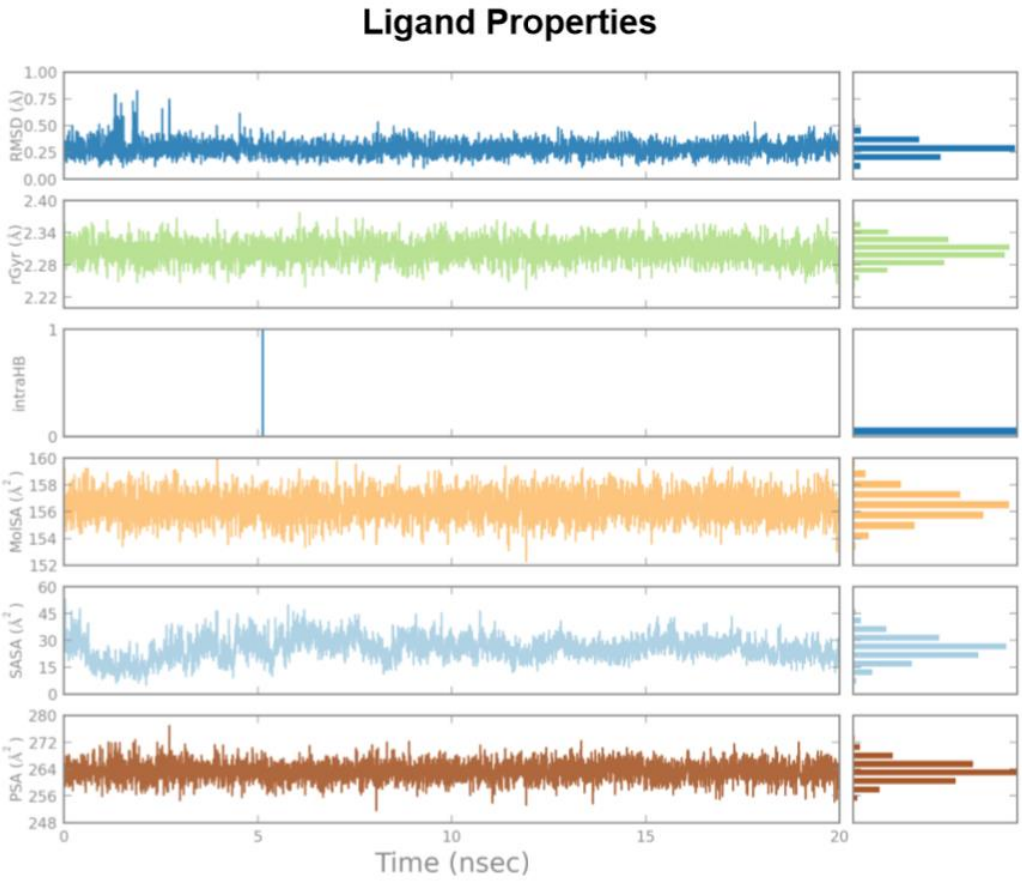


**Figure 61 Summary of ligand properties throughout 20ns simulation time which includes Ligand RMSD, radius of Gyration (rGyr), intramolecular hydrogen bonds, Molecular surface area (MolSA) Solvent accessible surface area (SASA) and Polar surface area (PSA). Ligand RMSD: RMSD value indicates the root mean square deviation of a ligand based on the time t=0 which is regard as reference time. Radius of Gyration (rGyr): Based on the principal moment of inertia and it measures the "extendedness" of ligand. Intramolecular Hydrogen Bonds (intraHB): Number of internal hydrogen bonds (HB) within a ligand molecule. Molecular Surface Area (MolSA): This value equivalent to Van der Waals surface area. Solvent Accessible Surface Area (SASA): Considered as a surface area of a molecule accessible by a water molecule. Polar Surface Area (PSA): Solvent accessible surface area in a molecule contributed only by oxygen and nitrogen atoms.**

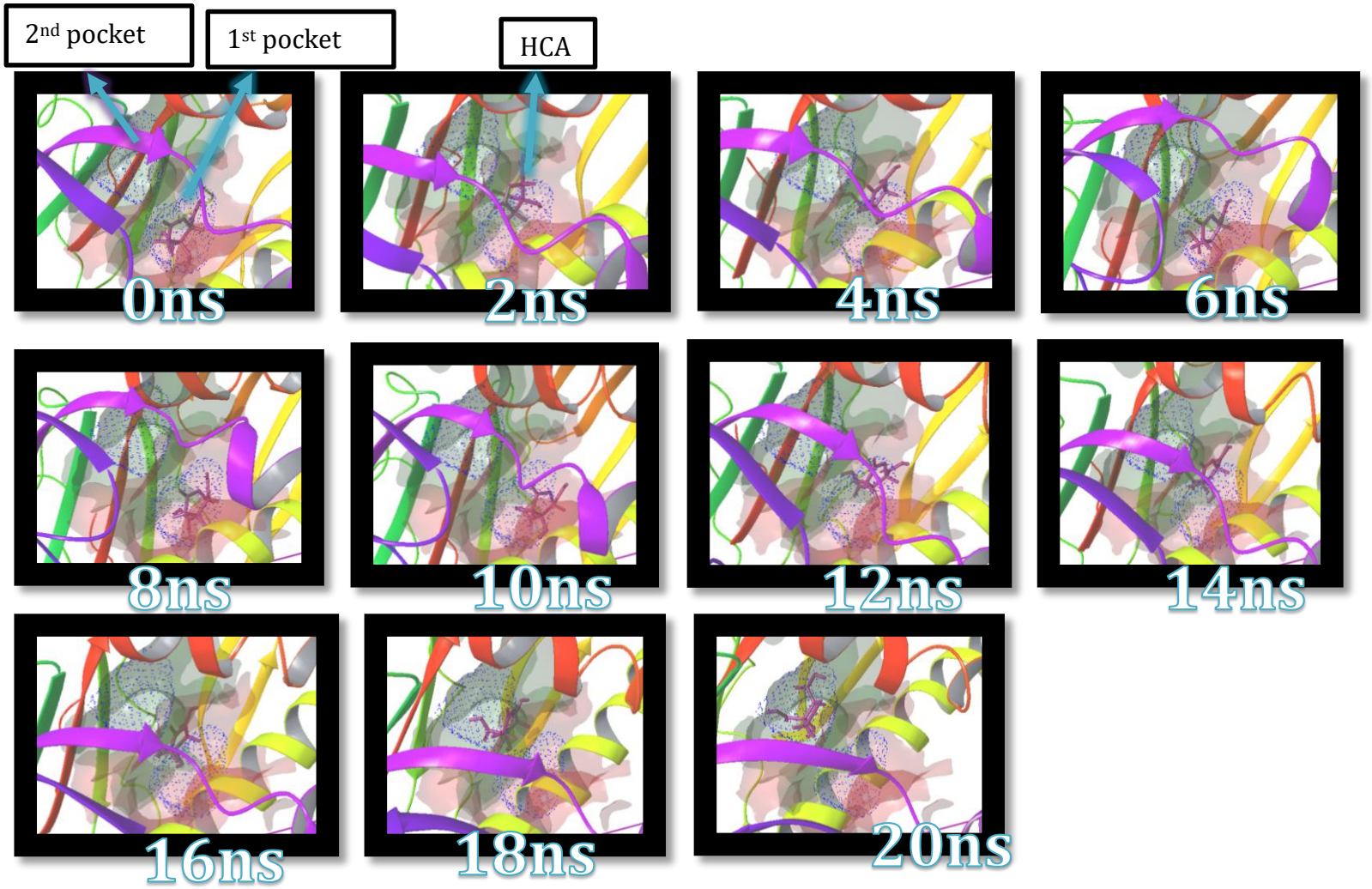


**Figure 62 Screenshot of MD simulation starting from 0ns to 20ns. There are two pockets that is being coloured purple. The first pocket is the place where HCA is situated before simulation run and the second pocket is the place where HCA is situated after 20ns simulation run. The purple colour stick structure is HCA**

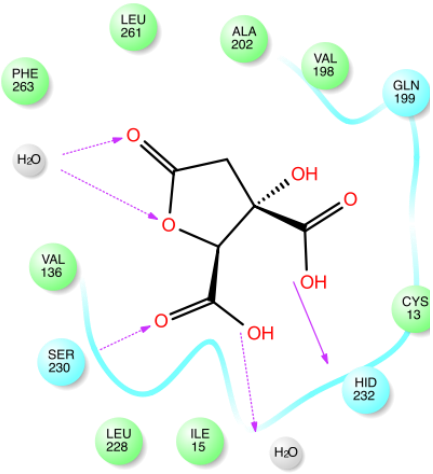


**0ns**

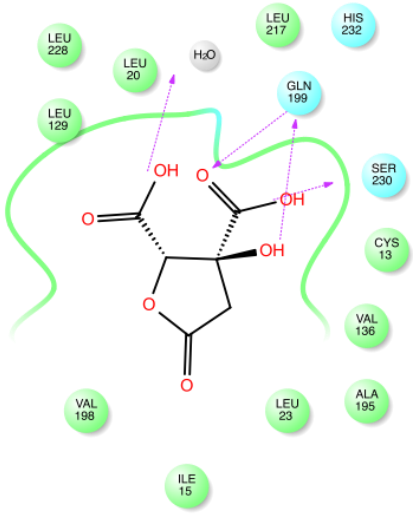


**20ns**

**Figure 63 2D representation of the ligand-receptor interaction between HCA and residue model obtained from docking using Glide during 0ns and 20ns simulation run, showing hydrogen bonds involving backbone atoms (solid purple arrows) and hydrogen bonds involving side-chain atoms (dashed purple arrows). Polar and hydrophobic residues are depicted with light blue and green circles respectively.**

Based on figure 62 the ligand does show stable bonding inside the CETP tunnel. This can be proven when HCA does not move outside the tunnel whenever pressure was applied for 20ns

timescale during the MD simulation. This indicate the stability of the HCA-CETP complex (Alonso *et al.*, 2006). And based on the figure 63, the comparison of the ligand interaction can be seen between before and after MD simulation. At 0ns, HCA forms hydrogen bonding between SER230 and HIS232. And after 20ns of MD simulation, HCA forms hydrogen bonding between GLN199 and SER230. And based on this analysis, HCA does not deviate too far and the hydrogen binding to SER230 shows the stability of the complex.

These simulations run give rise to valuable new predictions about the dynamics of HCA-CETP complex and provide meaningful insights in general into the reliability and reproducibility of the molecular modeling methods. Overall, the results of HCA binding towards CETP are very encouraging.

## 4.8 Structure activity relationship study of HCA analogues.

The final part of this thesis is to study the structure-activity relationship (SAR) between readily available HCA analogues chemical structure that are available in ZINC 3D database

and to assess its possible anti CETP effects through in vitro study and the possible binding site in the CETP tunnel through in-silico study.

ZINC 3D database, the web accessible chemical structure (http://blaster.docking.org/zinc)(Irwin & Shoichet, 2005) contain over 4.6million commercially available structures from over 50 compound vendors. In this part of chapter, searching through ZINC 3D database was being employed to see the activity relationship based on the structural similarity between HCA analogues and the potential inhibitory effects against CETP.

Based on ZINC 3D database, there are 9 analogues structure can be obtained. All of the analogues were then being subjected to molecular docking by GLIDE. Only two of the analogues are then being tested for structural activity relationship (SAR) study.

### 4.8.1 SAR studies of ZINC1656421

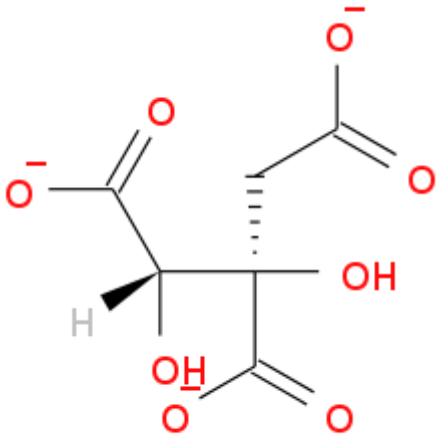


**Figure 64 Chemical structure of ZINC1656421**

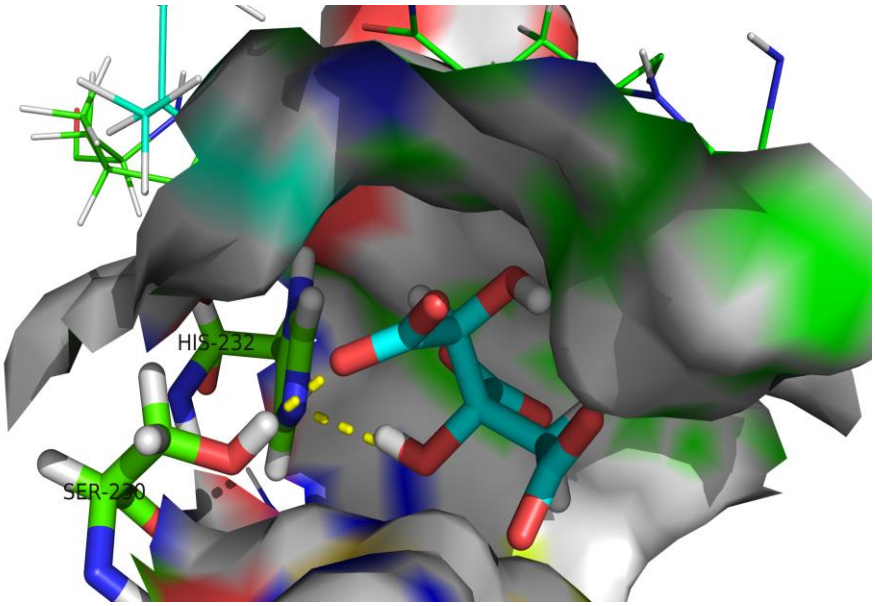


**Figure 65 3D image of docking between ZINC1656421. The yellow dotted lines shows the hydrogen bonding between ZINC1656421 and HIS232 and SER230.**

**Table 12 Docking Score result of ZINC1656421**

| | |
|---|---|
| **GLIDE gscore** | **-4.966** |
| **GLIDE emodel** | -25.859 |

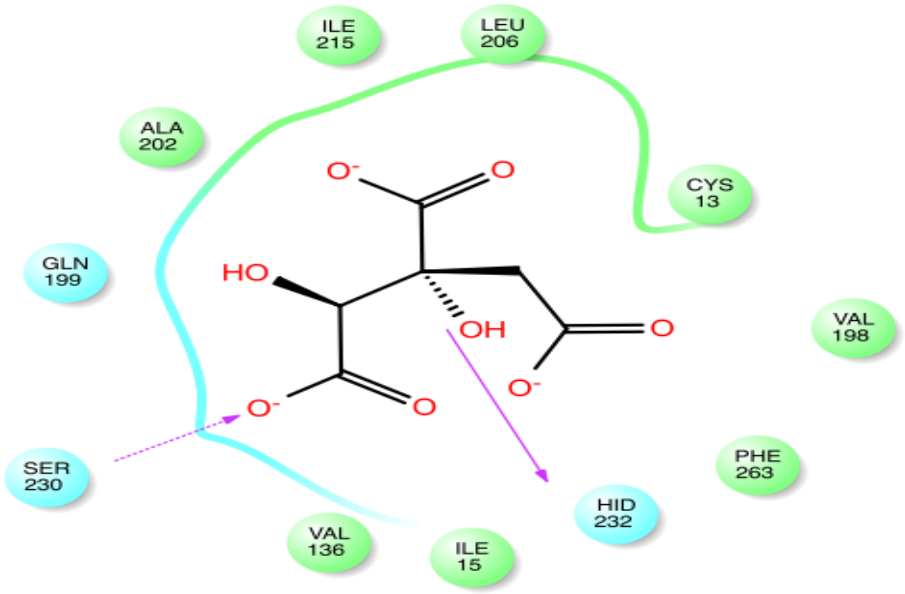


**Figure 66 2D representation of the ligand-receptor interaction between ZINC1656421 and residue model obtained from docking using Glide showing hydrogen bonds involving backbone atoms (solid purple arrows) and hydrogen bonds involving side-chain atoms (dashed purple arrows). Polar and hydrophobic residues are depicted with light blue and green circles respectively.**

Based on the docking result from GLIDE, ZINC1656421 does form hydrogen bonding towards SER230 and HIS232. And the docking score does show that ZINC1656421 does have good binding poses. The best pose and docking score for molecular docking of ZINC1656421 to CETP are being summarized in table 12. The GLIDE g-score reading is -4.966 and the GLIDE emodel value is -25.859. The GLIDE g-score that is being indicated in table 12 above shows the sum of the individual H-bond scores for H-bonds between the ligand and given residue. The more negative the score the stronger the H-bonding. Based on our results the negative values that was being obtained indicate that the H-bonding between ZINC1656421 and CETP is strong. Based on this experiment, multiple poses has been generated and GLIDE emodel helps in picking up the 'best' pose of a ligand. The results obtained in this experiment is the best rank among other poses.

### 4.8.2 SAR studies of ZINC895081

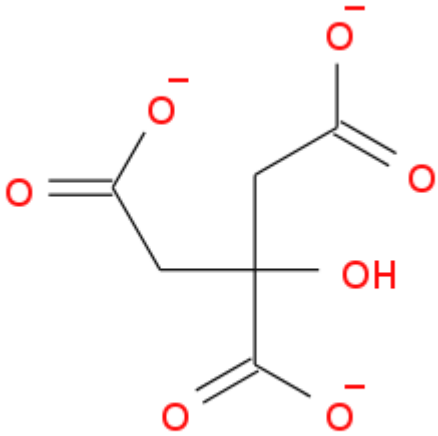


**Figure 67 Chemical Structure of ZINC895081**

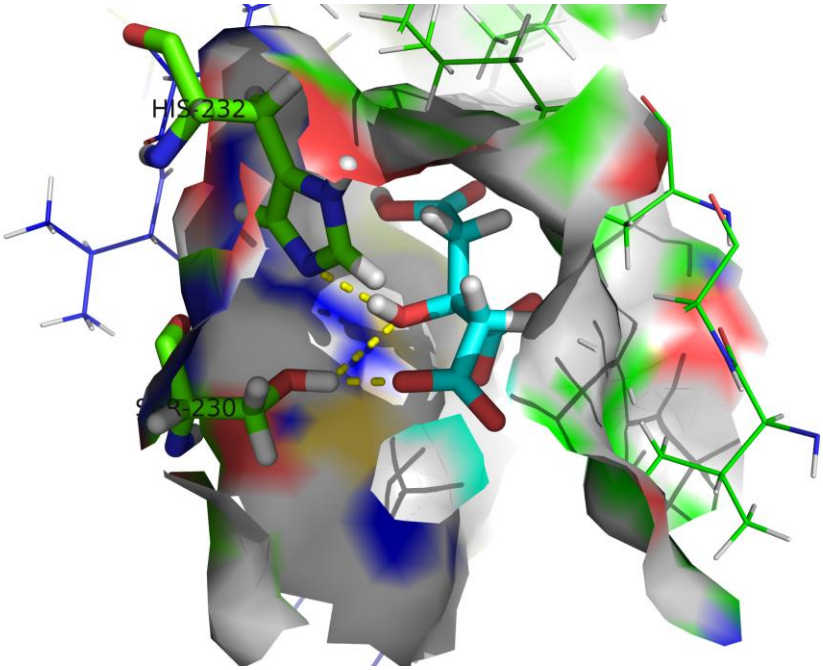


**Figure 68 3D view of docking between ZINC895081 and CETP. The yellow dotted lines shows the hydrogen bonding between HIS232 and SER230**

**Table 13 Docking Score result of ZINC895081**

| | |
|---|---|
| **GLIDE gscore** | **-4.732** |
| **GLIDE emodel** | -26.712 |

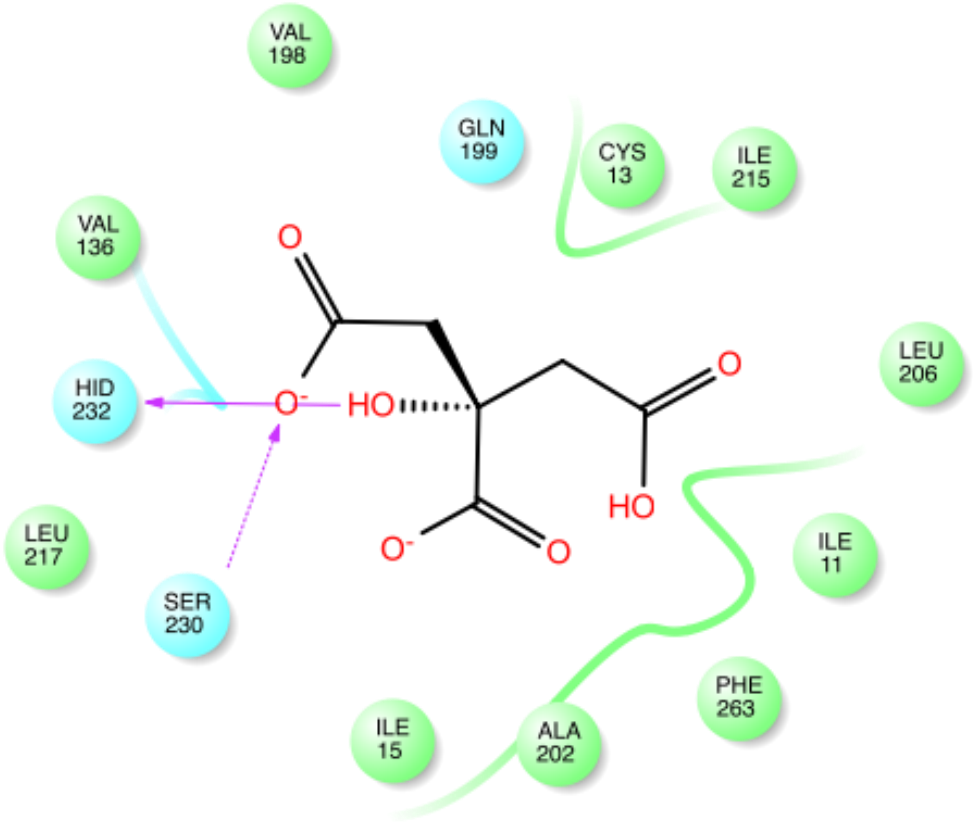


**Figure 69 2D representation of the ligand-receptor interaction between ZINC895081 and residue model obtained from docking using Glide showing hydrogen bonds involving backbone atoms (solid purple arrows) and hydrogen bonds involving side-chain atoms (dashed purple arrows). Polar and hydrophobic residues are depicted with light blue and green circles respectively.**

Hydrogen bonding that shows the stability of the complex also form between HIS232 residue and SER230 of CETP towards ZINC895081. The hydrogen bonds form due to the presence of hydroxyl group and the dissociate oxygen chain of ZINC895081. The best pose and

docking score for molecular docking of ZINC1656421 to CETP are being summarized in table 13. The GLIDE g-score reading is -4.732 and the GLIDE emodel value is -26.712. The GLIDE g-score that is being indicated in table 13 above shows the sum of the individual H-bond scores for H-bonds between the ligand and given residue. The more negative the score the stronger the H-bonding. Based on our results the negative values that was being obtained indicate that the H-bonding between ZINC895081 and CETP is strong. Based on this experiment, multiple poses has been generated and GLIDE emodel helps in picking up the 'best' pose of a ligand. The results obtained in this experiment is the best rank among other poses.

Two of the analogues that has been generated via ZINC 3D database has been chosen to undergo Structural Activity Relationship (SAR) study. Both of this analogues have been further tested for their inhibition towards CETP using in-vitro CETP assay. ZINC1656421 is also known as potassium hydroxycitrate tribasic monohydrate and ZNC895081 are also known as Isocitric acid.

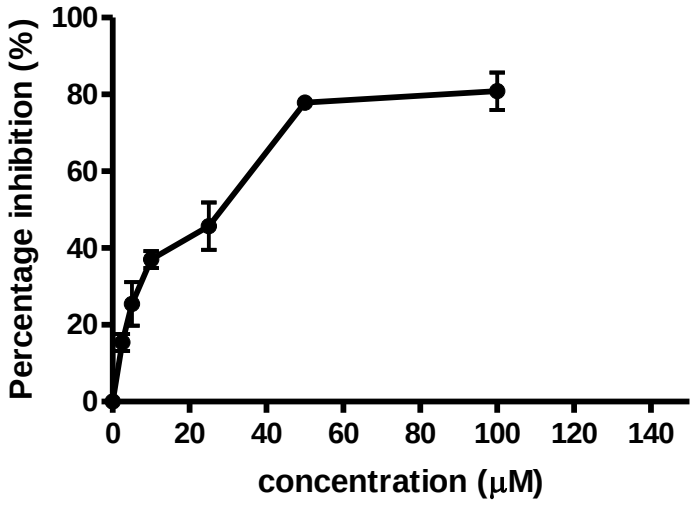


**Figure 70 Inhibition of CETP activity by ZINC1656421**

Based on CETP assay as summarized above, the IC50 obtained for ZINC1656421 is 29.87 ± 0.032 uM.

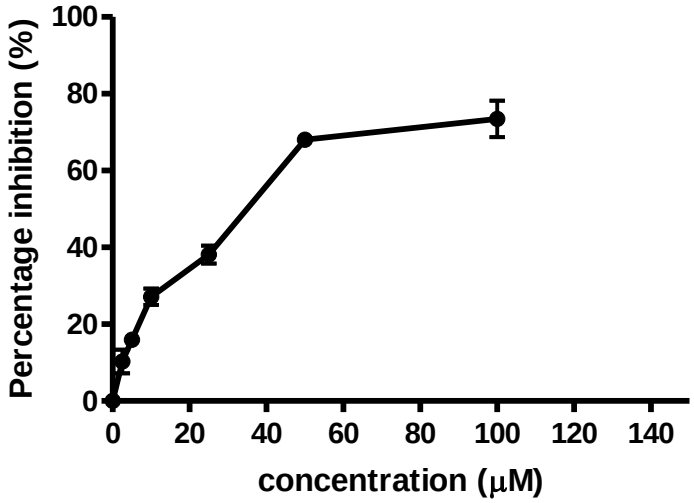


**Figure 71 Inhibition of CETP activity by ZINC895081**

Based on result above, compound 2 does shows inhibition towards CETP activity and the IC50 obtained is 35± 0.041uM.

Both of the analogues which are ZINC1656421 and ZINC895081 does shows promising results in the inhibition of CETP activity. Both of the analogues does shows promising results in the inhibition of CETP activity but the $IC_{50}$ values are higher than the $IC_{50}$ of pure compound of HCA and from this results suggests that HCA is more potent inhibitor compared to ZINC1656421 and ZINC895081. The higher the $IC_{50}$ values, the less potent the inhibitor is. . This explains that HCA is highly potent due to its properties which is easily soluble in water or hygroscopic (Lewis and Neelakantan, 1964) and compared to the other two analogues. This property giving HCA extra benefit because the presence of polar amino acids in the CETP tunnel which can easily forms strong hydrogen bonding with HCA. This further explains why HCA stablely binds to CETP.

The present results may have important implications for our understanding of the

pharmacological mechanisms of HCA and its analogues toward CETP activity and this study of structural features of HCA, its analogues and CETP are needed for the design of the new leads in the discovery of CETP inhibitor.

SAR knowledge reported herein will help to advance this chemical series further and provide template to produce more potent CETP inhibitors. Preliminary evaluations through in-silico studies and in vitro studies that the metabolic stability of HCA and its analogues series need to be improved via synthesis. Next goal is the conception of improved compounds which being obtained through synthesis activity, amenable to in-vivo target evaluation studies.

# Chapter 5: Conclusion

The main aim of this project is to assess the inhibitory effect of Malaysian plants on CETP activity. It is therefore, concluded from this present study that Malaysian local plant are sources for isolation of potential inhibitors of hypercholesterolaemic lowering agent that possesses inhibitory effect on CETP. Two different plants have been collected which are *Garcinia atroviridis* and *Garcinia parvifolia*. These two plants undergo methods of extraction and optimization which includes sample preparation for CETP assay. Two novel compounds which are clusianone and HCA are then tested on inhibitory effect against CETP activity. Based on the preliminary data obtained through screening of crude extracts, HCA were choosen for having an $IC_{50}$ of 20.07 ± 0.05 μM and this values shows that HCA is highly potent inhibitor on CETP activity. The inhibitory effect of HCA has been further revalidated using enzyme kinetic study, molecular docking study and molecular dynamic study.

HCA inhibition mechanism of action were done through enzyme kinetic study which acts as an important indicator to access the specific binding interaction that might be involved. Values generated from experimental results and plotted graph suggests that HCA possess noncompetitive inhibition characteristic in respect to CETP where Km is unchanged and Vmax is increasing as the substrate concentration increases. This very important result proves that HCA does possess drug like inhibitory characteristic as torcetrapib.

An in silico molecular modeling study further support and validate the assay results by pose and binding site validation and measuring the binding interaction between HCA and CETP. Our results suggest that HCA does binds to the same sites as torcetrapib in regards of CETP

tunnel. Molecular dynamic study has been done as part of this thesis in order to see the stability of the HCA-CETP complex in nanosecond time scale. The results obtained through this study suggest that the binding of HCA towards CETP is stable via the hydrogen bonds that exist at the SER 230 throughout 20ns simulation time.

In order to strengthen the results, two analogues of HCA which are being obtained through ZINC 3D database has been selected and being further tested their structure-activity relationship via molecular docking and CETP assay. The results suggest that HCA is potent compared to its analogues due to its properties which exhibit higher water solubility and this is strong evidence that HCA is a potent inhibitor as CETP tunnel is highly hydrophobic.

This work is mostly pioneering research concerning the interaction of CETP and HCA and thus paves the way to extend the scope of computational studies in order to gain a much deeper understanding concerning the inhibition of CETP. Overall, this PhD project gives a firm foundation for future research regarding HCA inhibition on CETP.

# Chapter 6: Future Perspectives

This study has successfully proved that Malaysian local plant as a source for secondary metabolites does have the potential ability to inhibit CETP. Hydroxycitric Acid (HCA) that is available commercially is surprisingly able to inhibit CETP activity. In order to gain deeper understanding regarding the inhibition of HCA against CETP, several recommendation that could be carried out to extend this study. This includes conducting this experiment in *in-vivo* level, synthesis of HCA to produce more potent analogues, and to see the interaction mechanism between HCA and CETP via X-ray crystallography.

Due to the positive results of inhibition of HCA against CETP in this PhD project, it could be extend to validate the HCA inhibition in animal context. This approach is important in order to see the efficacy of HCA inhibition in animal physiology. The recent advance in *in-vivo* approach is by using *in-vivo* molecular imaging system where we can see how does the HCA inhibition takes place in animal body enabling more complete understanding of the activity of a potential therapeutic. This is one of the interesting breakthrough that we could explore in CETP or atherosclerosis research at which we could see how does the interaction of HCA in real time imaging.

Synthesis approach whether it is total synthesis or semi synthesis is another potential area to be explored in CETP research. This can be carried out by synthesizing HCA or other potential CETP inhibitor by chemically adjusting the side chains in that active compounds to enhance binding affinity towards CETP and thus, increase the inhibitory activity. Hydroxyl

and amine group can be added in order to increase the hydrogen bonding between HCA and CETP.

Another interesting field to explore in the CETP research is X-ray crystallography. This enables us to understand the physical relationship between CETP and HCA. X-ray crystallography is one of the powerful techniques to gain significant understanding of the mechanism of inhibition by HCA at protein level. This approach can be used to involve HDL particle in order to better clarify the underlying mechanisms behind the inhibitory function of the drug.

The novel understanding could be used to develop new molecular agents to fight the progression of cardiovascular diseases since the existing medicines are not able to prevent all cardiovascular events. Overall, this piece of work gives a solid foundation for future research projects related to natural product and CETP.

# References


Agellon, L. B., Quinet, E. M., Gillette, T. G., Drayna, D. T., Brown, M. L., & Tall, A. R. (1990). Organization of the human cholesteryl ester transfer protein gene. *Biochemistry, 29*, 1372–1376.

Ambrose, J. A, & Barua, R. S. (2004). The pathophysiology of cigarette smoking and cardiovascular disease: an update. *Journal of the American College of Cardiology*, *43*(10), 1731–1737.

Amran, A. A., Zaiton, Z., Faizah, O., & Morat, P. (2009). Effects of *Garcinia atroviridis* on serum profiles and atherosclerotic lesions in the aorta of guinea pigs fed a high cholesterol diet. *Singapore Medical Journal*, 50, 295–299.

Anderson, T. J., Grégoire, J., Hegele, R. A., Couture, P., Mancini, G. B. J., McPherson, R., Francis, G. A., Poirier, P., Lau, D. C., Grover, S., Genest, J., Carpentier, A.C., Dufour, R., Gupta, M., Ward, R., Leiter, L. A., Lonn, E., Ng, D. S., Pearson, G. J., Yates, G. M., Stone, J. A., & Ur, E. (2013). 2012 update of the Canadian Cardiovascular Society guidelines for the diagnosis and treatment of dyslipidemia for the prevention of cardiovascular disease in the adult. *The Canadian Journal of Cardiology*, *29*(2), 151–67.

Ann S.B. (2013), Emerging modifiable ridk factors for cardiovascular disease in women, *Texas Heart Institute Journal,* 40(3), 293-295.

Atkinson, J.B. Hoover, R.L. Berry, K.K. Swift, L.L. (1989), Cholesterol-fed heterozygous Watanabe heritable hyperlipidemic rabbits: a new model for atherosclerosis, *Atherosclerosis,* 78, 123-136

Asztalos, B. F., Horvath, K. V, Kajinami, K., Nartsupha, C., Cox, C. E., Batista, M., Schaefer, E. J., Inazu, A., & Mabuchi, H. (2004). Apolipoprotein composition of HDL in cholesteryl ester transfer protein deficiency. *Journal of Lipid Research*, 45, 448–455.

Barrans, A., Collet, X., Barbaras, R., Jaspard, B., Manent, J., Vieu, C., Chap, H., & Perret, B. (1994). Hepatic lipase induces the formation of pre-$\beta_1$ High Density Lipoprotein (HDL) from triacylglycerol-rich $HDL_2$. A study comparing liver perfusion to in vitro incubation with lipases. *Journal of Biological Chemistry*, 269(15), 11572–11577.

Barter, P. (2009). Lessons Learned from the Investigation of Lipid Level Management to Understand its Impact in Atherosclerotic Events (ILLUMINATE) Trial. *American Journal of Cardiology*, 104(Suppl), 10E-15E.

Barter, P., Gotto, A. M., LaRosa, J. C., Maroni, J., Szarek, M., Grundy, S. M., Kastelein, J. J. P. , Bittner, V., & Fruchart, J.-C. (2007). HDL cholesterol, very low levels of LDL cholesterol, and cardiovascular events. *The New England Journal of Medicine*, *357*, 1301–1310.

Barter, P. J. (2003). Cholesteryl Ester Transfer Protein: A Novel Target for Raising HDL and Inhibiting Atherosclerosis. *Arteriosclerosis, Thrombosis, and Vascular Biology*, 23(2), 160–167.

Barter, P. J., Caulfield, M., Eriksson, M., Grundy, S. M., Kastelein, J. J. P., Komajda, M., Lopez-Sendon, J., Mosca, L., Tardif, J., Waters, D. D., Shear, C. L., Revkin, J. H., Buhr, K. A., Fisher, M. R., Tall, A. R., & Brewer, B. (2007). Effects of torcetrapib in patients at high risk for coronary events. *The New England Journal of Medicine*, 357(21), 2109–2122.

Barter, P. J., Nicholls, S., Rye, K. A., Anantharamaiah, G. M., Navab, M., & Fogelman, A. M. (2004). Antiinflammatory properties of HDL. *Circulation Research*, 94, 764-772.

Bentzon, J. F., Otsuka, F., Virmani, R., & Falk, E. (2014). Mechanisms of plaque formation and rupture. *Circulation Research*, 114(12), 1852–66.

Birtcher K.K. & Ballantyne C.M. (2004), Caretiology Patient Page: A patient perspective, *Circulation*, 110, e296-e297

Bloomfield, D., Carlson, G. L., Sapre, A., Tribble, D., McKenney, J. M., Littlejohn, Sisk, C. M., Mitchel, Y. & Pasternak, R. C. (2009). Efficacy and safety of the cholesteryl ester transfer protein inhibitor anacetrapib as monotherapy and coadministered with atorvastatin in dyslipidemic patients. *American Heart Journal*, 157,*352-360.*

Bocan, T.M.A. Mueller, S.B. Mazur, M.J. Uhlendorf, P.G. Brown, E.Q. and Kieft, K.A. (1993), The relationship between the degree of dietary-induced hypercholesterolaemia in the rabbit and the atherosclerotic lesion formation. *Atherosclerosis*, 102: 9-22.

Boden, W. E. (2000). High-density lipoprotein cholesterol as an independent risk factor in cardiovascular disease: assessing the data from framingham to the veterans affairs high-density lipoprotein intervention trial. *The American Journal of Cardiology*, 86(suppl), 19L-22L.

Boden, W.E. Probstfield, J.L. Anderson, T. Chaitman, B.R. Desvignes-Nickens, P. Koprowicz, K (2011), Niacin in patients with Low HDL cholesterol levels receivinb intensive statin therapy, *New England Journal of Medicine*, 365, 2255-2267.

Brosseau, M.E. Hoeg, J.M. (1999) Transgenic rabbits as models for atherosclerosis research, *J. Lipid Res*, 3, 365-375.

Bruce, C., Davidson, W. S.\, Kussie, P., Lund-Katz, S., Phillips, M. C. , Ghosh, R., & Tall, A. R. (1995). Molecular determinants of plasma cholesteryl ester transfer protein binding to high density lipoproteins. *Journal of Biological Chemistry*, 270(19), 11532–11542.

Buja, L.M. Kita, T. Goldstein, J.L. (1983), Cellular pathology of progressive atherosclerosis in the WHHL rabbit. AN animal model of familial hypercholesterolaemia, *Atherosclerosis*, 78, 123-136.

Burke, A. P., Kolodgie, F. D., Farb, A., Weber, D. K., Malcom, G. T., Smialek, J., & Virmani, R. (2001). Healed Plaque Ruptures and Sudden Coronary Death : Evidence

That Subclinical Rupture Has a Role in Plaque Progression. *Circulation*, 103(7), 934–940.

Burkill, I. H., Birtwistle, W., Foxworthy, F. W., Scrivenor, J. B., & Watson, J. G. (1966). *A Dictionary of the Economic Products of Malay Peninsula*., Kuala Lumpur, Malaysia, Ministry of Agriculture and Co-Operative.

Butler, M. S. (2004). The role of natural product chemistry in drug discovery. *Journal of Natural Products*, 67(12), 2141-2153. http://doi.org/10.1021/np040106y

Calabresi, L., Gomaraschi, M., & Franceschini, G. (2003). Endothelial protection by high-density lipoproteins: From bench to bedside. *Arteriosclerosis, Thrombosis, and Vascular Biology*, 23, 1724-1731.

Cao, G., Beyer, T. P., Zhang, Y., Schmidt, R. J., Chen, Y. Q., Cockerham, S. L., Zimmerman, K. M., Karathanasis, S. K., Cannady, E. A., Fields, T. & Mantlo, N. B. (2011). Evacetrapib is a novel, potent, and selective inhibitor of cholesteryl ester transfer protein that elevates HDL cholesterol without inducing aldosterone or increasing blood pressure. *The Journal of Lipid Research*, 52, 2169-2176, .

Chan, N. N., Colhoun, H. M., & Vallance, P. (2001). Cardiovascular risk factors as determinants of endothelium-dependent and endothelium-independent vascular reactivity in the general population. *Journal of the American College of Cardiology*, 38(7), 1814–1820.

Chasman, D. I., Paré, G., Mora, S., Hopewell, J. C., Peloso, G., Clarke, R., Cupples, L. A., Hamsten, A., Kathiresan, S., Malarstig, A., Ordovas, J. M., Ripatti, S., Miletich, J. P., & Ridker, P. M. (2009). Forty-three loci associated with plasma lipoprotein size, concentration, and cholesterol content in genome-wide analysis. *PLoS Genetics*, 5(11), 1-14.

Checovich, W.J. Fitch, W.L. Krauss, R.M. Smith, M.P. Rapacz, J. Smith, C.L. Attie, A.D. (1988), Defective catabolism and abnormal composition of low-density lipoproteins from mutant pigs with hypercholesterolaemia, *Biochemistry*,1, 1934-1941.

Cholesterol Treatment Trialists' (CTT) Collaboration, Baigent, C. Blackwell, L (2010), Efficacy and safety of more intensive lowering of LDL cholesterol, a meta analysis of data from 170,000 participants in 26 randomized trials, *Lancets*, 376, 1670-1681.

Clark, R. W., Ruggeri, R. B., Cunningham, D., & Bamberger, M. J. (2006). Description of the torcetrapib series of cholesteryl ester transfer protein inhibitors, including mechanism of action. *Journal of Lipid Research*, 47, 537–552.

Clay, M. A., Newnham, H. H., Forte, T. M., & Barter, P. I. (1992). Cholesteryl ester transfer protein and hepatic lipase activity promote shedding of apo A-I from HDL and subsequent formation of discoidal HDL. *Biochimica et Biophysica Acta - Lipids and Lipid Metabolism*, 1124, 52–58.

Connell, J. M. C., MacKenzie, S. M., Freel, E. M., Fraser, R., & Davies, E. (2008). A lifetime of aldosterone excess: Long-term consequences of altered regulation of aldosterone production for cardiovascular function. *Endocrine Reviews,* 29(2), 133-154.

Connelly, P. W. (1999). The role of hepatic lipase in lipoprotein metabolism. *Clinica Chimica Acta*, 286, 243–55.

Cooney, M.T. Dudina, A.L. Graham, I.M. (2009), Value and limitations of existing scores for the assessment of cardiovascular risk- A review for clinicians, *Journal of American college of cardiology,* 54; 1209-1227

Cook, N. C., & Samman, S. (1996). Flavonoids - Chemistry, metabolism, cardioprotective effects, and dietary sources. *Journal of Nutritional Biochemistry,* 7, 66-76.

Copeland, A. R. (2000). *Enzymes: A Practical Introduction to Structure, Mechanism, and Data Analysis*. New Jersey, USA: John Wiley & Sons.

Corsini, A. Bellosta, S. Baetta, R. Fumagalli, R. Bernini, F. (1999), New insights into the pharmacodynamics and pharmacokinetics properties of statins, *Pharmacology Therapy,* 84, 413-428.

Cortes, V.A. Busso, D. Mardones, P. Maiz, A. Arteaga, A. Nervi, F. and Rigotto, A. (2013). Advances in the physiological implications of cholesterol, *Biological reviews,* 3, 1-15

Critchley, J., Liu, J., Zhao, D., Wei, W., & Capewell, S. (2004). Explaining the increase in coronary heart disease mortality in Beijing between 1984 and 1999. *Circulation*, *110*(10), 1236–1244.

Crockett, E. L. (1998). Cholesterol Function in Plasma Membranes from Ectotherms: Membrane-Specific Roles in Adaptation to Temperature. *Integrative and Comparative Biology*, *38*(2), 291–304.

Crowther, M. a. (2005). Pathogenesis of atherosclerosis. *Hematology / the Education Program of the American Society of Hematology. American Society of Hematology. Education Program*, 436–441.

Cuchel, M., & Rader, D. J. (2006). Macrophage reverse cholesterol transport: key to the regression of atherosclerosis? ,*Circulation*, *113*(21), 2548–2555.

Cullen, P., & Lorkowski, J. R. S. (2005). The Pathogenesis of Atherosclerosis, *Handbook of Experimental Cardiology*, 170, 3–70.

Darden, T., Perera, L., Li, L., & Lee, P. (1999). New tricks for modelers from the crystallography toolkit: The particle mesh Ewald algorithm and its use in nucleic acid simulations. *Structure*, 7. R55-R60.

Davidson, M. H., & Rosenson, R. S. (2009). Novel Targets that Affect High-Density Lipoprotein Metabolism: The Next Frontier. *American Journal of Cardiology*, 104(suppl), 52E-57E.

Davis, H.R. Vesselinovitch, D. Wissler, R.W. (1984), Histochemical detection and quantification of macrophages in rhesus and cynomolgus monkey atherosclerotic lesions. *Journal of Histochemistry and Cytochemistry,* 12: 1319-1327

Dawson, P. A., & Rudel, L. L. (1999). Intestinal cholesterol absorption. *Current Opinion in Lipidology*, 10, 315–320.

De Grooth, G. J., Klerkx, A. H. E. M., Stroes, E. S. G., Stalenhoef, A. F. H., Kastelein, J. J. P., & Kuivenhoven, J. A. (2004). A review of CETP and its relation to atherosclerosis. *Journal of Lipid Research*, *45*(11), 1967–74.

Drayna, D., Jarnagin, A. S., McLean, J., Henzel, W., Kohr, W., Fielding, C., & Lawn, R. (1987). Cloning and sequencing of human cholesteryl ester transfer protein cDNA. *Nature*, 327, 632–634.

Fabricant, D. S., & Farnsworth, N. R. (2001). The value of plants used in traditional medicine for drug discovery. *Environmental Health Perspectives*, 109, 69–75.

Farnsworth, N. R., Akerele, O., Bingel, A. S., Soejarto, D. D., & Guo, Z. (1985). Medicinal plants in therapy. *Bulletin of the World Health Organization*, *63*, 965–981.

Fielding, C. J. (1978). Metabolism of cholesterol-rich chylomicrons. Mechanism of binding and uptake of cholesteryl esters by the vascular bed of the perfused rat heart. *Journal of Clinical Investigation*, *62*, 141–151.

Forrest, M. J., Bloomfield, D., Briscoe, R. J., Brown, P. N., Cumiskey, A.-M., Ehrhart, J., Hershey, J. C., Keller, W. J., McPherson, H. E., Messina, E., Peterson, L. B., Sharif-Rodriguez, W., Siegl, P. K. S., Sinclair, P. J., Sparrow, C. P., Stevenson, A. S., Sun, S. Y., Tsai, C, Vargas, H., Walker III, M., West, S. H., White, V., & Woltmann, R. F. (2008). Torcetrapib-induced blood pressure elevation is independent of CETP inhibition and is accompanied by increased circulating levels of aldosterone. *British Journal of Pharmacology*, 154, 1465–1473.

Forte, T. M., Subbanagounder, G., Berliner, J. A., Blanche, P. J., Clermont, A. O., Jia, Z., Oda, M. N., Krauss, R. M., & Bielicki, J. K. (2002). Altered activities of anti-atherogenic enzymes LCAT, paraoxonase, and platelet-activating factor acetylhydrolase in atherosclerosis-susceptible mice. *Journal of Lipid Research*, 43, 477–485.

Foti, R. S., & Fisher, M. B. (2004). Impact of incubation conditions on bufuralol human clearance predictions: Enzyme lability and nonspecific binding. *Drug Metabolism and Disposition*, 32, 295–304.

Frick, M.H. Elo, O. Haapa, K. Heinonen, O.P. Heinsalmi, P. Helo, P. Huttunen, J.K. Kaitaniemi, P. Koskinen, P. Manninen, V. Maenpaa, H. Maikonen, M. Manttari, M. Norola, S. Pasternack, A. (1987), Helsinki HEART study: Primary intervention trial with gemfibrozil in middle-aged men with safety of treatment, changes in risk factors and incidence of coronary heart disease, *New England Journal*, 317(20), 1237-1245.

Friesner, R. A., Banks, J. L., Murphy, R. B., Halgren, T. A., Klicic, J. J., Mainz, D. T., Repasky, M. P., Knoll, E. H., Shelly, M., Perry, J. K., Shaw, D. E., Francis, P. &

Shenkin, P. S. (2004). Glide: A New Approach for Rapid, Accurate Docking and Scoring. 1. Method and Assessment of Docking Accuracy. *Journal of Medicinal Chemistry*, 47, 1739–1749.

Friesner, R. A.; Murphy, R. B.; Repasky, M. P.; Frye, L. L.; Greenwood, J. R.; Halgren, T. A.; Sanschagrin, P. C.; Mainz, D. T., (2006). "Extra Precision Glide: Docking and Scoring Incorporating a Model of Hydrophobic Enclosure for Protein-Ligand Complexes," *Journal of Medicinal Chemistry*, 49, 6177–6196.

Funder, J.W. (2006), Mineralocorticoid Receptors and Cardiovascular Damage: It's not just aldosterone, *Hypertension,* 47, 634-635.

Funder, J. W. (2010). Aldosterone, hypertension and heart failure: insights from clinical trials. *Hypertension Research : Official Journal of the Japanese Society of Hypertension*, 33, 872–875.

García-García, H. M., Mintz, G. S., Lerman, A., Vince, G., Margolis, P., van Es, G. A., Morel, M. A., Nair, A., Virmani, R., Burke, A. P., Stone, G. W., & Serruys, P. W. (2009). Tissue characterisation using intravascular radiofrequency data analysis: Recommendations for acquisition, analysis, interpretation and reporting. *EuroIntervention*, 5, 177–189.

Gauthier, B., Robb, M., Gaudet, F., Ginsburg, G. S., & Mcpherson, R. (1999). Characterization of a cholesterol response element ( CRE ) in the promoter of the cholesteryl ester transfer protein gene : functional role of the transcription factors SREBP-1a, -2, and YY1, *Journal Lipid of Research*, 40, 1284-1293.

Gerrity, R.G. Goss, J.A. Soby, L. (1985), Control of monocyte recruitment by chemotactic factor(s) in lesion-prone areas of swine aorta, *Artherosclerosis, 5:* 55-66

Gerrity, R.G. Natarajan, R. Nadler, J.L. Kimsey, T. (2001), Diabetes-induced accelerated atherosclerosis in swine, *Diabetes,* 1654-1665.

Glomset, J. A. (1968). The plasma lecithins:cholesterol acyltransferase reaction. *Journal of Lipid Research*, 9, 155–167.

Gordon, D. J., Probstfield, J. L., Garrison, R. J., Neaton, J. D., Castelli, W. P., Knoke, J. D., Jacobs, D. R., Bangdiwala, S., & Tyroler, H. A. (1989). *High-density lipoprotein cholesterol and cardiovascular disease. Four prospective American studies. Circulation*, 79, 8-15.

Gotto, A. M., Havel, R. J., & Pownall, H. J. (1986). Introduction to the plasma lipoproteins. *Methods in Enzymology*, 128(1947), 3–41.

Grover, S.A. Lowenstyn, I. Joseph, 1. (2007), Patients knowledge of coronary risk profile imporves the effectiveness of dyslipidaemia therapy, the check up study: a randomized controlled trial, *Architectural Internal Medicine,* 167: 2296-2303.

Grover, S.A. Coupal, L. Kaouche, M. Lovenstyne, I. (2007), Preventing cardiovascular disease among Canadians: What are the potential benefits of treating hypertension or dyslipidaemia?, *Canadian Journal Cardiology,* 23,467-473.

Guo, J., Hurley, M. M., Wright, J. B., & Lushington, G. H. (2004). A docking score function for estimating ligand-protein interactions: Application to acetylcholinesterase inhibition. *Journal of Medicinal Chemistry*, 47, 5492–5500.

Guo, Z.; Mohanty, U.; Noehre, J.; Sawyer, T. K.; Sherman, W.; Krilov, G., (2010). "Probing the α-Helical Structural Stability of Stapled p53 Peptides: Molecular Dynamics Simulations and Analysis," *Chemistry Biological Drug Design.*,75, 348-359

Halgren, T. A.; Murphy, R. B.; Friesner, R. A.; Beard, H. S.; Frye, L. L.; Pollard, W. T.; Banks, J. L., (2004). "Glide: A New Approach for Rapid, Accurate Docking and Scoring. 2. Enrichment Factors in Database Screening," *Journal Medicinal Chemistry*, 47, 1750–1759

Hamilton, J. A., & Deckelbaum, R. J. (2007). Crystal structure of CETP: new hopes for raising HDL to decrease risk of cardiovascular disease? *Nature Structural & Molecular Biology*, 14(2), 95-97.

Hassall, D. G., Owen, J. S., & Bruckdorfer, K. R. (1983). The aggregation of isolated human platelets in the presence of lipoproteins and prostacyclin. *The Biochemical Journal*, 216, 43–49.

Hassan, H. H., Denis, M., Lee, D.-Y. D., Iatan, I., Nyholt, D., Ruel, I., Krimbou, L., & Genest, J. (2007). Identification of an ABCA1-dependent phospholipid-rich plasma membrane apolipoprotein A-I binding site for nascent HDL formation: implications for current models of HDL biogenesis. *Journal of Lipid Research*, 48(11), 2428–2442.

Heinecke, J. (2011). HDL and Cardiovascular-Disease Risk — Time for a New Approach? *New England Journal of Medicine*., 364, 170-171.

Hobbs F.D.R. (2004), Cardiovascular disease: Different strategies for primary and secondary prevention?, *Heart,* 90(10), 1217-1223.

Hu, X., Dietz, J. D., Xia, C., Knight, D. R., Loging, W. T., Smith, A. H., Yuan, H., Perry, D. A. & Keiser, J. (2009). Torcetrapib induces aldosterone and cortisol production by an intracellular calcium-mediated mechanism independently of cholesteryl ester transfer protein inhibition. *Endocrinology*, *150*, 2211–2219.

Hughes, J.R. (2003), Motivating and helping smokers to stop smoking, *Journal of General Internal Medicine,* 18(2), 1053-1057.

Ibañez, B., Badimon, J. J., & Garcia, M. J. (2009). Diagnosis of Atherosclerosis by Imaging. *American Journal of Medicine*, 122, S15-S25.

Igbinosa, O. O., Igbinosa, E. O., & Aiyegoro, O. A. (2009). Antimicrobial activity and phytochemical screening of stem bark extracts from *Jatropha curcas* (Linn). *African Journal of Pharmacy and Pharmacology*, 3, 58–62.

Insull, W. (2009). The Pathology of Atherosclerosis: Plaque Development and Plaque Responses to Medical Treatment. *American Journal of Medicine*, 122 (Suppl), S3-S14.

Irwin, J. J., & Shoichet, B. K. (2005). ZINC - A free database of commercially available compounds for virtual screening. *Journal of Chemical Information and Modeling*, 45, 177–182.

Irwin, J. J., Sterling, T., Mysinger, M. M., Bolstad, E. S., & Coleman, R. G. (2012). ZINC: A free tool to discover chemistry for biology. *Journal of Chemical Information and Modeling*, 52, 1757-1768.

Ishibashi, S., Brown, M. S., Goldstein, J. L., Gerard, R. D., Hammer, R. E., & Herz, J. (1993). Hypercholesterolemia in low density lipoprotein receptor knockout mice and its reversal by adenovirus-mediated gene delivery. *The Journal of Clinical Investigation*, 92, 883–893.

Istvan, E. (2003). Statin inhibition of HMG-CoA reductase: A 3-dimensional view. In *Atherosclerosis Supplements*, 4, 3-8.

Jean, D. (2004), Beneficial cardiovascular Pleiotropic effects of statin, *Circulation,* 109, 111-39-111-43.

Jena, B. S., Jayaprakasha, G. K., Singh, R. P., & Sakariah, K. K. (2002). Chemistry and biochemistry of (-)-hydroxycitric acid from Garcinia. *Journal of Agricultural and Food Chemistry*.50, 10-22.

Jiang, X. C., Moulin, P., Quinet, E., Goldberg, I. J., Yacoub, L. K., Agellon, L. B., Compton, D., Schnitzer-Polokoff, R. & Tall, A. R. (1991). Mammalian adipose tissue and muscle are major sources of lipid transfer protein mRNA. *Journal of Biological Chemistry*, 266, 4631–4639.

Johs, A., Hammel, M., Waldner, I., May, R. P., Laggner, P., & Prassl, R. (2006). Modular structure of solubilized human apolipoprotein B-100: low resolution model revealed by small angle neutron scattering. *Journal of Biological Chemistry*, 281, 19732–19739.

Jonas, A. (2002). Lipoprotein structure. In D. E. Vance & J. E. Vance (Eds.), *Biochemistry of Lipids, Lipoproteins and Membranes (4th Edn).*, 483-504, Illinois, USA, Elsevier Science B.V.

Jonas, A., Kézdy, K. E., Williams, M. I., & Rye, K. A. (1988). Lipid transfers between reconstituted high density lipoprotein complexes and low density lipoproteins: effects of plasma protein factors. *Journal of Lipid Research*, 29, 1349–1357.

Kevin J. Bowers, Edmond Chow, Huafeng Xu, Ron O. Dror, Michael P. Eastwood, Brent A. Gregersen, John L. Klepeis, Istvan Kolossvary, Mark A. Moraes, Federico D. Sacerdoti, John K. Salmon, Yibing Shan, and David E. Shaw, (2006), "Scalable Algorithms for Molecular Dynamics Simulations on Commodity Clusters," *Proceedings of the ACM/IEEE Conference on Supercomputing (SC06), Tampa, Florida*, November 11-17.

Khurana, M. Sharma, D. Khandelwal, P.D. (2000), Lipid profiles in smokers and tobacco chewers: a comparative study, *Journal of Association Physicians India,* 48(9): 895-897.

Kirchmair, R., Ebenbichler, C. F., & Patsch, J. R. (1995). Post-prandial lipaemia. *Bailliere's Clinical Endocrinology and Metabolism*, 9, 705-719.

Ko, K. W., Taira, O., & Yokoyama, S. (1994). Triglyceride Transfer Is Required for Net Cholesteryl Ester Transfer between Lipoproteins in Plasma by Lipid Transfer Protein, *Journal of Biological Chemistry*, 269(45), 28206–28213.

Konstantinov, I. E., & Jankovic, G. M. (2013). Alexander I. Ignatowski: A pioneer in the study of atherosclerosis, *Historical Perspectives*, 40(3), 247–249.

Kosin, J., Ruangrungsi, N., Ito, C., & Furukawa, H. (1998). A xanthone from Garcinia atroviridis. *Phytochemistry*, 47, 1167–1168.

Kumar, S., Sharma, S., & Chattopadhyay, S. K. (2013). The potential health benefit of polyisoprenylated benzophenones from Garcinia and related genera: Ethnobotanical and therapeutic importance. *Fitoterapia*, 89, 86-125.

Kuvin, J. T., Rämet, M. E., Patel, A. R., Pandian, N. G., Mendelsohn, M. E., & Karas, R. H. (2002). A novel mechanism for the beneficial vascular effects of high-density lipoprotein cholesterol: Enhanced vasorelaxation and increased endothelial nitric oxide synthase expression. *American Heart Journal*, 144, 165–172.

Kwiterovich, P. O. (2000). The metabolic pathways of high-density lipoprotein, low-density lipoprotein, and triglycerides: a current review. *The American Journal of Cardiology*, 86, 5L–10L.

Leonhardt, M., Balkan, B., & Langhans, W. (2004). Effect of hydroxycitrate on respiratory quotient, energy expenditure, and glucose tolerance in male rats after a period of restrictive feeding. *Nutrition*, 20(10), 911–915.

Leonhardt, M., Hrupka, B., & Langhans, W. (2001). Effect of hydroxycitrate on food intake and body weight regain after a period of restrictive feeding in male rats. *Physiology and Behavior*, 74(1-2), 191–196.

Lewis, Y. S. (1965). (-)-Hydroxycitric acid - The principal acid in the fruits of *Garcinia Cambogia* , *Phytochemistry*, 4 , 619-625.

Li, A. C., & Glass, C. K. (2002). The macrophage foam cell as a target, *Nature Medicine*, 8(11), 1235–1242.

Libby, P., Ridker, P. M., & Hansson, G. K. (2011). Progress and challenges in translating the biology of atherosclerosis. *Nature*, 473(7347), 317–25.

Lippi, G., & Guidi, G. (2000). Lipoprotein(a): from ancestral benefit to modern pathogen? *QJM : Monthly Journal of the Association of Physicians*, 93, 75–84.

Liu, S., Mistry, A., Reynolds, J. M., Lloyd, D. B., Griffor, M. C., Perry, D. A, Ruggeri, R. B., Clark, R. W., & Qiu, X. (2012). Crystal structures of cholesteryl ester transfer protein in complex with inhibitors. *The Journal of Biological Chemistry*, 287(44), 37321–9.

Lusis, A. J., Zollman, S., Sparkes, R. S., Klisak, I., Mohandas, T., Drayna, D., & Lawn, R. M. (1987). Assignment of the human gene for cholesteryl ester transfer protein to chromosome 16q12-16q21. *Genomics*, 1, 232–235.

Mackeen, M. M., Ali, A. M., Lajis, N. H., Kawazu, K., Hassan, Z., Amran, M., Habsah, M., Mooi, L. Y. & Mohamed, S. M. (2000). Antimicrobial, antioxidant, antitumour-promoting and cytotoxic activities of different plant part extracts of *Garcinia atroviridis* Griff. ex T. Anders. *Journal of Ethnopharmacology*, 72, 395–402.

Mackeen, M. M., Ali, A. M., Lajis, N., Kawazu, K., Kikuzaki, H., & Nakatani, N. (2002). Antifungal garcinia acid esters from the fruits of *Garcinia atroviridis*. *Zeitschrift Fur Naturforschung - Section C Journal of Biosciences*, 57, 291–295.

Mackness, B., Hine, D., Liu, Y., Mastorikou, M., & Mackness, M. (2004). Paraoxonase-1 inhibits oxidised LDL-induced MCP-1 production by endothelial cells. *Biochemical and Biophysical Research Communications*, 318, 680–683.

Mahley, R. W. (1996). Heparan sulfate proteoglycan/low density lipoprotein receptor-related protein pathway involved in type III hyperlipoproteinemia and Alzheimer's disease. *Israel Journal of Medical Sciences*, 32, 414–429.

Martyna, G. J., Tobias, D. J., & Klein, M. L. (1994). Constant pressure molecular dynamics algorithms. *The Journal of Chemical Physics*, 101, 4177-4189.

Martyna, G., Klein, M. L., & Tuckerman, M. E. (1992). Nose-Hoover chains: the canonical ensemble via continous dynamics. *The Journal of Chemical Physical*, 97, 2635–2643.

Masson, D. (2009). Anacetrapib, a cholesterol ester transfer protein (CETP) inhibitor for the treatment of atherosclerosis. *Current Opinion in Investigational Drugs*, 10, 980–987.

Masucci-Magoulas, L., Moulin, P., Xian Cheng Jiang, Richardson, H., Walsh, A., Breslow, J. L., & Tall, A. (1995). Decreased cholesteryl ester transfer protein (CETP) mRNA and protein and increased high density lipoprotein following lipopolysaccharide administration in human CETP transgenic mice. *Journal of Clinical Investigation*, *95,* 1587–1594.

Mathers, C. D., & Loncar, D. (2006). Projections of global mortality and burden of disease from 2002 to 2030. *PLoS Medicine*, 3(11), 2011–2030.

Milliez, P., Girerd, X., Plouin, P.-F., Blacher, J., Safar, M. E., & Mourad, J.-J. (2005). Evidence for an increased rate of cardiovascular events in patients with primary aldosteronism. *Journal of the American College of Cardiology*, 45(8), 1243-1248.

Mott, G.E. Jacksom, E.M. McMahan, C.A. McGill Jr, H.C. (1992), Dietary cholesterol and type of fat diiferentially affect cholesterol metabolism and atherosclerosis in baboon, *Journal of Nutrition,* 122, 1397-1406.

Khalili, R., Norhayati, A. H., Rokiah, M. Y., Asmah, R., Siti Muskinah, M., & Abdul Manaf, A. (2009). Hypocholesterolemic effect of red pitaya (*Hylocereus* sp.) on hypercholesterolemia induced rats. *International Food Research Journal*, 16, 431–440.

Koskinas, K.C. Feldman, C.L. Chatzizisis, Y.S. Coskun, A.U. Jonas, M. Maynard, C. Baker, A.B. Papafaklis, M.I. Edelman, E.R. Stone, P.H. (2010), Natural history of experimental coronary atherosclerosis and vascular remodelling in relation to endothelial shear stress: a serial, in vivo intravascular ultrasound study, *Circulation*, 19, 2092-2101.

Kumar, S. Rai, H. Kapoor, A. Tewari, S. Sinha, N. (2013), Pharmacological measures to increase HDL-C among risk isolated low HDL cases : A randomized study amongst north Indian, *Indian Journal of medical reviews*, 138(6), 873-881

Medina, M.W. & Krauss, R.W. (2009), The role of HMGCR alternative splicing in statin efficacy, *Trends in cardiovascular medicine*, 19(5), 173-177.

Morton, R. E., & Greene, D. J. (2003). The surface cholesteryl ester content of donor and acceptor particles regulates CETP: a liposome-based approach to assess the substrate properties of lipoproteins. *Journal of Lipid Research*, 44, 1364–1372.

Morton, R. E., & Zilversmit, D. B. (1983). Inter-relationship of lipids transferred by the lipid-transfer protein isolated from human lipoprotein-deficient plasma. *Journal of Biological Chemistry*, 258, 11751–11757.

Muller, J. E., & Tofler, G. H. (1992). Triggering and hourly variation of onset of arterial thrombosis. *Annals of Epidemiology*, 2, 393–405.

Nagashima, M., McLean, J. W., & Lawn, R. M. (1988). Cloning and mRNA tissue distribution of rabbit cholesteryl ester transfer protein. *Journal of Lipid Research*, 29, 1643–1649.

Ng, Y. F., & Mariam, O. S. (2009). Diversity of butterfly (Lepidoptera: Rhopalocera) communities at three habitats in Hulu Langat, Selangor, Peninsular Malaysia. *Journal of Science and Technology in the Tropic*, 5(2), 105.

Nichols, M., Townsend, N., Scarborough, P., & Rayner, M. (2013). Cardiovascular disease in Europe: Epidemiological update. *European Heart Journal*, 34, 3028-3034.

Nordestgaard, B.G. Zilversmit, D.B. (1988), Large lipoproteins are excluded from the arterial wall in diabetic cholesterol-fed rabbits, *Journal Lipid Research*, 1491-1500.

Okamoto, H., Yonemori, F., Wakitani, K., Minowa, T., Maeda, K., & Shinkai, H. (2000). A cholesteryl ester transfer protein inhibitor attenuates atherosclerosis in rabbits. *Nature*, 406, 203–207.

Oram, J. F., & Vaughan, A. M. (2006). ATP-Binding cassette cholesterol transporters and cardiovascular disease. *Circulation Research*, 99(10), 1031–1043.

Ordovas, J. M., Cupples, L. A., Corella, D., Otvos, J. D., Osgood, D., Martinez, A., Schaefer, E. J. (2000). Association of cholesteryl ester transfer protein-TaqIB polymorphism with

variations in lipoprotein subclasses and coronary heart disease risk: the Framingham study. *Arteriosclerosis, Thrombosis, and Vascular Biology*, 20, 1323–1329.

Packard, C. J., Demant, T., Stewart, J. P., Bedford, D., Caslake, M. J., Schwertfeger, G., Bedynek, A., Shepherd, J. & Seidel, D. (2000). Apolipoprotein B metabolism and the distribution of VLDL and LDL subfractions. *Journal of Lipid Research*, 41, 305–318.

Patsch, J. (1998). Influence of lipolysis on chylomicron clearance and HDL cholesterol levels. *European Heart Journal*, 19 Suppl *H*, H2–H6.

Permana, D., Abas, F., Maulidiani, Shaari, K., Stanslas, J., Ali, A. M., & Lajis, N. H. (2005). Atrovirisidone B, a new prenylated depsidone with cytotoxic property from the roots of Garcinia atroviridis. *Zeitschrift Fur Naturforschung - Section C Journal of Biosciences*, 60, 523–526.

Permana, D., Lajis, N. H., Mackeen, M. M., Ali, A. M., Aimi, N., Kitajima, M., & Takayama, H. (2001). Isolation and bioactivities of constitutents of the roots of Garcinia atroviridis. *Journal of Natural Products*, 64, 976–979.

Plump, A. S., Smith, J. D., Hayek, T., Aalto-Setälä, K., Walsh, A., Verstuyft, J. G., Rubin, E. M., & Breslow, J. L. (1992). Severe hypercholesterolemia and atherosclerosis in apolipoprotein E-deficient mice created by homologous recombination in ES cells. *Cell*, 71, 343–353.

Portman, O.W. Andrus, S.B. (1965), Comparative evaluation of three species of new world monkeys for studies of dietary factors, tissue lipids, and atherogenesis, *Journal of Nutrition.* 87, 429-438

Prescott, M.F. McBride, C.H. Hasler-Rapacz, J. Von Linden, J. Rapacz, J. (1991) Development of complex atherosclerotic lesions in pigs with inherited hyper-LDL cholesterolemia bearing mutant allelles for apolipoprotein B, *Americal Journal of Pathology*, 139: 139-147

Preuss, H. G., Bagchi, M., & Bagchi, D. (2006). Comparison of the effects of three different (-)-hydroxycitric acid preparations on food intake in rats: response. *Nutrition & Metabolism*.,1, 1-2,

Prochaska, J.J. Prochaska, J.O. (2013), A review of multiple health behavior change interventions fro primary prevention, *American Journal of Lifestyle Medicine,* 5(3), 1-21.

Qiu, X., Mistry, A., Ammirati, M. J., Chrunyk, B. a, Clark, R. W., Cong, Y., Culp, J. S., Danley, D. E., Freeman, T. B., Geoghegan, K. F., Griffor, M. C., Hawrylik, S. J., Hayward, C. M., Hensley, P., Hoth, L. R., Karam, G. A., Lira, M. E., Lloyd, D. B., McGrath, K. M., Stutzman-Engwall, K. J., Subashi, A. K., Subashi, T. A., Thompson, J. F., Wang, I. K., Zhao, H. & Seddon, A. P. (2007). Crystal structure of cholesteryl ester transfer protein reveals a long tunnel and four bound lipid molecules. *Nature Structural & Molecular Biology*, 14(2), 106–113.

Ranalletta, M., Bierilo, K. K., Chen, Y., Milot, D., Chen, Q., Tung, E., Houde, C., Elowe, N. H., Garcia-Calvo, M., Porter, G., Eveland, S., Frantz-Wattley, B., Kavana, M., Addona, G., Sinclair, P., Sparrow, C., O'Neill, E. A., Kobian, K. S., Sitlani, A., Hubbard, B., & Fisher, T. S. (2010). Biochemical characterization of cholesteryl ester transfer protein inhibitors. *Journal of Lipid Research*, 51, 2739–2752.

Rao, R. N., & Sakariah, K. K. (1988). Lipid-lowering and antiobesity effect of (−)hydroxycitric acid. *Nutrition Research*, 8, 209-212.

Rea, T. J., Demattos, R. B., Pape, M. E., & Arbor, A. (1993). Hepatic expression of genes regulating lipid metabolism in rabbits, *Journal of Lipid Research*, 34, 1901-1910.

Rehman, I. and Bonfield, W. (1997). Characterization of hydroxyapatite and carbonate apatite by photo acoustic FTIR spectroscopy. *Journal of Material Science:Material in Medical*, 8,1-4.

Reiner, Z. Catapano, A.L. De-Backer, G. Graham, I. Taskinen, M.R. Wiklund, O. Agewall, S. Alegria, E. Chapman, M.J. Durrington, P. Erdine, S. Halcox, J. Hobbs, R. Kjekshus, J. Filardi, P.P Riccardi, G Storey, R.F. Wood, D. (2011), ESC/EAS Guidelines for the management of dyslipidaemias: the Task force for the management of dyslipidemia of the European Society of Cardiology (ESC) and the European Atherosclerosis Society (EAS), *European Heart Journal*, 32(14), 1769-1818.

Reiser, R. Sorrels, M.F. Williams, M.C. (1959), Influence of high levels of dietary fats and cholesterol on atherosclerosis and lipid distribution in swine, *Circulation Research*, 7, 835-846.

Robbesyn, F., Garcia, V., Auge, N., Vieira, O., Frisach, M. F., Salvayre, R., & Negre-Salvayre, A. (2003). HDL counterbalance the proinflammatory effect of oxidized LDL by inhibiting intracellular reactive oxygen species rise, proteasome activation, and subsequent NF-kappaB activation in smooth muscle cells. *The FASEB Journal : Official Publication of the Federation of American Societies for Experimental Biology*, 17(6), 743–745.

Rye, K. A., Clay, M. A., & Barter, P. J. (1999). Remodelling of high density lipoproteins by plasma factors. *Atherosclerosis*, 145, 227-238.

Saland, J. M., & Ginsberg, H. N. (2007). Lipoprotein metabolism in chronic renal insufficiency. *Pediatric Nephrology (Berlin, Germany)*, 22, 1095–1112.

Satoh, K., Imaizumi, T., Kawamura, Y., Yoshida, H., Hiramoto, M., Takamatsu, S., & Takamatsu, M. (1991). Platelet-activating factor (PAF) stimulates the production of PAF acetylhydrolase by the human hepatoma cell line, HepG2. *Journal of Clinical Investigation*, 87, 476–481.

Savithramma, N., & Rao, M. (2011). Screening of Medicinal Plants for Secondary Metabolites. *Middle-East Journal of Scientific*, 8, 579–584.

Schmelzle, J. Rosser, W.W. Birthwistle, R. (2008), Update on pharmacologic and non pharmacologic therapies for smoking cessation, *Canadian family physicians,*54(7), 994-999.

Schmitt, J. and Flemming, H.C. (1998). FTIR-spectroscopy in microbial and material analysis. *International Biodeterioration & Biodegradation*, 41,l-11.

Schrödinger Release 2015-3**:** Desmond Molecular Dynamics System, version 4.3, D. E. Shaw Research, New York, NY, 2015. Maestro-Desmond Interoperability Tools, version 4.3, Schrödinger, New York, NY, 2015.

Schrödinger Release 2015-3**:** Maestro, version 10.3, Schrödinger, LLC, New York, NY, 2015

Schwartz, G. G., Olsson, A. G., Ballantyne, C. M., Barter, P. J., Holme, I. M., Kallend, D., Leiter, L. A., Leiterdorf, E., McMurray, J. J. V., Shah, P. K., Tardif, J. C., Chaitman, B. R., Duttlinger-Maddux, R., & Mathieson, J. (2009). Rationale and design of the dal-OUTCOMES trial: Efficacy and safety of dalcetrapib in patients with recent acute coronary syndrome. *American Heart Journal*, 158, 896-901.

Shiomi, M. Ito, T. (2009), The watanabe heritable hyperlipidemic (WHHL) rabbits, its characteristic and history development: a tribute to the late Dr. Yoshio Watanabe, *Atherosclerosis*, 207,1-7.

Sehayek, E. Butbul, E. Avner, R. (1994). Enhanced cellular metabolism of very low density lipoprotein by simvastation: A novel mechanism of action of HMG-COA reductase inhibitors, *European Journal of Clinical Investment*, 24, 173-178.

Serdyuk, A. P., & Morton, R. E. (1999). Lipid transfer inhibitor protein defines the participation of lipoproteins in lipid transfer reactions: CETP has no preference for cholesteryl esters in HDL versus LDL. *Arteriosclerosis, Thrombosis, and Vascular Biology*, 19, 718–726.

Shiomi, M. Ito, T. Shiraishi, M. Watanabe, Y. (1992), Inheritability of atherosclerosis and the role of lipoproteins as risk factors in the development of atherosclerosis in the WHHL rabbits: risk factors related to coronary atherosclerosis are different from those related to aortic atherosclerosis, *Atherosclerosis,* 96, 43-52.

Shivakumar, D.; Williams, J.; Wu, Y.; Damm, W.; Shelley, J.; Sherman, W., (2010). "Prediction of Absolute Solvation Free Energies using Molecular Dynamics Free Energy Perturbation and the OPLS Force Field," *Journal of Chemical Theory Computation,* 6, 1509–1519

Singh, R. B., Mengi, S. A., Xu, Y., Arneja, A. S., & Dalla, N. S. (2002). Pathogenesis of atherosclerosis : A multifactorial process, *Experimental and Clinical Cardiology*, 7(1), 40-53.

Skold, B.H. Getty, R. Ramsey, F.K. (1966), Spontaneous atherosclerosis in the arterial system of aging swine, *American Journal of Veterinary Research*, 27, 257-273.

Small-Molecule Drug Discovery Suite 2015-3: Glide, version 6.8, Schrödinger, LLC, New York, NY, 2015.

Smith, J.D. James, D. Dansky, H.M. Wittkowski, K.M. Moore, K.J. Breslow, J.L. (2003), In silico quantitative trait locus map for atherosclerosis susceptibility in lipoprotein E-deficient mice, *Atheriosclerosis, Thrombosis and Vascular Biology*, 23, 117-122.

Spieker, L. E., Sudano, I., Hürlimann, D., Lerch, P. G., Lang, M. G., Binggeli, C., Corti, R., Ruschitzka, F., Luscher, T. F., & Noll, G. (2002). High-density lipoprotein restores endothelial function in hypercholesterolemic men. *Circulation*, 105, 1399–1402.

Stuart-Shor, E. M. Berra, K.A. Kamau, M.W. Kumanyika, S.K. (2012), Behavioral strategies for cardiovascular risk reduction in dverse and underserved racial/ethnic group, *circulation,* 125-171-184.

Steals, B. Dallongeville, J. Auwerx, J. Schoonjans, K. Leitersdorf, E, Fruchart, J.C. (2013), Mechanism of action of fibrates on lipid and lipoprotein metabolism, *circulation*, 98, 2088-2093.

Subbaiah, P. V, Liu, M., Senz, J., Wang, X., & Pritchard, P. H. (1994). Substrate and positional specificities of human and mouse lecithin-cholesterol acyltransferases. Studies with wild type recombinant and chimeric enzymes expressed in vitro. *Biochimica et Biophysica Acta*, 1215, 150–156.

Sugatani, J., Miwa, M., Komiyama, Y., & Ito, S. (1996). High-density lipoprotein inhibits the synthesis of platelet-activating factor in human vascular endothelial cells. *Journal of Lipid Mediators and Cell Signalling*, 13, 73–88.

Sundt, T. M. (2007). Intramural hematoma and penetrating atherosclerotic ulcer of the aorta. *The Annals of Thoracic Surgery*, 83(2), S835–41.

Sung, J. H., Lee, S.-J., Park, K. H., & Moon, T. W. (2004). Isoflavones inhibit 3-hydroxy-3-methylglutaryl coenzyme A reductase in vitro. *Bioscience, Biotechnology, and Biochemistry*, 68, 428–432.

Tall, A. R. (1993). Plasma cholesteryl ester transfer protein, *Journal of Lipid Research*, 34, 1255–1274.

Tan, W. N., Wong, K. C., Khairuddean, M., Eldeen, I. M., Asmawi, M. Z., & Sulaiman, B. (2013). Volatile constituents of the fruit of *Garcinia atroviridis* and their antibacterial and anti-inflammatory activities. *Flavour and Fragrance Journal*, 28, 2–9.

Taylor, A.J. Sullenberger, L.E. Lee, H.J. Lee, J.K. Grace, K.A. (2004), Arterial biology for the biology for the investigation of the treatment effects of reducing cholesterol (ARBITER)2: a double blide placebo-controlled study of extended released niacin on atherosclerosis progression in seconday prevention patients treated with statin, *circulation,* 110, 3512-3517.

Teupser, D. Tan, M. Persky, A.D. Breslow, J.L. (2006) Atherosclerosis quantitative trait loci are sex and lineage dependent in an intercross of C56BL/6 and FVB/N low density

lipoprotein receptor -/- mice, *Proceeding of Natural Academic Science Asia*, 103: 123-128.

Terasaka, N., Yu, S., Yvan-Charvet, L., Wang, N., Mzhavia, N., Langlois, R., Pagler, T., Li, R., Welch, C. L., Goldberg, I. J. & Tall, A. R. (2008). ABCG1 and HDL protect against endothelial dysfunction in mice fed a high-cholesterol diet. *Journal of Clinical Investigation*, 118, 3701–3713.

Testai, L., Martelli, A., Cristofaro, M., Breschi, M. C., & Calderone, V. (2013). Cardioprotective effects of different flavonoids against myocardial ischaemia/reperfusion injury in Langendorff-perfused rat hearts. *Journal of Pharmacy and Pharmacology*, 65(5), 750–756.

Tiwari, P., Kumar, B., Mandeep, K., Kaur, G., & Kaur, H. (2011). Phytochemical screening and Extraction: A Review. *Internationale Pharmaceutica Sciencia*, 1, 98–106.

Tobias, P. S., & Curtiss, L. K. (2007). Toll-like receptors in atherosclerosis. *Biochemical Society Transactions*, 35(Pt 6), 1453–1455.

Tunstall-Pedoe, H., Kuulasmaa, K., Mähönen, M., Tolonen, H., Ruokokoski, E., & Amouyel, P. (1999). Contribution of trends in survival and coronary-event rates to changes in coronary heart disease mortality: 10-year results from 37 WHO MONICA Project populations. *Lancet*, 353(9164), 1547–1557.

Van Linthout, S., Spillmann, F., Lorenz, M., Meloni, M., Jacobs, F., Egorova, M., … Tschöpe, C. (2009). Vascular-protective effects of high-density lipoprotein include the downregulation of the angiotensin II type 1 receptor. *Hypertension*, 53, 682–687.

Van Sickle, W. A., Wilcox, H. G., & Nasjletti, A. (1986). HDL-induced cardiac prostacyclin synthesis: relative contribution of HDL apoprotein and lipid. *Biochemical and Biophysical Research Communications*, 139, 416–423.

Varban, M. L., Rinninger, F., Wang, N., Fairchild-Huntress, V., Dunmore, J. H., Fang, Q.,Gosselin, M. L., Dixon, K. L., Deeds, J. D., Acton, S. L., Tall, A. R., & Huszar, D. (1998). Targeted mutation reveals a central role for SR-BI in hepatic selective uptake of high density lipoprotein cholesterol. *Proceedings of the National Academy of Sciences of the United States of America*, 95, 4619–4624.

Vedhachalam, C., Duong, P. T., Nickel, M., Nguyen, D., Dhanasekaran, P., Saito, H., Rothblat, G. H., Lund-Katz, S., & Phillips, M. C. (2007). Mechanism of ATP-binding cassette transporter A1-mediated cellular lipid efflux to apolipoprotein A-I and formation of high density lipoprotein particles. *The Journal of Biological Chemistry*, 282(34), 25123–30.

Verdonk, M. L., Cole, J. C., Hartshorn, M. J., Murray, C. W., & Taylor, R. D. (2003). Improved protein-ligand docking using GOLD. *Proteins: Structure, Function and Genetics*, *52*, 609–623.

Vesselinovitch, D. Gets, G.S. Hughes, R.H. Wissler, R.W. (1974), Atherosclerosis in the rhesus monkey fed three food fats, *Atherosclerosis*, 2, 303-321

Virmani, R., Burke, A. P., Kolodgie, F. D., & Farb, A. (2003). Pathology of the Thin-Cap Fibroatheroma:. A Type of Vulnerable Plaque. *Journal of Interventional Cardiology*, 16(3), 267–272.

Virmani, R., Kolodgie, F. D., Burke, A. P., Farb, A., & Schwartz, S. M. (2000). Lessons From Sudden Coronary Death: A comprehensive Morphological classification scheme for atherosclerotic lesions, *Journal of the American Heart Association*, 20, 1262–1275..

Wal, A. C. Van Der, & Becker, A. E. (1999). Atherosclerotic plaque rupture – pathologic basis of plaque stability and instability, *Cardiovascular Research*, 41, 334–344.

Whittle, B. J., Moncada, S., Whiting, F., & Vane, J. R. (1980). Carbacyclin--a potent stable prostacyclin analogue for the inhibition of platelet aggregation. *Prostaglandins*, 19, 605–627.

Whitman, S.C. (2004), A practical approach to using mice in atherosclerosis, *Clinical Biochemistry Review*, 25(1), 81-93.

Wolfe, M.S. Sawyer, J.K. Morgan, T.M. Bullock, B.C. Rudel, L.L. (1994), Dietary polyunsaturated fat decreases coronary artery atherosclerosis in a pediatric-aged population of African green monkeys, *Atheriosclerosis Thrombus*, 4, 587-597.

Wong, J.P.C. (2013), 3-hydroxy-3-methylglutaryl coenzyme A (HMG-CoA) reductase inhibitors from plant secondary metabolites as hypercholesterolaemic lowering agent (Doctoral thesis), University of Nottingham.

World Health Organisation (WHO) (2010), Non-communicable diseases country profile. WHO Global Reports, Geneva.

World Health Organisation (WHO) (2014), Non-communicable diseases country profile. WHO Global Reports, Geneva.

Xia, P., Vadas, M. A., Rye, K. A., Barter, P. J., & Gamble, J. R. (1999). High density lipoproteins (HDL) interrupt the sphingosine kinase signaling pathway. A possible mechanism for protection against atherosclerosis by HDL. *The Journal of Biological Chemistry*, 274, 33143–33147.

Yamanashi, Y., Takada, T., Yoshikado, T., Shoda, J., & Suzuki, H. (2011). NPC2 regulates biliary cholesterol secretion via stimulation of ABCG5/G8-mediated cholesterol transport. *Gastroenterology*, 140, 1664–1674.

Yang, X. Peterson, L. Thieringer, R. Deignan, J.L. Wang, X. Zhu, J. Wang, S. Zhong, H. Stepaniants, S. Beaulaurier, J. Wang, I.M. Rosa, R. Cumiskey, A.M. Luo, J.M. Luo, Q. Shah, K. Xiao, J. Nickle, D. Plump, A. Schadt, E.E. Lusis, A.J. Lum, P.Y. (2010), Identification and validation of genes affecting aortic lesions in mice, *Journal of Clinical Investigation.* 120: 2414-2422

Yokoyama, S. (2000). Release of cellular cholesterol: Molecular mechanism for cholesterol homeostasis in cells and in the body. *Biochimica et Biophysica Acta*, 1529, 231-244..

Yoshida, K., Tanaka, T., Hirose, Y., Yamaguchi, F., Kohno, H., Toida, M., Hara, A., Sugie, S., Shibata, T & Mori, H. (2005). Dietary garcinol inhibits 4-nitroquinoline 1-oxide-induced tongue carcinogenesis in rats. *Cancer Letters*, 221(1), 29–39.

Yoshida, Y., & Niki, E. (2003). Antioxidant effects of phytosterol and its components. *Journal of Nutritional Science and Vitaminology*, 49(4), 277–280.

Yuhanna, I. S., Zhu, Y., Cox, B. E., Hahner, L. D., Osborne-Lawrence, S., Lu, P., Marcel, Y. L., Anderson, R. G. W., Mendelsohn, M. E., Hobbs, H. H., & Shaul, P. W. (2001). High-density lipoprotein binding to scavenger receptor-BI activates endothelial nitric oxide synthase. *Nature Medicine*, 7, 853–857.

Yusuf, S. Hawken, S. Stephanie, D.T. Avezum, A. Lanas, F. Mcqueen, M. Budaj, A. Pais, P. Varigos, J. Lisheng, L. (2004), Effects of potentially modifiable risk factors associated with myocardial infarction in 52 countries (The INTERHEART study): Case control study, *Lancet*, 364(9438), P937-952.

Zannis, V. I., Chroni, A., & Krieger, M. (2006). Role of apoA-I, ABCA1, LCAT, and SR-BI in the biogenesis of HDL. *Journal of Molecular Medicine*, 84, 276-294.

Zhang, Y., Proenca, R., Maffei, M., Barone, M., Leopold, L., & Friedman, J. M. (1994). Positional cloning of the mouse obese gene and its human homologue. *Nature*, 372, 425–432.

Zhou, H., Li, Z., Hojjati, M. R., Jang, D., Beyer, T. P., Cao, G., Tall, A. R., & Jiang, X.-C. (2006). Adipose tissue-specific CETP expression in mice: impact on plasma lipoprotein metabolism. *Journal of Lipid Research*, 47, 2011–2019.

**APPENDIX A – Parameters for GLIDE**

**AI. Table for Protein preparation**

| Parameters | Action |
|---|---|
| **Ligands** | Delete |
| **Bond order** | Assign |
| **Hydrogen Bonds** | Add |
| **Zero order bonds to metal** | Add |
| **Disulphide bonds** | Add |
| **Convert selenomethionines to methionines** | Add |
| **Fill in missing side chains using Prime** | Add |
| **Fill in missing loops using Prime** | Add |
| **Cap termini** | Add |
| **Delete water** | Add – within 5Å from het groups |

**AII Table for Docking run**

| Parameters | Action |
|---|---|
| Precision | **SP (standard precision)** |
| Ligand sampling | **-Flexible**<br>**-Sample nitrogen inversions**<br>**-sample ring conformations** |
| Epik state penalties to docking score | **Add** |
| Scaling of Van der Waals | **-Scaling factor : 0.8**<br>**-partial charge cutoff: 0.15** |

**APPENDIX B – Parameters for GOLD**

**BI Table for parameters for GOLD**

| Parameter | Action |
|---|---|
| **Input structure** | Protein target: 2OBD<br>Observed ligands: HCA<br>Number of docking: 10 |
| **Early termination settings** | Allow termination if top 3 solutions are within 1.5Å RMSD |
| **Scoring function** | Chemscore |
| **GA parameters** | Population size: 100<br>Selection pressure: 1.1<br>Number of operations: 30000<br>Number of islands: 3<br>Niche size: 2<br>Migrate 10<br>Mutate 95<br>Crossover 95 |

**APPENDIX C – Parameters for DESMOND**

**C1 Table for parameters for protein preparation**

| Parameters | Action |
|---|---|
| Pre-process and analyse structure | **Assign bond orders**<br>**Add H**<br>**Treat metals**<br>**Delete water : 5Å** |
| H- bond assignment | **Sample water orientations** |
| Impref minimization | **RMSD (Å) :0.30**<br>**Force field: OPLS 2005** |

**Table CII Table for Generation of solvated system**

| Parameters | actions |
|---|---|
| Solvent model | **SPC** |
| Boundary conditions | **Box shape: Orthothombic**<br>**Box size calculation method: Buffer**<br>**Distances (Å): a: 10.0 b:10.0 c: 10.0** |
| Neutralize system | **Excluded region: Exclude ion and salt placement within 7.0 Å**<br>**Ion placement: Neutralize**<br>**Add salt: Salt concentration = 0.15M**<br>**Salt positive ion : $Na^+$**<br>**Salt negative ion: $Cl^-$** |

**CIII Table for simulation parameters**

| Parameters | Actions |
|---|---|
| Model system | **Load from workspace : docking model of HCA-CETP** |
| Simulation | **Simulation time : 20ns, elapsed: 0.0**<br>**Recording interval : 1.0 ps trajectory 20**<br>**Ensemble class: NPT**<br>**Temperature (K) : 300.0**<br>**Pressure bar: 1.01325**<br>**Relax model before simulation: Default** |

**APPENDIX D – Number of poses for HCA-CETP docking using GLIDE**

| No of poses | GLIDE gscore | GLIDE gmodel |
|---|---|---|
| **1** | -4.573 | -31.665 |
| **2** | -4.436 | -31.624 |
| **3** | -4.501 | -31.621 |
| **4** | -4.522 | -31.618 |
| **5** | -4.516 | -31.607 |
| **6** | -.4.307 | -31.601 |
| **7** | -.4.467 | -31.596 |
| **8** | -4.493 | -31.582 |
| **9** | -4.512 | -31.578 |
| **10** | -4.533 | -31.563 |
| **11** | -4.559 | -31.551 |
| **12** | -4.413 | -31.548 |
| **13** | -4.492 | -31.541 |
| **14** | -4.431 | -31.535 |
| **15** | -4.215 | -31.501 |
| **16** | -4.390 | -31.492 |
| **17** | -4.214 | -31.484 |
| **18** | -4.108 | -31.470 |
| **19** | -4.215 | -31.462 |
| **20** | -4.331 | -31.458 |

**APPENDIX D – Number of poses for HCA-CETP docking using GOLD**

| No of poses | chemscore | Ranking |
|---|---|---|
| **1** | 38.6 | 1 |
| **2** | 36.4 | 2 |
| **3** | 35.9 | 3 |
| **4** | 33.7 | 4 |
| **5** | 32.0 | 5 |
| **6** | 31.6 | 6 |
| **7** | 29.9 | 7 |
| **8** | 28.1 | 8 |
| **9** | 27.4 | 9 |
| **10** | 23.6 | 10 |

**APPENDIX E – Docking results of HCA analogues using ZINC 3D database**

| Structure name | GLIDE gscore | GLIDE gmodel |
|---|---|---|
| **ZINC1656421** | -4.966 | -25.859 |
| **ZINC1656422** | -4.907 | -24.974 |
| **ZINC1656423** | -4.822 | -24.550 |
| **ZINC1656424** | -4.806 | -22.568 |
| **ZINC895175** | -4.902 | -22.957 |
| **ZINC895081** | -4.732 | -26.712 |
| **ZINC895176** | -4.686 | -30.467 |
| **ZINC895179** | -4.878 | -24.131 |
| **ZINC895180** | -4.754 | -21.725 |

**APPENDIX F – Publication**

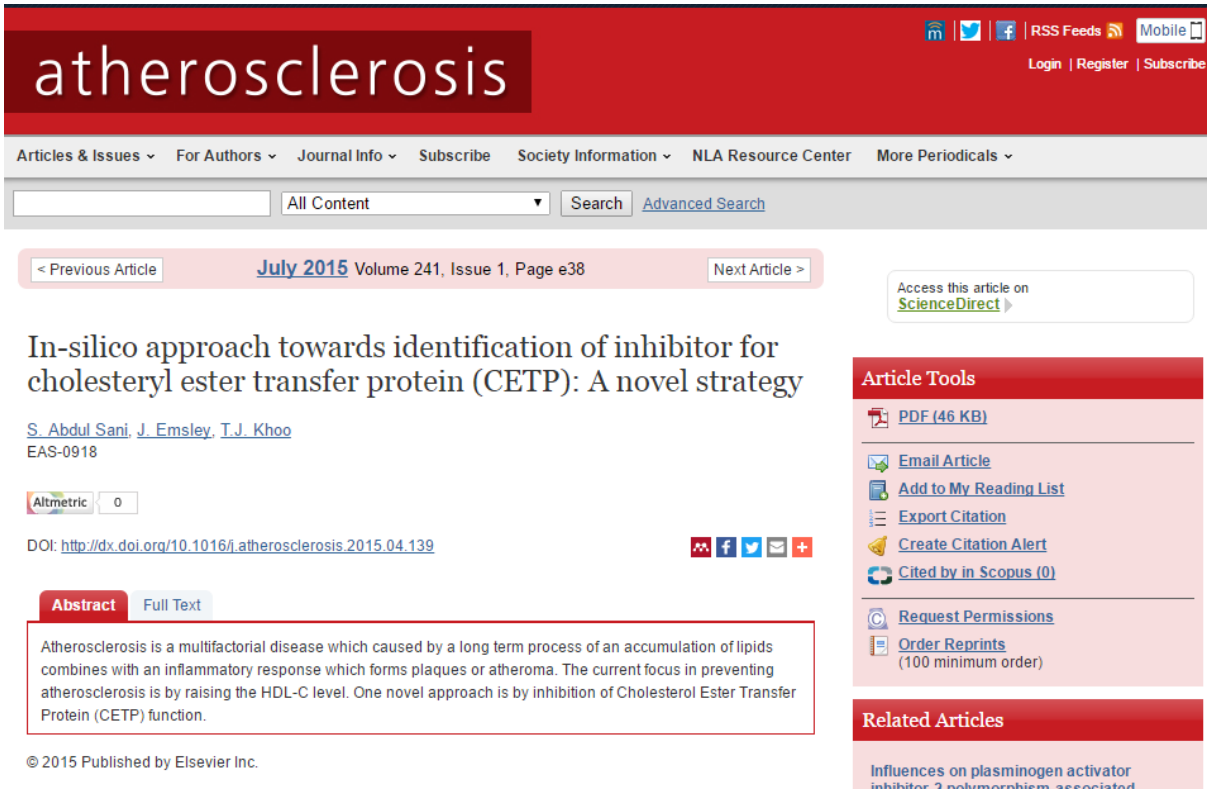

atherosclerosis

RSS Feeds Mobile
Login | Register | Subscribe

Articles & Issues | For Authors | Journal Info | Subscribe | Society Information | NLA Resource Center | More Periodicals

All Content | Search | Advanced Search

< Previous Article | July 2015 Volume 241, Issue 1, Page e38 | Next Article >

# In-silico approach towards identification of inhibitor for cholesteryl ester transfer protein (CETP): A novel strategy

S. Abdul Sani, J. Emsley, T.J. Khoo

EAS-0918

Altmetric 0

DOI: http://dx.doi.org/10.1016/j.atherosclerosis.2015.04.139

Abstract | Full Text

Atherosclerosis is a multifactorial disease which caused by a long term process of an accumulation of lipids combines with an inflammatory response which forms plaques or atheroma. The current focus in preventing atherosclerosis is by raising the HDL-C level. One novel approach is by inhibition of Cholesterol Ester Transfer Protein (CETP) function.